PNL-2500 PT4
UC-48

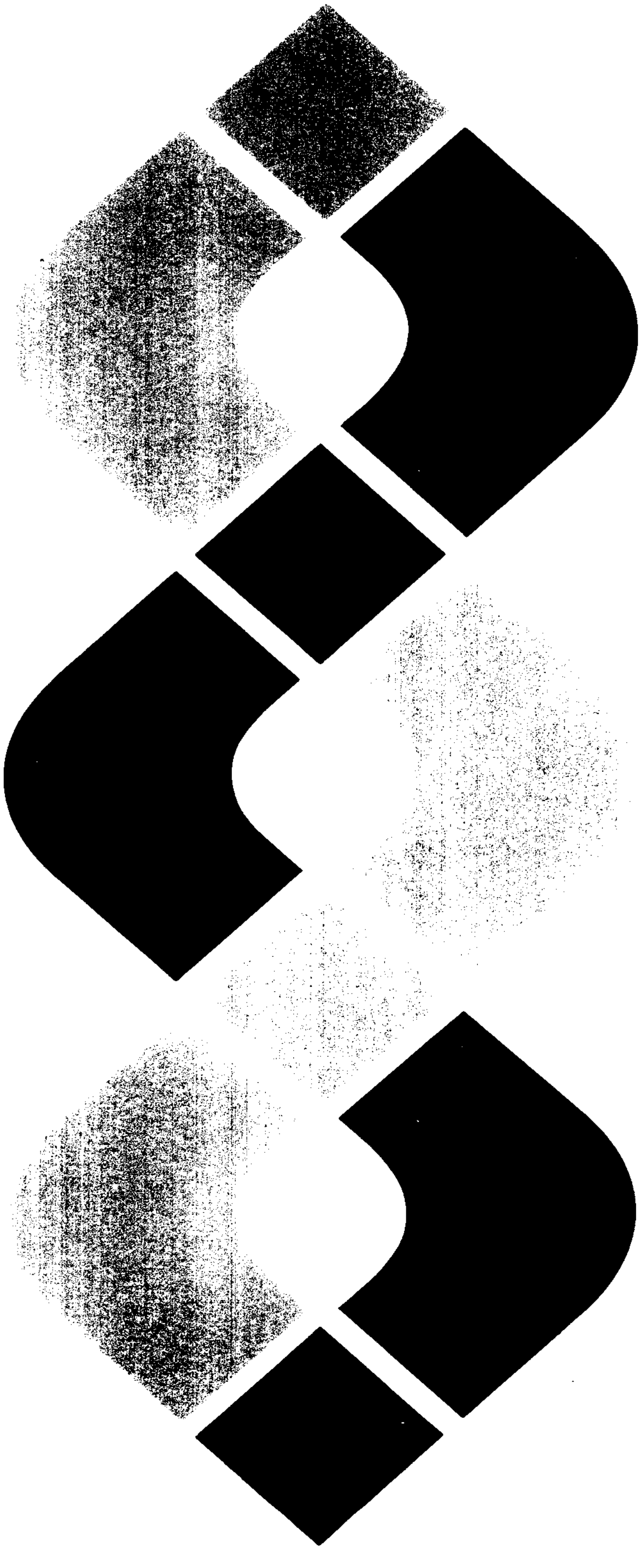

Pacific Northwest Laboratory
Annual Report for 1977
to the DOE Assistant Secretary
for Environment

February 1978

Part 4

Physical Sciences

Prepared for the
U.S. Department of Energy
under Contract EY-76-C-06-1830

PNL-2500 PT4

Battelle
Pacific Northwest Laboratories

PACIFIC NORTHWEST LABORATORY
operated by
BATTELLE
for the
UNITED STATES DEPARTMENT OF ENERGY
Under Contract EY-76-C-06-1830

Printed in the United States of America
Available from
National Technical Information Service
United States Department of Commerce
5285 Port Royal Road
Springfield, Virginia 22151

Price: Printed Copy $_____*; Microfiche $3.00

*Pages	NTIS Selling Price
001-025	$4.50
026-050	$5.00
051-075	$5.50
076-100	$6.00
101-125	$6.50
126-150	$7.00
151-175	$7.75
176-200	$8.50
201-225	$8.75
226-250	$9.00
251-275	$10.00
276-300	$10.25

PNL-2500 PT4
UC-48

Pacific Northwest Laboratory Annual Report for 1977 to the DOE Assistant Secretary for Environment

Part 4 Physical Sciences

by
J. M. Nielsen and Staff Members
of Pacific Northwest Laboratory

February 1978

Battelle
Pacific Northwest Laboratories
Richland, Washington 99352

PREFACE

The 1977 Annual Report from Pacific Northwest Laboratory (PNL) to the DOE Assistant Secretary for Environment introduces a new cover. The earth-green color used on past annual reports has been replaced by the "environmental colors," blue and green. The cover's abstract design is not intended to represent anything specific, but we would not be unhappy if it suggests something environmental or biological to the reader. The blue and green color pattern on the cover is different for each part of this report to help distinguish the five parts.

The five parts of the Report are oriented to particular segments of our program. Parts 1-4 report research performed for the DOE Office of Biomedical and Environmental Research. Part 5 reports progress on all other research performed for the Assistant Secretary for Environment, including the Office of Environmental Control Technology, Office of Technology Impact, and Office of Operational and Environmental Safety.

Each part consists of project reports authored by scientists from several PNL research departments, reflecting the interdisciplinary nature of the research effort. Parts 1-4 are organized primarily by energy technology, although it is recognized that much of the research performed at PNL is applicable to more than one energy technology.

The parts of the 1977 Annual Report are:

Part 1: Biomedical Sciences
Program Manager - W. R. Wiley   R. C. Thompson, Report Coordinator
D. L. Felton, Editor

Part 2: Ecological Sciences
Program Manager - B. E. Vaughan   B. E. Vaughan, Report Coordinator
J. L. Helbling, Editor

Part 3: Atmospheric Sciences
Program Manager - C. L. Simpson   R. L. Drake, Report Coordinator
C. M. Gilchrist, Editor

Part 4: Physical Sciences
Program Manager - J. M. Nielsen   J. M. Nielsen, Report Coordinator
G. M. Garnant/L. Carson, Editors

Part 5: Control Technology, Overview, Health, Safety,
and Policy Analysis

Program Managers - N. E. Carter
D. B. Cearlock
J. C. Fox
D. L. Hessel
H. V. Larson W. J. Bair, Report Coordinator
S. Marks R. W. Baalman, Editor

Activities of the scientists whose work is described in this Annual Report are broader in scope than the articles indicate. Knowledge and experience obtained by PNL staff in carrying out research in the Environment, Health, and Safety Research program have contributed to many other DOE interests. These include assistance in the preparation of several Environmental Development Plans for the Assistant Secretary for Environment, preparation of environmental statements for which the Laboratory is responsible, key membership in several national and international organizations, and numerous responses to the media on research projects of public interest.

W. J. Bair, Manager
S. Marks, Associate Manager
Environment, Health, and Safety Research
Program

Previous Reports in this Series:

Annual Report for

1951	W-25021, HW-25709
1952	HW-27814, HW-28636
1953	HW-30437, HW-30464
1954	HW-30306, HW-33128, HW-35905, HW-35917
1955	HW-39558, HW-41315, HW-41500
1956	HW-47500
1957	HW-53500
1958	HW-59500
1959	HW-63824, HW-65500
1960	HW-69500, HW-70050
1961	HW-72500, HW-73337
1962	HW-76000, HW-77609
1963	HW-80500, HW-81746
1964	BNWL-122
1965	BNWL-280, BNWL-235, Vol. 1-4, BNWL-36I
1966	BNWL-480, Vol. 1, BNWL-481, Vol. 2, Pt 1-4
1967	BNWL-714, Vol. 1, BNWL-715, Vol. 2, Pt 1-4
1968	BNWL-1050, Vol. 1, Pt. 1-2, BNWL-1051, Vol. 2, Pt. 1-3
1969	BNWL-1306, Vol. 1, Pt. 1-2, BNWL-1307, Vol. 2, Pt. 1-3
1970	BNWL-1550, Vol. 1, Pt. 1-2, BNWL-1551, Vol. 2, Pt. 1-2
1971	BNWL-1650, Vol. 1, Pt. 1-2, BNWL-1651, Vol. 2, Pt. 1-2
1972	BNWL-1750, Vol. 1, Pt. 1-2, BNWL-1751, Vol. 2, Pt. 1-2
1973	BNWL-1850, Pt. 1-4
1974	BNWL-1950, Pt. 1-4
1975	BNWL-2000, Pt. 1-4
1976	BNWL-2100, Pt. 1-5

FOREWORD

Part 4 of the Pacific Northwest Laboratories' Annual Report for 1977 to the Assistant Secretary for Environment, DOE, includes those programs funded under the title "Physical and Technological Programs." The 189 program studies reports are grouped under the most directly applicable energy technology heading. Each energy technology section is introduced by a divider page which indicates the 189s reported in that section. These reports only briefly indicate progress made during 1977, so for details the reader should contact the principal investigators named or examine the publications cited.

CONTENTS

1.0 COAL

2.0 FISSION

3.0 GEOTHERMAL

4.0 OIL SHALE

5.0 MULTITECHNOLOGY

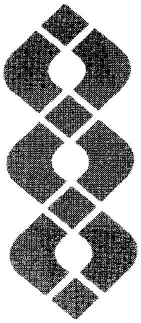

1.0

Coal

COAL

- **Reaction Kinetics of Combustion Processes**
- **In Situ Coal Gasification**

- Bullet Denotes 189 Title

• Reaction Kinetics of Combustion Processes

The goal of the Reaction Kinetics of Combustion Processes is to determine the conditions, mechanism, and chemical reactions which control the identity and concentrations of emissions from coal combustion processes. The first two years of this program have emphasized analysis of fly ash and the development of a model for its formation. The model successfully rationalizes the large enrichment observed for many trace elements in fly ash emitted from coal-fired steam plants. Mass spectrometric techniques have been developed for the study of the high temperature kinetics relevant to coal combustion, with specific emphasis on techniques which will allow investigation of the mechanism and rates of formation for toxic and carcinogenic organic compounds.

Formation of Fly Ash in Coal Combustion

R. D. Smith and J. A. Campbell

It has been established that the smaller flyash particles formed during coal combustion show a significant enrichment of several volatile trace elements. The most reasonable mechanism for trace element enrichment in flyash formation involves the volatilization of these elements during combustion, followed by condensation or adsorption over the available matrix material (composed primarily of the nonvolatile oxides of Al, Mg, and Si). The larger surface-to-volume ratio of the smaller particles leads to a trace element concentration which is inversely related to the particle diameter. We have found flyash surfaces to be enriched in several of the same trace elements, supporting this mechanism. The smaller particles, which show the highest concentrations of several potentially toxic trace metals, are not efficiently collected by pollution control devices. These particles also have the highest atmospheric mobilities and are deposited preferentially in the pulmonary and bronchial regions of the respiratory system.

In the past year we have collected flyash from two coal-fired steam plants for separation into 9 to 17 well-defined size fractions using a Bahco Microparticle Classifier. Separate aliquots of each size fraction were analyzed for 43 major, minor and trace elements by X-ray fluorescence, atomic absorption, and instrumental neutron activation to establish the concentration-particle size dependence for each element. These results show a strong dependence on particle size for a number of elements, as expected for volatilization and subsequent condensation.

A model to semi-quantitatively predict the concentration versus particle size behavior observed in these flyash samples has been developed. The theory divides the trace elements in coal into three fractions: 1) a component which is always volatilized and is primarily associated with the organic matter in coal; 2) a potentially volatile component associated with the mineral matter in coal for which the fraction volatilized is controlled by diffusion-limited processes in the particle; and 3) a nonvolatile component associated with the mineral matter. Experiments are presently in progress which are designed to test the relationship between the organic affinity of trace elements in coal and the enrichment in the smaller flyash particles. Figure 1.1 shows the experimental results obtained for Rb, Mn, As, and Se, and the fit obtained using a simplified version of our volatilization-condensation model. With further theoretical advancement, fueled by experimental developments, we hope to be able to semi-quantitatively predict such concentration profiles given only analyses of the coal (including concentration and organic affinity of each element) and a knowledge of the

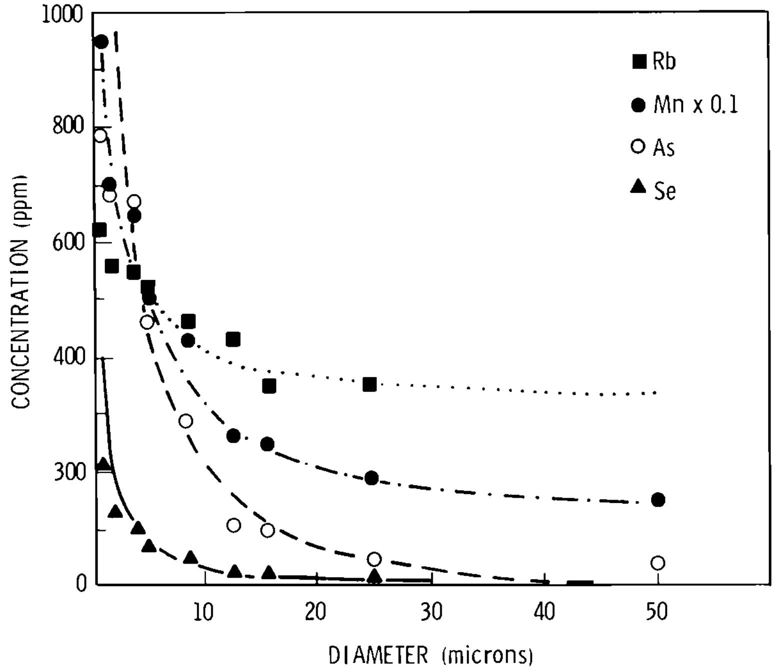

FIGURE 1.1. Concentration of Four Elements in Fly Ash as a Function of Particle Size

operating parameters and time-temperature profile for the coal-fired plant.

Mass Spectrometric Studies of Combustion Related Reactions

R. D. Smith

To understand the complex chemical processes which occur in the combustion and post-combustion region of coal-fired plants, knowledge is required of the rate constants for important unimolecular (pyrolysis), bimolecular, gas-solid, and more complex reactions. In the past year we have developed mass spectrometric techniques to perform experimental measurements for each reaction type.

Unimolecular reactions of important polynuclear aromatic compounds formed in the pyrolysis of coal can be studied using the very low pressure pyrolysis (VLPP) method developed by Benson and coworkers.(1) In these experiments, we use a high temperature Knudsen cell capable of operation up to 3300°K and equipped with a gas inlet. For the study of rapid bimolecular (or more complex) reactions, a flow-tube is interfaced with a modulated molecular beam mass spectrometer. A flow-tube capable of operation at temperatures up to 500°C has been constructed and a second flow-tube furnace for operation up to 2200°C is being constructed.

For high pressure studies, an atmospheric pressure flow-tube (equipped with a movable combustion region) has been constructed and demonstrated. This system allows extraction of material from atmospheric pressure through a water-cooled sampling cone and a series of beam skimmers into the modulated beam mass spectrometer for analysis. Very slow reactions at elevated pressures may also be studied using a static system from which a small sample is continually leaked into the mass spectrometer. This combination of techniques allows the measurement essentially of any rate constant for gas phase reactions. The VLPP method, of course, also allows the study of gas-solid pyrolysis reactions using selected surfaces.

The flexibility of the modulated beam mass spectrometer developed for this work has been shown in other applications. For example, the high temperature Knudsen cell allows the determination of thermodynamic information, as well as identification of species present in the vapors of high temperature systems. We have used this capability to examine the vapors over fly ash in vacuum, under oxidizing and reducing atmospheres, at temperatures up to 1800°C. Other experimental configurations may be readily constructed to meet the needs of each experiment. For example, Figure 1.2 shows how a low temperature (20° to 700°C) arrangement has been used to identify species sublimed

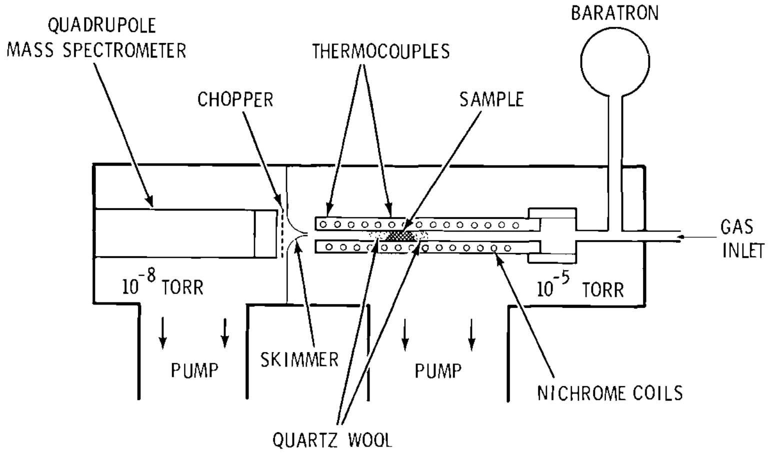

FIGURE 1.2. Experimental Configuration for Flyash Heating Experiments

from fly ash over various inert and reactive gases at pressures of 1 to 10 torr. Figure 1.3 shows the results of such a study for fly ash heated to 500°C in an inert gas (He). These results show that significant quantities of SO_2 and CO_2 are liberated at relatively low temperatures. In addition, a large number of organic species are liberated with a maximum at approximately 350°C. Analyses of the mass spectra show these species to be primarily organic acids. This result is consistent with the reported gaseous emissions of organic acids from coal-fired plants which have been shown to be on the order of 10^2 greater than emissions of polynuclear aromatics.

We are in the process of determining the mechanisms for formation of the organic emissions from coal-fired plants, with particular emphasis on determining the rates for formation and reaction of potentially toxic and carcinogenic organic species.

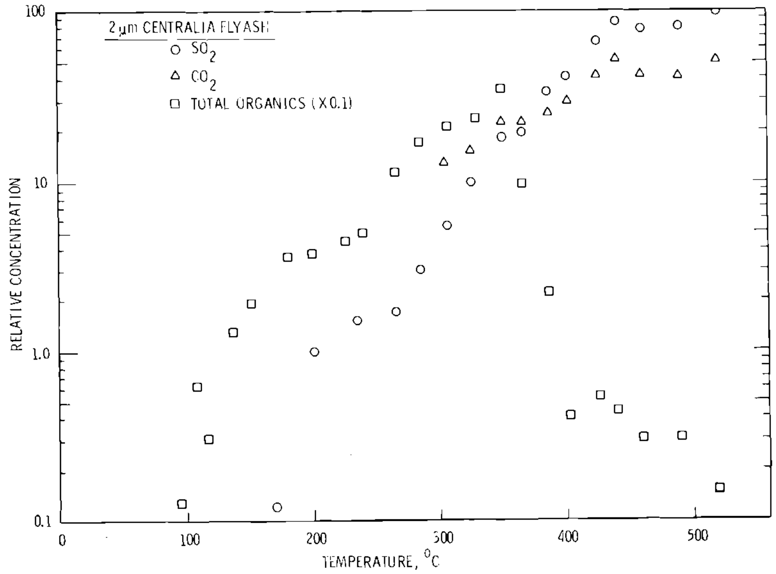

FIGURE 1.3. Relative Concentrations of Species Volatilized from a Sample of Fly Ash

• In Situ Coal Gasification

During the Hanna III in situ coal gasification burn, the raw product gas was analyzed for gaseous inorganic species. Of the elements for which analyses were performed, only arsenic and mercury were detected in the gas phase.

Characterization of Gaseous Effluents From In Situ Coal Gasification

J. A. Campbell and M. R. Petersen

In situ coal gasification looks promising as a means of recovering energy from coal resources without extensive surface disturbances or undue exposure to workers. With this technology, low grade coal or narrow seams could yield energy in the form of low Btu gas.

At the site in Hanna, Wyoming, the process consists of drilling two wells, then firing the seam at the bottom of one well and injecting high pressure air down the neighboring well. The flame front then slowly migrates to the source of air in the injection well. Once link-up has occurred, then gas production begins by forcing large volumes of air underground and recovering the gas flowing from the production well.

A series of 10 sampling runs were made over a one-month period to investigate the volatile inorganic species in the raw product gas. The hot gas (up to 900°F) was drawn off the production well line, filtered to remove entrained particulates, and passed through various impinger solutions. The solutions were analyzed by X-ray fluorescence and atomic absorption spectroscopy for Hg, Pb, Br, Cd, Se, Na, K, Li, and Ce. These elements were below the detection limits ($\sim$10-100 ppb) or near concentrations of the blank during every sampling run. For increased sensitivity, selective absorption traps were used specifically for arsenic and mercury species. The concentration of mercury as the element only was about 1000 ng/ℓ, which is consistent if the mercury in the coal was volatilized during combustion. No arsenic species were detected.

1.0 REFERENCES

1. D. M. Golden, G. N. Spokes and S. W. Benson, "Very Low-Pressure Pyrolysis (VLPP); A Versatile Kinetic Tool." Angew. Chem. Int. Ed. Engl. 12:534, 1973.

2.0
Fission

FISSION

- Radiation Physics
  - Initial Interaction Processes
  - Track Structure
  - Energy Transport
- Radiation Dosimetry and Radiation Biophysics
- Microdosimetry of Internal Sources
- Dosimetry of Internal Emitters
- Real-Time Measurement of Pu in Air at Below-MPC Levels
- Analytical Techniques for Measurement of ^{99}Tc in Environmental Samples
- Radiation Instrumentation—Radiological Chemistry

• Radiation Physics

The Radiation Physics project continues in the investigation of basic mechanisms of energy deposition by fast charged particles and the subsequent transport and degradation of that energy in leading to the formation of chemically active molecular species. Energy deposition is studied through the measurement of interaction cross sections which, when compared to theory, provide insight into the mechanisms of energy deposition in biologically significant matter and which provide the data base required for energy transport studies. Our effort in energy transport and degradation combines the use of Monte Carlo calculations to provide detailed information on the initial formation of the particle track with theoretical investigation of condensed-phase chemical kinetics to provide the link between initial energy deposition and the final observation of chemically active molecular species. Definitive tests of the theoretical results are provided by time-resolved measurements of fluorescence from liquid systems excited by irradiation with pulsed beams of fast charged particles and UV light. Understanding the mechanisms by which energy is deposited and subsequently converted to chemically active species is of direct value in the interpretation of dose-response relationships in terms of quantifiable chemical and physical processes.

Molecular Effects in Ionization by Fast Protons

L. H. Toburen, W. E. Wilson,
L. E. Porter,* and T. L. Criswell**

The effects of radiation on biological matter depend strongly on the manner in which energy is initially deposited by the radiation field. Determination of the probability of interaction and quantity of energy deposited, including the effects of the chemical environment on these interactions, provides insight into the biological effectiveness of radiation. These interaction probabilities are determined from basic interaction cross sections for molecular targets under irradiation by fast charged particles. The charged particles are chosen to be typical of those encountered in irradiated tissue.

The investigation of the effects of molecular structure of electron emission cross sections continues as an important component of our cross section measurements. During the past year, two studies bearing on this problem have been completed. Cross sections for water vapor, molecular oxygen and molecular hydrogen were measured for incident protons in the energy range 0.3 to 1.5 MeV. These results were analyzed in terms of Bragg-rule additivity and were compared for scalability with previous measurements of molecules with constituents of low atomic number. The principal findings of this study were that both additivity and scaling work well within this proton energy range for double differential cross sections for emission of electrons with energies greater than about 100 eV. For lower electron energies, molecular structure plays an important role in establishing the electron energy spectra. Because of the large number of low energy electrons ejected in ionizing collisions, the effects of molecular structure will be important in determining quantities such as total ionization cross sections and W values. Low energy electrons are also known to play an important role in establishing the yield of chemically active species. Our results for proton ionization of H_2O, O_2, and H_2 have been published in J. Chem. Phys. 66, 5202-5213 (1977).

The degree of success in understanding cross sections obtained for molecules of low-Z constituents encouraged us to look for further systematics in complex molecules and those containing high-Z elements. Measurements were conducted for ionization of SF_6 and TeF_6 molecules by protons in the energy range 0.3 to 1.8 MeV. Again, molecular structure effects were observed in the low energy portion of the ejected electron energy spectra. Autoionization was observed at electron energies less than 10 eV and attributed to excitation of electrons from "inner well" states to continuum states which subsequently autoionize. Attempts to scale cross sections in the manner found successful for less complex low-Z molecules failed. Within the proton energy range studied, the probability for ejecting electrons from the various inner shells is strongly dependent on proton energy which renders derivation of a simple scaling parameter impractical. Any requirement of differential ionization cross sections for molecules involving high-Z atoms will continue to require specific measurements until a sufficient data base has been generated to derive the systematics needed to determine appropriate scaling parameters. A paper presenting this study in detail has recently been published in Journal of Chemical Physics, 67:4212-4221 (1977).

The Radiation Physics project has also progressed in the study of ionization by heavy ions and by low energy protons. A study of the ionization of argon by 5-50 keV protons was completed and published in Phys. Rev. A 16, 508 (1977). In addition to accumulation of data for 5 to 50 keV proton on molecular nitrogen, we have initial data

---

*Dept. of Physics, University of Montana, Missoula, Montana 59812.

**Temporary assignment. Permanent address: Bevatron Group, Lawrence Berkeley Laboratory, Berkeley, California 94720.

on molecular oxygen and molecular hydrogen. We intend to investigate water vapor soon. These low energy data are important in providing a complete picture of the proton track as the particle stops.

Systematics in Electron Energy Spectra Resulting from Proton Impact Ionization

L. H. Toburen and S. T. Manson*

Several years ago, Y.-K. Kim demonstrated a method based on simple theoretical techniques of extrapolating and/or interpolating differential cross sections into regions where measurements were nonexistent.(1-3) Although the model was originally tested for ionization by electron impact, in principle, the theory applies equally well for protons of sufficiently high velocities.

During the past year, an extensive investigation of proton ionization of He, Ne, and Ar was undertaken in collaboration with Y. -K. Kim of Argonne National Laboratory and S. T. Manson of Georgia State University, to determine the applicability of this theoretical model for proton impact. Both experimental and theoretical cross sections were studied using the theoretical analysis proposed by Kim. Our findings show that Kim's technqiue is very useful for proton energies above a few MeV. Below 1 MeV, the proton velocity is too low for the simple theoretical analysis used in this analysis to be valid. Even at high energies, the model must be used with care when atoms, or molecules, containing multiple inner shells are concerned. The details of this study have recently been submitted for publication in the Physical Review A. See also contribution to X ICPEAC, Abstracts of Papers, edited by M. Barat and J. Reinhardt (Commissariat A'l'Energy Atomique, Paris, 1977), p. 988-989, 990-991.

Ionization by Helium Ions and Alpha Particles

L. H. Toburen, J. H. Miller, R. J. Popowich,** and W. E. Wilson

An extensive investigation of ionization by alpha particles and singly charged helium ions was initiated during the past year. This work was given high priority because of the importance of understanding energy deposition by alpha particles associated with the decay of elements such as plutonium which may be encountered as airborne contamination at various stages of the nuclear reactor fuel cycle. Of particular interest is determination of the range of applicability of Z^2 scaling for alpha particle cross sections and investigation of the effects of screening by the bound electron for He^+ cross sections. Also of importance are the atomic and molecular effects associated with the target.

Measurements now have been completed for incident He^+ and He^{++} ion energies of 0.3, 0.8, 1.2, 1.6, and 2.0 MeV/amu on targets of water vapor and argon. Preliminary results of these measurements were presented at the Radiation Research Society meeting -- see Radiation Research 70, 618 (1977) and BNWL-SA-6216. For the most part, differential ionization cross sections for alpha particles readily scale by Z^2 from measured proton cross sections when the projectile velocities are equal. Differences do exist, however, for low energy ejected electrons. It should also be noted that the lowest alpha particle energy considered in this comparison was 1.2 MeV because proton data are not available at equivalent velocities for lower energies.

The results shown in Figure 2.1 represent the difference between alpha particle results and scaled ($Z^2=4$) proton cross sections for ionization of argon by 0.3 and 0.5 MeV/amu particles. The dashed and solid line represented expected Z^3 contributions for projectile energies of 0.3 and 0.5 MeV/amu, respectively, based on higher order Born terms using the model of Ashley, et al.(4) Although this theory is in excellent agreement for energy loss between 4 and 8 Ry where small variations from Z^2 scaling are observed, large discrepancies exist for smaller energy loss where the differences from Z^2 scaling are largest and the Z^3 correction appears to have the wrong sign.

It should be noted that some uncertainty in the low energy electron measurement is to be expected based on instrumental difficulties, but one would not expect the uncertainties to be large enough to encompass the large differences observed in Figure 2.1. Variations from Z^2 scaling observed for energy loss in the range 10 to 17 Ry are attributed to two factors. First, for 0.3 MeV/amu ions, charge transfer to the continuum is expected to enhance the alpha particle spectrum over the proton results. This is based on discussions with A. Salin (Laboratory d'Astrophysique, Talenc, France), whose calculations indicate that continuum charge transfer should depend on Z^3. Second, the region around 15 Ry is dominated by Auger transitions (LMM Auger transitions in argon) and these transitions have

---

*Consultant, Dept. of Physics, Georgia State University, Atlanta, Georgia.

**Graduate student, University of Washington.

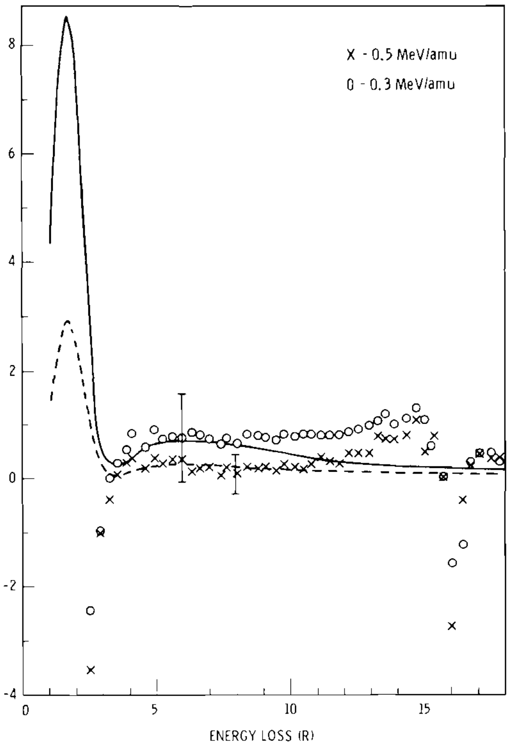

FIGURE 2.1. The Difference Between $\sigma(\epsilon)$ Measured for Alpha Particles and 4 $\sigma(\epsilon)$ Measured for Equal Velocity Protons. The Solid and Dashed Lines Represent Z^3 Corrections to the Born Calculation of $\sigma(\epsilon)$ Calculated According to the Theory of Ashley, et al (Ref.4) for Particle Energies of 0.3 and 0.5 MeV/amu, Respectively

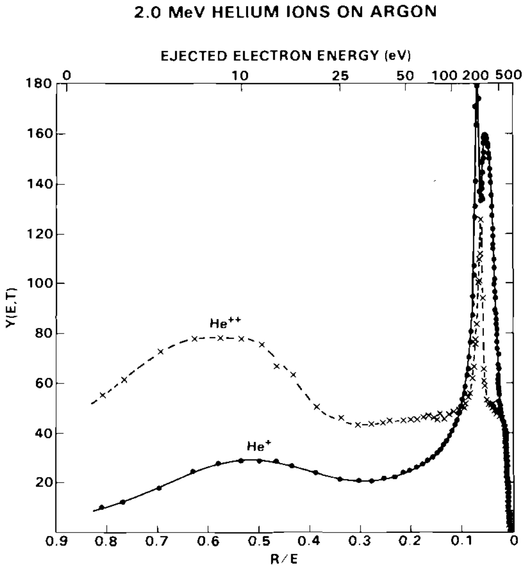

FIGURE 2.2. The Ratio of Measured Electron Energy Spectra $\sigma(\epsilon)$ to the Corresponding Rutherford Cross Section for 2 MeV Helium Ions Plotted Against the Reciprocal of the Energy Loss

previously been shown to deviate from Z^2 scaling.(5) Details of our analysis of the Z^3 effect have been published in the Physical Review A 16:2478-2479 (1977).

Because an alpha particle undergoes charge changing collisions as it slows, it is important to determine the effect that electron capture has on the subsequent secondary electron yield and spectral shape. An example of the effect of the bound electron is shown in Figure 2.2 where the electron ejection cross sections are compared for 2.0 MeV He^+ and He^{++} ionization of argon. The quantity Y(E,T) plotted in Figure 2.2 is simply the ratio of measured cross sections to the corresponding Rutherford cross section per target electron. Plotted in the manner of Figure 2.2, equal areas under the curve contribute equally to the total ionization cross sections, and the relative importance of electrons of various energies can be assessed. Note that screening by the electron bound to He^+ reduces the yield of slow electrons by as much as a factor of 4 relative to the corresponding He^{++} spectra. At high energies of ejected electrons, He^+ and He^{++} give nearly identical results. The broad peak (in addition to the Auger peak at 200 eV) at about 300 eV is due to stripping of the bound electron from the He^+ ion. An important radiological result derived from these measurements is that the mean energy of electrons ejected in ionizing collisions by He^+ can be much greater than that for alpha particles. Since any reliable model of track structure or dosimetric calculation must include the probability for charge transfer as alpha particles slow down, the widely varying secondary electron distributions for differing charge states of the ions must be known if the radiation effects of alpha particles are to be understood.

Analytical Expression for Cross Section Data

W. E. Wilson

The spatial distribution of energy along a charged particle track determines the subsequent chemical kinetics. Since energy transport via electron collisions occurs in an extremely short time (10^{-15}-10^{-12} sec), one cannot follow track evolution experimentally. To obtain detailed information regarding the spatial distribution of energy deposited near a particle track, one must resort to calculational techniques. Monte Carlo codes are particularly well suited for these calculations.

Detailed information regarding charged particle track structure requires extensive use of experimental input data. Of particular importance are accurate cross sections for the energy and angular dependence of secondary electrons. Experimental results in the form of cross sections, however, require too much computer memory to be used efficiently in tabular form. For the most efficient use, the cross sections need to be represented in some simple analytic form.

In order to provide such an analytical representation of the initial proton ionization process for our track structure calculations, we have developed a semi-empirical phenomenological model of the double differential cross sections (DDCS) for electron ejection from poly-atomic molecules. Inasmuch as tissue is composed of 85% water, we have based our model on the DDCS for that molecule. The basic approach used has been previously described;(6) therefore, only the improvements will be discussed here.

The DDCS for a given proton energy E_p, electron energy ε, and electron emission angle θ, are first scaled according to the following expression:

$$Y(\varepsilon,\theta) = \frac{4T^3[(\varepsilon+I_p)/4T]^2}{\pi a_0^2 R^2 N_e}\,\sigma(\varepsilon,\theta) \qquad (1)$$

where R is the Rydberg unit of energy (13.606 eV), a_0 is the Bohr radius, I_p is the first ionization potential of the target molecule (12.6 eV for H_2O), T is the kinetic energy of an electron having velocity equal to that of the proton of energy E_p, and N_e is the number of weakly bound electrons in the molecule (N_e=8 for H_2O).

For a given secondary electron energy ε, the resulting angular distributions, $Y(\varepsilon,\theta)$, are fitted in the least-squares sense with the nonlinear expression,

$$Y(\varepsilon,\theta) = A_1 e^{-Z(\theta)} + A_4 + A_5/K(\theta) \qquad (2)$$

where

$$Z(\theta) = [(\cos(\theta) - A_3)/A_2]^2 \qquad (3)$$

and

$$K(\theta) = \sqrt{\frac{M_e}{2}\,[v_p^2 + v_e^2 - 2v_p v_e \cos(\theta)]^{1/2}} \qquad (4)$$

where v_p and v_e are the velocities of the proton and electron, respectively, and the A_i are adjustable fitting parameters which contain the ε and E_p dependence of Y. Fitting the angular distributions over the range of values of ε gives the dependence of each A_i on ε.

The parameterization of coefficients A_1-A_5 in Equations (2) and (3) have been discussed before.(6) Previously, A_1 required two different representations, each valid in a different region of electron energy ε. We have discovered a single parameterization of the coefficient A_1 that is sufficiently accurate over the whole range of energy loss. This expression, derived from fitting techniques of Daniel and Wood,(7) is

$$A_1 = a\,x^b\,e^{cx} \qquad (5)$$

where x is energy loss in units of 4T, and a, b, and c are adjustable parameters containing the dependence on E_p. It was assumed that a, b, and c depend linearly on E_p since the proton energy range covered is small. Under this assumption, Equation (5) then becomes the algorithm for A_1 and is compared in Figure 2.3 with the coefficients obtained from least-squares fitting the angular distribution.

Coefficients A_4 and A_5 obtained by fitting the angular distributions are less well behaved in their dependence on energy loss and proton energy; however, the DDCS are not strongly dependent on them. Therefore, the assumption that A_4 and A_5 depend logarithmically on x was made resulting in

$$A_4 = a + b \log x, \qquad (6)$$

and with a similar expression for A_5. In these expressions, a and b are linear functions of E_p.

Using the parameterization described here coupled with that presented previously(6) for the five coefficients as functions of the energy loss and proton energies, an analytical expression has been constructed which is being used to simulate the DDCS in track structure calculations for ion energies less than about 2 MeV/amu. As it presently is developed, the model returns accurate cross sections for proton energies from 0.3 to 1.5 MeV where fits to experimental data were possible. Extension of the phenomenological model to higher ion energies will necessarily rely on theoretical calculations and/or experimental data for molecules other than water vapor.

Primary Ionization Source Term for Track Structure Calculations

W. E. Wilson

The development of an analytical representation of experimental cross sections discussed in the preceding report was necessary for efficient utilization of experimental cross section data. The model returns cross sections which now must be converted to probabilities which are compatible with the Monte Carlo code. Our first efforts in this direction have been to use the phenomenological model to provide an algorithm for selecting the emission angle for the secondary electron from primary ionization.

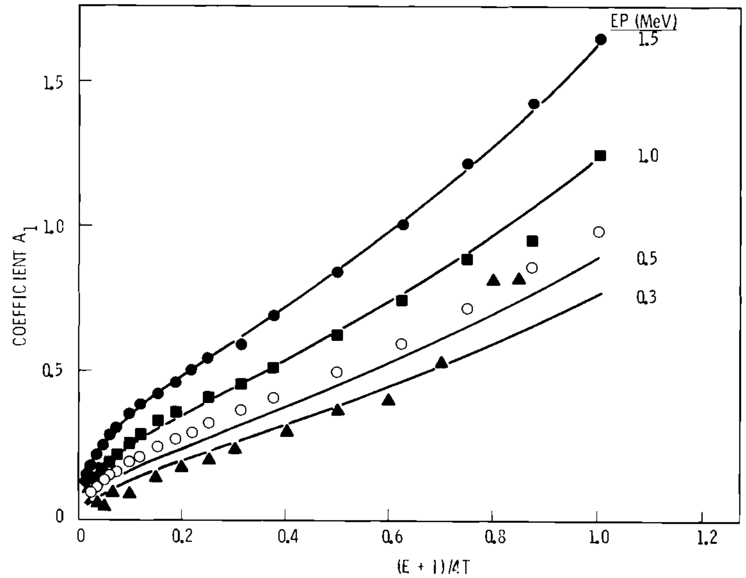

FIGURE 2.3. Coefficient A_1 as a Function of Energy Loss. Data Points Indicate the Results of Least-Squares Fitting Eq. (2) to the Experimental Angular Distributions. Solid Lines Indicate the Result of the Phenomenological Algorithm for A_1, Including an Assumed Linear Dependence on E_p for the Coefficients in Eq. (5)

To put the DDCS into a practical form for use in Monte Carlo calculations, the following integral equation is inverted to provide cos θ as the dependent variable:

$$P(\cos\theta,\varepsilon) = \int_{+1}^{\cos\theta} \sigma(\varepsilon,\theta)\, d\Omega \Bigg/ \int_{+1}^{-1} \sigma(\varepsilon,\theta)\, d\Omega \qquad (7)$$

A linear interpolation scheme for inverting Equation (7) is sufficiently accurate since the analytical representation for $\sigma(\varepsilon,\theta)$ allows one to obtain $P(\cos\theta,\varepsilon)$ at arbitrarily close spaced intervals. Inversion of Equation (7) provides a table of cos(θ) as a function of probability at uniformly spaced probability intervals. The computer generation of a random number determines a specific cosine value from the table.

Several typical tables of cosine values for different secondary electron energies generated with the model are shown in Figure 2.4 for 1 MeV/amu protons. By combining this table with a preselected electron energy, the ejection angle (cosine of the angle) is obtained from a random number generated by the code. We are presently studying the results of implementing this change in the Monte Carlo code and incorporating the model for the determination of electron energy as well as emission angle.

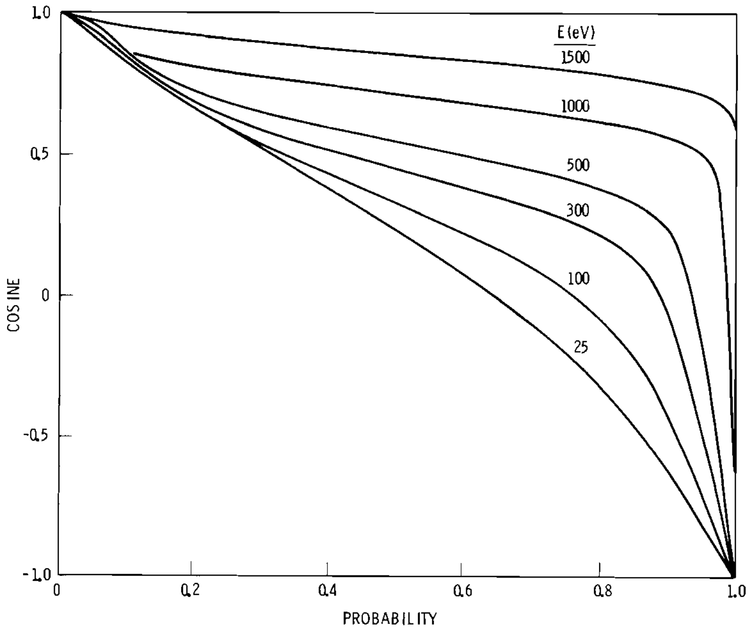

FIGURE 2.4. Cosine of Emission Angle for Ejection of Secondary Electrons with Energy ε by 1 MeV/amu Protons

Track Structure Effects in Radiation Chemistry

J. H. Miller and M. L. West

The spatial distribution of absorbed dose influences the yield of chemically active species in a medium exposed to radiation. Through the study of nonhomogeneous kinetics of radiation chemistry in simple liquid systems, we will gain insight into the chemical bases for radiation quality factors such as Relative Biological Effectiveness (RBE) and Oxygen Enhancement Ratio (OER). This insight contributes to the scientific basis for radiation protection standards and to the effective use of radiation in medical applications.

The diffusive motion of molecules rapidly destroys the initial distribution of primary species in most liquids. Hence, stroboscopic techniques must be used to directly observe the effects of nonhomogeneous chemical kinetics. Pulsed radiolysis with electrons has been used extensively to probe the subnanosecond time region. However, the application of this method to other types of radiation, in particular, radiations with high linear energy transfer (LET) is limited by the requirement of large dose per pulse to achieve a significant absorption signal for the chemical species under investigation.

The use of fluorescence, rather than absorption, to detect the presence of chemical species circumvents this difficulty. By time-resolve, emission spectroscopy, the evolution of a small population of excited states can be studied under varied radiation conditions with subnanosecond time resolution. Through fluorescence quenching, the time evolution of the concentration of nonradiative species can also be investigated.

Figure 2.5 compares time-resolved emission from benzene in cyclohexane excited by pulsed proton irradiation at three proton energies with the fluorescence decay observed using ultraviolet (UV) irradiation. The nonexponential character of the fluorescence decay with proton irradiation results from a time dependent concentration of quenching species not present under UV excitation. We have published a detailed analysis of this effect in J. Chem. Phys. 67, 2793 (1977). The time dependence of the quencher concentration can be explained by the diffusion of chemical species out of the region of initial energy deposition. The initial concentration of the quenching species is proportional to the LET of the radiation. Hence, more quenching is observed as the energy of proton irradiation decreases.

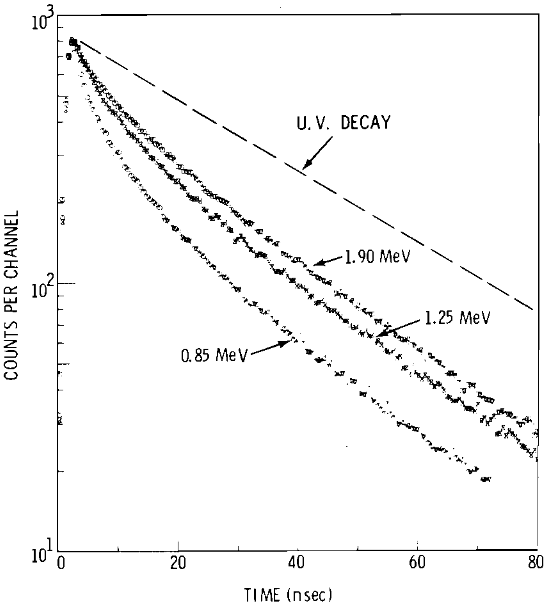

FIGURE 2.5. Time-Resolved Singlet Emission from Benzene in Cylohexane Excited by Pulsed Proton and Ultraviolet Irradiation

Analysis of the energy dependence of the fluorescence decay in terms of the LET of the radiation ignores the radial distribution of the initial energy deposition. This is a good approximation over the range of projectile energies achievable with the 2 MV accelerator; however, with more energic heavy ions, transport of energy away from the track core by secondary electrons results in a more diffuse pattern of energy deposition at equal values of LET. This difference in radial distribution of absorbed dose modifies the RBE of the radiation.

A model is being developed to estimate the effect of the radial distribution of absorbed dose on the decay of fluorescence induced by protons and alpha particles of the same LET. The model is based on the assumption that excited states and quenchers are formed in spurs centered about the initial sites of ionization of the medium. The distribution of chemical species within each spur is assumed to be Gaussian with a variance $\sigma^2(t) = r_0^2 + 2Dt$, where r_0 is the initial spur radius and D is the diffusion coefficient of quenchers and excited states. The model predicts a fluorescence decay of the form

$$-\frac{1}{N_\star}\frac{dN_\star}{dt} = k_{uv} + k_{spur}\,(1 + \langle g(\vec{r};t)\rangle) \qquad (8)$$

where k_{uv} is the quenching rate observed with UV irradiation, k_{spur} is the rate of quenching in isolated spurs, and

$$g(\vec{r};t) = \sum_{\vec{r}_j \neq \vec{r}} \exp\,(-(\vec{r}-\vec{r}_j)^2/4\sigma^2(t)) \qquad (9)$$

is the probability that an excited state at position $\vec{r}$ will be quenched by chemical species from other sites of ionization. We call this the "spur overlap."

The goal of our model calculations is to evaluate the expectation value of the spur overlap by Monte Carlo track simulation and to study its relationship to the radial distribution of absorbed dose. When radial dispersion of the ionizations is ignored, the mean spur overlap is $2\pi^{1/2}\sigma S/W$, where S is the projectile stopping power and W is the mean energy absorbed per ionization. Preliminary Monte Carlo results show that this is a good approximation when the spur radius is much greater than the track core radius.(8) If the spur radius is comparable to the track core radius, the mean spur overlap is significantly smaller due to the contribution from ionization outside of the track core. Calculations of the expected fluorescence decay with energetic alpha particles are in progress. The model calculations will then be tested against measurements of the time-resolved emission induced by alpha irradiation from the accelerator facilities at the University of Washington Nuclear Physics Laboratory.

Temperature Studies

M. L. West and J. H. Miller

In a recent publication,(9) we attributed proton-induced fluorescence decay to dynamic quenching from a time dependent concentration of radiation produced radicals. In addition, there is quenching by intramolecular processes thermally activated through solvent perturbation. A study of the temperature dependence of radioluminescence provides additional information about the dynamic quenching and thermally activated processes. Results of this study have been recently submitted for publication in J. Phys. Chem.

Dilute solutions of benzene in cyclohexane were irradiated with subnanosecond pulses of protons and changes in the time-resolved emission were studied as a function of solvent temperature. These data were compared to our model which predicts a time dependence for proton-induced fluorescence of the form

$$I(t) = I_0 \exp\,(-kt - \alpha \ln\,(1 + t/t_0)) \qquad (10)$$

where k is the decay rate observed for ultraviolet excitation, α is the ratio of the interaction radius for quenching by radicals to the mean number of radicals per unit track length, and t_0 is the time required to reduce the concentration of radicals to one-half its initial value due to diffusion. Estimates of the parameters k, α, and t_0 were obtained at each temperature by fitting the proton-induced fluorescence decay. The results are shown in Table 2.1. The asymptotic decay rate k obtained at each temperature from these proton data agrees well with the decay that was measured using ultraviolet excitation. Estimates of the parameters α and t_0 which characterize the intratrack quenching do not exhibit any systematic temperature variation when the experimental uncertainties are considered. This suggests that the principal temperature dependence of the proton-induced fluorescence is from thermally activated intramolecular quenching. Quenching by radicals formed in the proton track is approximately independent of temperature over the range investigated.

The absence of a temperature variation in α supports the conclusions that radicals quench excited states on every encounter and

TABLE 2.1 Parameters of the Intra-Track Quenching Model[a]

T(°K)	k(10^7 sec^{-1})	α	t_0 (10^{-9} sec)
288	2.7	.34	3.0
290	2.8	.35	3.1
292	3.0	.34	2.7
294	3.2	.35	3.1
296	3.4	.36	3.2
300	3.8	.33	2.7
306	4.5	.34	2.8
308	4.5	.36	3.3
313	5.4	.38	3.5

(a)Defined by Eq. (10) of text.

that this interaction does not require thermal activation. The principal temperature dependence of t_0 is embodied in the diffusion rate of radicals. If this diffusion rate obeys the Stokes-Einstein relation(10) we expect t_0 to change by a factor of 2 over the temperature range studied, decreasing as the temperature increases. The absence of such a temperature variation may suggest that the initial track radius increases more rapidly with temperature than predicted through change in solvent density. We hesitate to draw this conclusion, however, until more reliable estimates of t_0 can be determined. Reliable estimates of t_0 require a detailed investigation of the first 5 nsec of fluorescence response and this will require improved time resolution. Work in this direction is currently in progress. The effects on estimates of t_0 of finite formation times of excited states and of time dependence in the quenching rate constant are also being investigated.

Data for the experimental investigation of temperature dependence of fluorescence decay discussed above were taken with a detection system limited by photomultiplier response to about 1.5 nsec FWHM. Reliable estimates of t_0 require a better time resolution and additional information about the system response. We have just recently achieved a time resolution of 0.7 nsec FWHM by using improved electronics and a new phototube of reduced background, less time jitter, and minimized afterpulsing. The absence of afterpulsing has resulted in a more symmetric time response and has lead to successful unfolding of the system time resolution function from measured fluorescence decay. Rapid fluorescence decay of the 3914 Å line of N_2^+ is used for the resolution measurements. At atmospheric pressure, this state exhibits exponential decay with a lifetime of about 100 psec. All experimental parameters including beam optics, electronic timing and phototube operating characteristics have been optimized for maximum performance. Preliminary data taken with this new timing system for proton-induced fluorescence indicates that our earlier estimates of t_0 may be too large. A complete temperature study with this new detection system is in progress.

• Radiation Dosimetry and Radiation Biophysics

The joint purpose of these two closely integrated programs is to explore the connections between the primary physical events produced by radiation and their biological consequences in cellular systems. The radiation dosimetry program includes theoretical description of the primary events and their connection with the observable effects and experimental realization and measurement of the physical parameters needed by the theory. The radiation biophysics program tests or makes use of the theoretical developments and gathers information needed for the theories by experiments on cellular systems. This year several different studies converged and led to finding in *Chlamydomonas reinhardi* and in mammalian cells a recovery process faster than the well-known Elkind-Sutton effect. Experimental and theoretical studies of the process are still going on. Early theoretical results indicate it may have a great influence on how laboratory data are extrapolated to the low doses and dose rates relevant in radiation protection. Identification of the effect is permitting interpretation of our results on the change in radiation killing with temperature and on the absence of pool effects on recovery. Development of synchronous, stationary populations of CHO cells for long-period dose-rate and split-dose experiments has begun.

Dose-Rate and Fractionation Theory for Multiple Recovery Processes

W. C. Roesch

X rays, gamma rays, and fast electrons are major concerns in the protection of workers and the public from the effects of energy generation by either fission or fusion. Experiments with them at the low doses and dose rates relevant to protection would require such large animal populations that they are impractical. Consequently, the theory of the phenomena they produce at higher doses and rates is important because it enables confident extrapolation to low doses and rates. We have studied how changes in dose rate and dose fractionation affect this extrapolation because of a recovery process discovered by Elkind and Sutton.(11) Our studies have now led us to find evidence for another recovery process, one that proceeds faster than the Elkind-Sutton process. Analysis of the new process suggests that it too will strongly influence how we extrapolate experimental data to estimate radiation hazards.

Our interest in other kinds of recovery began several years ago. From theoretical studies of LET effects(12) we deduced a recovery might be found in synchronized mitotic cells. An increase in RBE with increasing LET would have signaled the presence of such a process. Such data were not available so we proposed the necessary experiment. But recently, with the help of W. K. Sinclair of Argonne National Laboratory, we found related evidence that indicates the fast recovery may be present in mitosis.

In unsynchronized cells the assumed fast recovery would be present with the Elkind-Sutton recovery. This led us to extend our modeling to multiple recovery processes. Our earlier model (see "Hit Theory for Low-LET Radiation," *Rad. Res.* *51*:480, 1972) had radiation produce a single kind of product subject to recovery; death resulted from interaction of two of the damaged entities. To contrast with the models below, we now call this the One-Product Model. Two kinds of recovery can appear in at least the following three ways:

- Two-Mode Model -- radiation kills in two stochastically independent One-Product-Model ways,

- Two-Product Model -- radiation produces two kinds of products, each subject to recovery at its own rate; death results from interaction between one each of the two products, and

- Two-Step Kinetic Model -- radiation produces two kinds of products; one kind must undergo a biochemical transformation to become active; death results from interaction between one of these activated products and one of the other kind of direct product.

Combinations of these and the One-Product Model give rise to models with three or more recovery processes.

Formulas for the survival in single and split-dose irradiations were derived for the three models. Figure 2.6 shows -ln(S)/D curves calculated for them. Part A is for a Two-Mode Model. At very high dose rates, -ln(S)/D is a straight line; at intermediate rates, it becomes straight after some initial curvature and is lower than at high rates; at low rates, it is horizontal over most of its length and is lower still. Part A also serves for the Two-Product Model if the slope approached at the intermediate rates is one-half the slope at high rates. Part B is for a Two-Step Kinetic Model. At very high dose rates, -ln(S)/D is a curve and is lower than for some lower rates. In other words, in this dose-rate range survival increases with increasing dose rate, the reverse of what is ordinarily expected. At intermediate rates, -ln(S)/D is nearly a straight line; and at low rates it is mostly horizontal.

These models were compared with the few very high dose-rate survival curves in the literature. Most of the data are for HeLa cells and gave nothing interpretable in terms of the models. On the other hand, Todd et al.(13) used T_1 cells and obtained two curves like 1 and 2 in Figure 2.6.A. The slope of curve 2 was close to one-half that of curve 1. Concluding that T_1 cells behave like the Two-Product Model is not yet safe, however, because no experimental points were obtained in the curving part at low doses. I estimated the mean recovery time for the fast process to be 2 min.

Our first report (W. C. Roesch, "Models of the Radiation Sensitivity of Mammalian Cells")(14) on the above models had just been submitted when Malcolm and Little(15) reported to the Radiation Research Society that split-dose experiments with plateau-phase V79 and 10T1/2 cells showed fast recovery with half times from 2 to 5 min in addition to the normal Elkind-Sutton process.

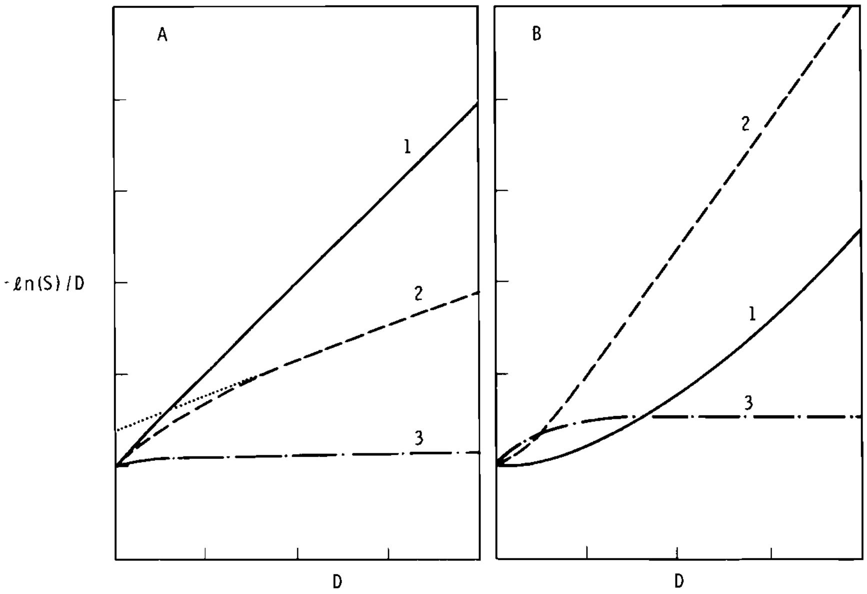

FIGURE 2.6. -ln(S)/D Curves for: (A) the Two-Mode Model (and the Two-Product Model, in some Circumstances), and (B) the Two-Step Kinetic Model. Curves 1 are for Very High Dose Rates, 2 for Intermediate Dose Rates, and 3 for Very Low Dose Rates

A reversed dose-rate effect such as shown in Figure 2.6.B appeared in the data of Ben Hur et al.(16) for V79 cells at a very high temperature, 42°C. This could be the effect of a recovery process that is so fast at ordinary temperatures as to have escaped observation but that is slowed down at high temperatures. Their result led us to extend our split-dose experiments with *C. reinhardi*(17) to higher temperatures and shorter interfraction times. We found that *C. reinhardi* does have a fast recovery in addition to the slow recovery we have been studying, and in the next article we will describe our first measurements of it.

The presence of two (or more) recovery processes may have important consequences on how we extrapolate laboratory data to low doses and dose rates to choose radiation protection limits. Typical data, on -ln(S)/D plots such as in Figure 2.6, intercept the vertical axis at a non-zero value, the proper sensitivity to use at low doses. This intercept is interpreted as due to killing by single charged-particle events and, therefore, as being independent of dose rate. Curve 2 in Figure 2.6.A is a typical result for ordinary laboratory dose rates for two recovery processes. Further, data on the curving portion at low doses may be missing because the survival is high and measurements consequently difficult. Then the investigator would probably extrapolate along the dotted line in the figure to an intercept that is higher than the true value. Indeed, the data of Todd et al. for T_1 suggest that the true intercept may be nearly zero, that there may be no true single-event lethal process. (But, some killing by single events will probably always occur. The different products in the models above can both be produced in a single event as well as in separate events.) In other words, the presence of an unsuspected fast recovery process can lead an observer to overestimate his system's low-dose sensitivity. Also, his estimate would depend on the dose rate and different observers might disagree without recognizing different rates as the cause.

Fast Recovery in Chlamydomonas Reinhardi

J. M. Nelson, L. A. Braby, and W. C. Roesch

During the study of how temperature influences radiation killing in *C. reinhardi* described in the next article, we had difficulty analyzing data at temperatures above 25°C. In the split-dose plot ($\ln(S_m/S)$ vs t; t = interfraction time, S = survival, S_m = survival for large t), the point for zero interfraction time was always higher than expected and points for small (3 min or less) times were also consistently high. At about this time, the development of the fast recovery concept described in the last article was going on. We hypothesized our difficulties might stem from a fast recovery process rather than to lack of heat tolerance of the cells. To test the hypothesis, we changed our irradiation technique to employ a dose rate of 10^5 rad/min and repeated the split-dose measurements, adding interfraction times of 0.25 to 5 min. They did show a fast recovery process was present.

The upper part of Figure 2.7 shows a typical result. For interfraction times greater than 5 min, the points define a straight line whose slope gives a (slow) recovery time of 23 min, which is consistent with our measurements at lower temperatures. Below 5 min, the points all lie above this line. Subtracting the values of the slow-recovery line from the data points gives the plot in the lower part of the figure. We have interpreted them as another straight line due to a fast recovery process with a mean recovery time of about 1 min.

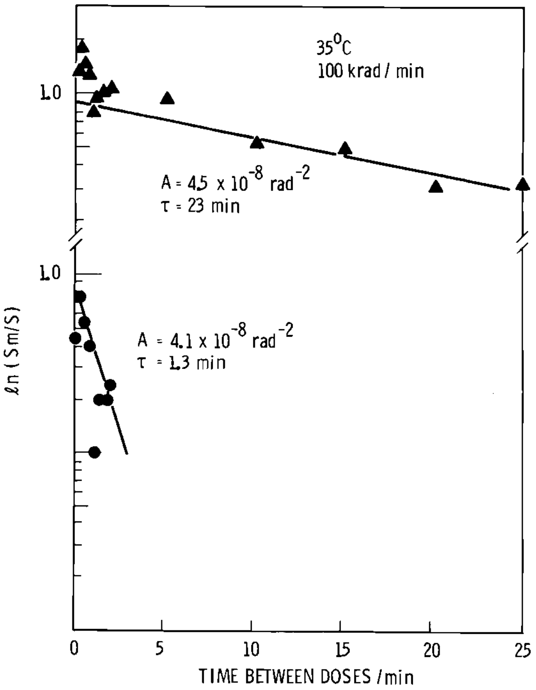

FIGURE 2.7. A Typical Split-Dose Experiment with *C. Reinhardi*

Similar curves were obtained for temperatures from 25°C to 37°C giving fast recovery times from 1 to 3 min. The points are scattered with no pattern discernible through the errors; but a pattern presumably exists, because the effect disappears below 25°C.

The data in Figure 2.7 are compatible with either a Two-Mode Model or a Two-Product Model. Indeed, the method of analysis just described was based on the models. A Two-Step Kinetic Model would have had the points for small times below the slow-recovery line instead of above. The intercepts of the two recovery lines on the vertical axis are about equal. They must be equal for a Two-Product Model; they may be for a Two-Mode Model.

Inactiviation and Recovery in Chlamydomonas Reinhardi as a Function of Temperature

L. A. Braby, J. M. Nelson, and W. C. Roesch

Last year(17) we began to measure how temperature influences radiation killing of C. reinhardi. The aim was to be able to correct laboratory measurements and to obtain thermodynamic data that might shed light on how the cell reacts to radiation. We found we could separate changes in recovery rate from changes in radiosensitivity. The recovery is an enzymatic process. The lethal action is in competition with some other process. This work was set aside while investigating the fast recovery reported above and a possible correction that had been suggested to us (see next article), since both might have influenced our conclusions. These investigations gave us more data and confirmed the earlier results.

Figure 2.8 shows the Arrhenius plot of the slow recovery time for temperatures below 25°C where the fast recovery does not interfere. The Xs are last year's data, obtained at 5 krad/min; the Os this year's, at 100 krad/min. They agree within the accuracy of the experiment and give an activation energy of 19 kcal/mole. This happens to agree with the 19.1 kcal/mole Donlon and Norman(18) measured for the rejoining of single-strand breaks in human lymphocyte DNA. It makes attractive the hypothesis that single-strand breaks are the major sublethal damage in C. reinhardi. But the activation energy for rejoining has not been measured in C. reinhardi and other processes may give deceptively similar values; therefore, it remains only a hypothesis for now.

Figure 2.9 shows the two-event factor, a measure of radiosensitivity. The new data agree with the old. We still look on these results as indicating the presence of a process competing with lethality and deduce the activation energies of the two must differ by 5 kcal/mole.

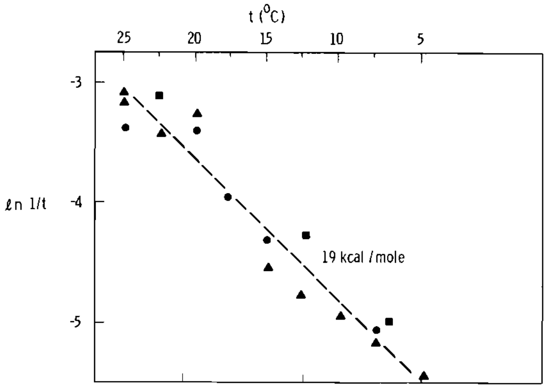

FIGURE 2.8. Arrhenius Plot of the Mean Recovery Times Measured for C. *Reinhardi.* X, 5 krad/min, and ●, 100 krad/min, by the Dose-Rate Method; ■, by the Split-Dose Method

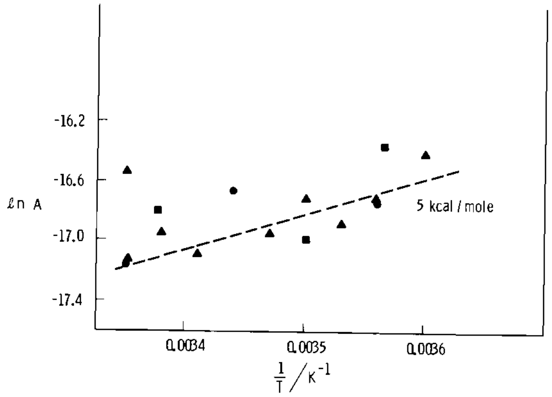

FIGURE 2.9. Two-Event Factor; Same as Figure 2.8

Reduced Radiation Sensitivity After Recovery from Sublethal Damage

L. A. Braby and W. C. Roesch

On hearing of our studies with C. reinhardi (preceding article), P. E. Bryant of London's Hammersmith Hospital warned that an increased radioresistance he had observed after times following a first dose of radiation long enough to permit recovery from sublethal damage might be interfering with our split-dose measurements. We confirmed his findings but concluded the increased resistance has a negligible effect on our results.

Following Bryant, we gave cells a dose sufficient to kill 90% of them. Two hours later we determined a survival curve for the survivors of the first dose. The survivors had a 40% lower two-event factor. For a conditioning dose equal to the first dose in our split-dose experiments, enough to kill about 50% of the cells, the two-event factor was reduced only 20% at 25°C but the reduction increased to 40% at 30°C.

To determine the effect of the increased resistance on our measurements, we calculated the split-dose $\ln(S_m/S)$ curve for a Two-Product Model having mean recovery times of 2 and 25 min and allowing for a change in two-event factor of the size reported above. Calculations were made both for linear and exponential changes in the factor with time. The heavy line in Figure 2.10 is a typical result. The Bryant effect does not affect the fast-recovery part of the curve. At longer times the curve has a greater slope than in the absence of the change in the factor (light line): the slope (dashed line) gives a recovery time of 20 min instead of 25 min. At much longer times the curve abruptly breaks away. We have observed the break at temperatures above 25°C but not at lower temperatures, even with interfraction times as long as 400 min. We concluded that the error in the (slow) mean recovery time was not worse than the other experimental errors. The error in the value of the two-event factor determined from the extrapolated intercept on the vertical axis is quite small, 10% or less.

Absence of Pool Effects in the Recovery of Chlamydomonas Reinhardi

J. M. Nelson, L. A. Braby, and W. C. Roesch

Laurie et al.,(19) following a suggestion by E. L. Powers, hypothesized that a pool or pools of consumable materials used in the repair processes might exist within irradiated cells. Furthermore, they deduced that recovery parameters determined by dose-rate and split-dose experiments might differ, one reflecting the rate of consumption, the other the rate of refilling the pool. This pool hypothesis aroused our interest because it differs markedly from the models we have been using (under this 189). The existence of a pool has never been demonstrated, albeit this fact in itself does not prove its non-existence. We

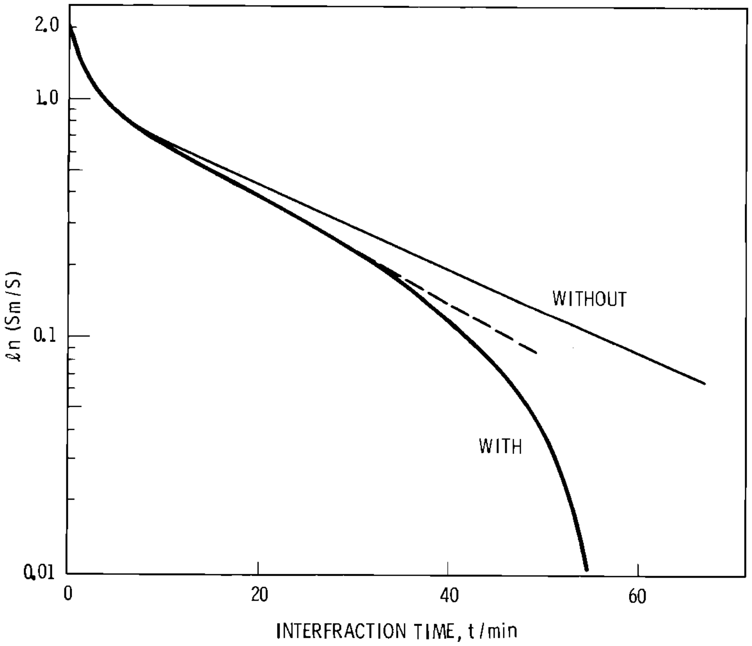

FIGURE 2.10. The Effect of the Reduction in Radiation Sensitivity Following Recovery from Sublethal Damage. Light Line, Calculated Without Such Recovery; Heavy Line, With.

decided to test the model by measuring the mean recovery times in dose-rate and split-dose experiments to look for the difference it predicts. We found no significant difference and, hence, cannot support the pool hypothesis.

Preliminary dose-rate and split-dose studies(20,21) using the eukaryotic alga *Chlamydomonas reinhardi* had not indicated different mean recovery times, but differences might have gone unnoticed because of temperature changes during the experiment. Consequently, new experiments were made to determine the recovery times by both methods as a function of temperature. In protracted irradiation, dose rates ranged from 100,000 rad/min down to 25 to 50 rad/min, giving irradiation times from about 1 sec to more than 7 hr. Split-dose irradiations were generally made at 5000 rad/min or greater with interfraction times up to 320 min.

Values for the mean recovery times and two-event factors determined by these two methods were shown in Figures 2.8 and 2.9. There is no significant difference between values determined by the split-dose and the dose-rate methods below 25°C. Interference by the fast recovery discussed in preceding articles, unrecognized at the time these measurements were made, prevented analysis of data derived from experiments at higher temperatures. The mean recovery time varies from about 240 min at 5°C to a minimum of about 20 min at 25°C.

Our data do not lend support to the pool hypothesis and we conclude that, if a pool or pools of consumable materials exists in this system, the associated rate constants must be very high and the transit times very short, relative to the irradiation times, so as to be unobserved by these techniques.

Plateau-Phase Chinese Hamster Ovary Cells

J. M. Nelson

For several years past, experiments done under this project to test models or obtain information for modeling have used the eukaryotic green alga *Chlamydomonas reinhardi*. Synchronized *C. reinhardi* have a period of almost ten hours in which their radiation sensitivity does not change. This enables the long experiments required in the dose-rate and split-dose methods of studying recovery. Mammalian cells move through their cycle to new states of sensitivity so fast that such experiments are not possible. However, mammalian cells can be stopped in certain phases of their cycle. We hope to find such synchronized, but stationary, populations we can use as we have used *Chlamydomonas*. We have begun investigating the use of cells in plateau phase for this purpose, preferring them to drug-blocked cells to avoid side effects of the drug.

We have equipped the cell culture facility and are now carrying the Chinese hamster ovary (CHO) cell line. The CHO cells are particularly adapted to this sort of experimentation because they are easily cultured by conventional techniques and readily assayed for surviving fractions of clonogenic cells, and they may be grown either as monolayers or suspensions with little change of techniques. They are maintained in our lab by serial passage as monolayers and are stored in liquid nitrogen for purposes of continuity.

Our plans require the development of techniques to stop logarithmic growth and establish a parasynchronous, nonproliferating or resting cell population. Resting cell populations are generally associated with nutritional and/or density-contact inhibition; both are phenomena characteristic of population plateau conditions. Unfortunately, the existence of the plateau is not in itself evidence of resting cells or even of greatly attenuated growth. Some systems can maintain an equilibrium density with a relatively high cellular turnover and near normal renewal rate. We do not know how the CHO cells will behave. It is necessary, therefore, to assess proliferative activity directly and correlate this with cell population growth in order to determine the physiological status of the population.

Preliminary experiments to determine growth parameters of plateau-phase CHO cells have established the existence of resting cells although further development of the techniques is necessary. Figure 2.11 shows the relationship between cell density and DNA-synthetic activity of the same sub-population from a typical experiment. These cells have been nutritionally inhibited.

Note that both the pulse ^{125}I-UdR uptake (a measure of DNA-synthetic activity) and the continuous ^{125}I-UdR uptake (a quantity corresponding to the growth fraction), fall exponentially from the 6th or 7th day through the 20th day, while the total cell number remains relatively high and constant. The unexplained variability in uptake cannot be tolerated, but appears to be dependent on the labeling technique. Further work should not only confirm the ability to maintain a population of resting cells, but should give us better techniques by which we can readily assess the kinetic

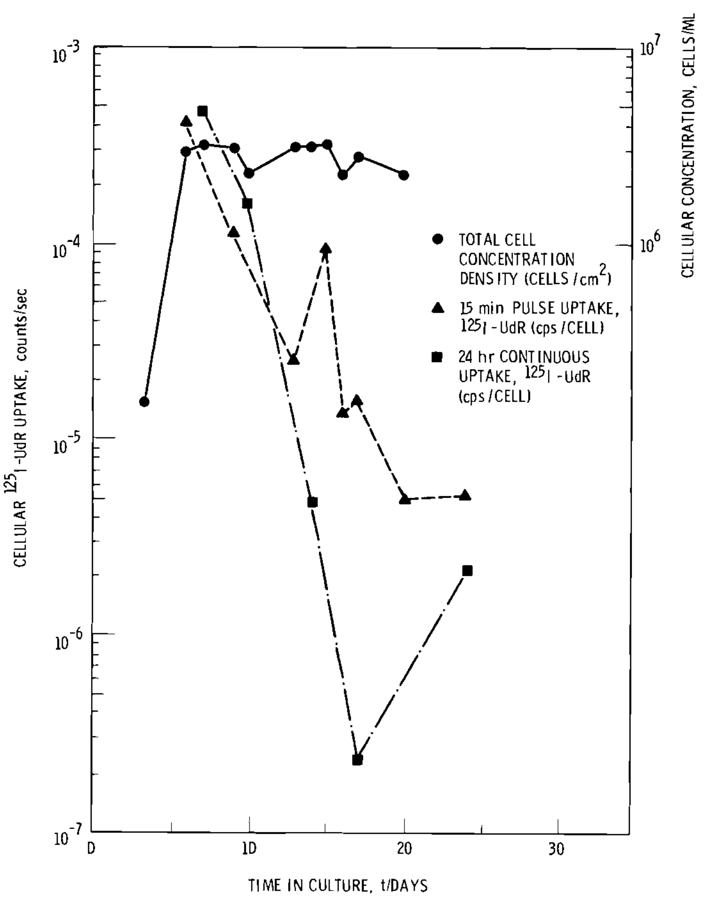

FIGURE 2.11. Growth Parameters of Plateau-Phase CHO Cells

status of such populations. Experiments associated with development of this methodology are in progress.

Electron Van de Graaff Accelerator Irradiations

L. A. Braby

The fast recovery process reported above made necessary changes to our Van de Graaff electron accelerator. Split-dose experiments require large doses in times short compared to the mean recovery time and interfraction times comparable to the recovery time. Dose-rate experiments require control of dose rate so irradiation times can range from very much less to very much more than the recovery time. The slow recovery (recovery time say 20 min) offers no difficulty, and previous changes to the accelerator were designed for recovery times of the order of microseconds. But the fast recovery, with recovery times of about a minute, needed a new way of turning the accelerator on and off.

Electron beams of 10^{-9} to 5×10^{-5}A emerge from an accelerator window and reflect from a graphite block to give dose rates from 2 to 100,000 rad/min. The electronics for microsecond pulsing was changed to direct coupling and a relay added to turn the beam current on and off in response to a light signal from a light-emitting diode at the base of the accelerator. This system can turn the beam current on or off in a few milliseconds. The charge delivered to the graphite block is measured with a digital charge integrator whose pulses are counted by a preset counter set to turn the beam off when the desired dose is reached. Single exposures as short as 20 ms are reproducible. Hand operation for split doses separated by as little as 15 sec is satisfactory; for separations as small as 10 ms we plan to use a second preset counter driven by a pulser.

]

• Dosimetry of Internal Emitters

Dosimetric guidance was provided to many of the radiobiology programs at Pacific Northwest Laboratory. In particular, organ and whole-body doses were calculated and measured in experiments aimed at elucidating the dose-effect relationships from exposure to ^{85}Kr gas, $^{239}Pu(NO_3)_4$ aerosols and cervical implants of ^{252}Cf and ^{226}Ra.

Dosimetric Support of Radiobiology Studies

F. T. Cross and G. W. R. Endres

Considerable effort was expended in support of the Toxicology of Tritium and the Noble Gases Program. Past estimates of the hazards from ^{85}Kr indicated the surface dose to the total body to be the limiting factor in exposure but internal dose, especially to the lung, has not been adequately treated. Doses to both rats and beagle dogs have been calculated from assumed or measured tissue concentrations and also determined from thermoluminescent (Tl) dosimeter measurements. There has not yet been total agreement between the doses derived from tissue concentrations and those measured by Tl dosimeters. Some of the difficulty is due to uncertainty in the calibration of the Tl dosimeters to ^{85}Kr gas exposures, a problem we hope to solve in the near future. Part of this effort included the determination of the shielding effect of rodent fur during ^{85}Kr exposures. Assessing biologic effect to skin from beta emitting aerosols must take this factor into account as man, except for clothes, hasn't such a protective layer for his skin. The fur from the back of rats was found to additionally reduce the dose to skin, and presumably, if representative of fur on the rest of the animal, reduces the dose to the whole body by 17%. These experiments accounted for gas penetration amongst the fur, for when the experiments were repeated with a thin film separating the fur and the gas environment, the shielding effect of the fur was higher, reducing the dose by 25%.

Dosimetric guidance and support was provided to many other radiobiology programs at Pacific Northwest Laboratories. Dose and organ burden modeling along ICRP methodology was contrasted with separate digital computer system modeling of the early translocation of inhaled $^{239}Pu(NO_3)_4$ in beagle dogs. Preliminary data of this continuing project were reported at the July 1977 Annual Meeting of the Health Physics Society. Neutron and photon doses and associated relative biological effectiveness (RBE) factors to organ systems within swine were determined as part of an ongoing program to assess the response to normal tissues from the cervical implant of ^{226}Ra and ^{252}Cf sources. Additionally, the data of our previous experiments to assess the health effects to the GI tract from reactor effluents have been prepared for publication and for presentation.

• Microdosimetry of Internal Sources

The purpose of this study is to develop practical methods for calculating microdosimetric distributions for soft tissue and for lung tissue in which plutonium or other alpha-emitting elements are deposited, particularly when deposited as particulates, to aid in correlating and extrapolating radiation effects measured at different levels of exposure and in different species. Computational methods will be developed and tested in the Radiological Physics Section; concurrently, the Radiological Health Section will develop cell and tissue models in which those methods will be applied. This year the development of a computer code for single-event densities was completed, previous codes for using these densities were updated and described, and a study made of moving particulates.

Calculation of Single-Event Distributions for Point Source Alpha Emitters

W. E. Wilson

A method for calculating the single-event distribtion in energy imparted for point-source alpha emitters has been devised. The need for these distributions arises as a practical matter in the microdosimetry of internal emitters.

The single-event distribution in energy imparted for a point alpha source at a distance r from a spherical volume of radius ρ is

$$F_1(e) = \int_{\Omega} n(\Omega) \quad f_1(e,\vec{r}) \, d\Omega \qquad (1)$$

where $n(\Omega)$ is the flux density, and $f_1(e,\vec{r})$ is the energy imparted by a single track at a distance $\vec{r}$ from the volume of interest. The volume of integration in Equation (1) must extend over all solid angles for which f_1 is non-zero, which, because of the finite range of the most energetic δ-rays, is slightly larger than the site volume.

For an isotropic source of activity, N, the problem has rotational symmetry, and then f_1 does not depend on ϕ, the azimuthal coordinate. In this case Equation (1) can be written

$$F_1(e) = \frac{N}{2} \int_0^{\pi} \sin\theta \; f_1(e,r,\theta) \, d\theta \qquad (2)$$

Furthermore, because of the rotational symmetry, the $f_1(e,r,\theta)$ can be characterized by $f_1(e,a)$, since all f_1's having the same impact parameter, a, are identical.

Monte Carlo techniques were used to evaluate $f_1(e,a)$ for the range of alpha particle energies 1-6 MeV and sites of radii 0.1-5.0 micrometers. The calculations were made using computer codes developed by Paretzke.(22) The results of the calculations, as expected, indicated that for individual alpha tracks passing through the site, the single-event distributions can be approximated by a Gaussian function of the form

$$f_1(e,a) = \frac{1}{\sqrt{2\pi}\,\sigma(a)} \; \mathrm{EXP}\left(-1/2 \; \frac{(e-\bar{\Delta}(a))^2}{\sigma(a)}\right) \qquad (3)$$

$\bar{\Delta}(a)$ is the mean and $\sigma(a)$ is the width of the distribution.

The Monte Carlo calculations indicated that $\bar{\Delta}$ is linearly related to the track length inside the site. This is to be expected because for the energies and site sizes considered here, the energy imparted to the site should nearly equal the energy lost by the alpha particle in passing through the site.

The dependence of the width of the distribution on radial position is such that the ratio, $\sigma/\overline{\Delta}$, is constant out to within 0.1 μm of the edge of the site, then it increases sharply. This sharp increase was phenomenologically approximated by an exponential.

The contribution to F_1 from tracks passing outside the site was estimated entirely from Monte Carlo calculations.

Single-event distributions were calculated for tracks passing up to 0.3 μm outside the site and for alpha energies from 1 to 6 MeV and for site radii of 0.1 to 5 μm. In summary, the single-event distribution for tracks which pass totally outside the site is not significantly dependent on alpha energy and can be adequately approximated with an algorithm exponential in energy imparted. The amplitude and the characteristic decay of the exponential are not strong functions of ρ.

Numerical integration of Equation (2) using Equation (3) and the observed dependences of $\overline{\Delta}$ and σ on a is sufficient to evaluate single-event distributions for tracks which pass through the site. The contribution from tracks passing outside the site is an additive feature simulated by the exponential algorithm described above.

Calculations for Microdosimetry of Internal Sources

W. C. Roesch

Last year we described computer programs for combining single-event densities, such as described in the preceding article, into microdosimetric distributions for any distribution of particulates in a homogeneous tissue. These programs have been rearranged in a more orderly fashion than they were in after the development period so they can be understood and used by other programmers. A laboratory report describing the mathematical methods and approximations used in the programs and the combinations of programs used in typical applications is nearing completion.

Microdosimetry of Moving Particulates

W. C. Roesch

Last year we reported a number of examples of microdosimetric distributions for alpha-particle emitting particulates, but they were all stationary particulates. Usually, particulates move about, at least during the early stages of their history in the body. Consequently, we enlarged our theoretical study to include moving particulates. But, as a result, we concluded that corrections for motion are seldom necessary.

Because of the correlation between alpha particles emitted at different points along the tracks of moving particulates, the microdosimetric distribution produced in a site by a field of moving particulates differs from that produced by stationary particulates whose number per unit volume equals the time-average number of moving particulates. This correlation, however, is ineffective if the particulate emits alpha particles so slowly that the chance of a site being hit by more than one alpha particle from a particulate is small. A site cannot be hit by more alpha particles than the particulate emits while within alpha-particle range of the site. This number is about AR/v (A = activity of particulate, R = alpha-particle range, v = speed of particulate). For particulates containing 10^{-15} Ci of ^{239}Pu, for example, AR is 5 cm/year. If the particulate moves faster than this, the correlation can be ignored; at some lower speed, it will become significant.

To estimate this critical speed, the computer programs for stationary particulates were modified for calculations with moving particulates. The mathematical theory for moving particulates present little difficulty,(23) but the computing does. Many more calculations and much more computer memory are generally necessary. Fortuantely, for a uniform field of particulates moving with constant velocities, the computer memory requirement can be relaxed by using the same space successively for different quantities. Figure 2.12 shows densities in specific energy at four AR/v values for this condition. For AR/v = 1, the density is indistinguishable from that for a uniform stochastic distribution of stationary particulates. For the value 10

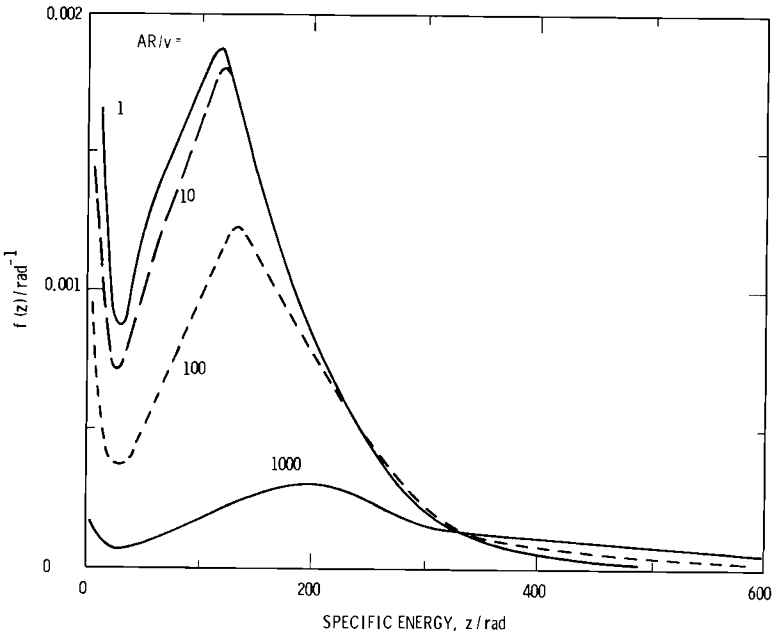

FIGURE 2.12. Densities in Specific Energy in Sites in Uniform Fields of ^{239}Pu Particulates Moving with Constant Velocities

it is noticeably different, but the difference is not particularly important until still higher.

In other words, in the example above, the particulates must be slower than 0.5 cm/year before the microdosimetric distribution is different from that of uniformly-spread stationary particulates. This speed is of the order of 10 cell diameters per year. A particulate is unlikely to move that slowly. Rather, it will probably move relatively rapidly from one position to another where it will remain a while. Then its microdosimetric effect is that of a series of stationary particulates. The use of the relatively difficult computer methods for moving particulates is unnecessary.

• Real-Time Measurement of Pu in Air at Below-MPC Levels

A direct-inlet mass spectrometer is being developed for monitoring low-level airborne plutonium on a real-time basis. The instrument will be capable of measuring plutonium concentrations below the MPC level. Developments during the year have improved several aspects of the instrument's performance. A minicomputer-based ion-burst measurement system has been completed. Instrument calibration for particle size measurement is continuing.

Direct-Inlet Mass-Spectrometer Development

J. J. Stoffels, P. J. Hof, and
T. P. Harrington

Current techniques for monitoring airborne plutonium are limited by the rate of radioactive decay which, for ^{239}Pu, amounts to only one disintegration per second for every 10^{12} atoms present. A new technique using direct-inlet mass spectrometry is being developed which will measure one ion count for approximately every 10^2 atoms of ^{239}Pu present and do this on an individual particle basis.

The direct-inlet mass spectrometric technique(24,25) and the direct-inlet mass spectrometer (DIMS) we have developed are described in previous PNL Annual Reports.(26-28) Further development of the ion detector has improved the gain. A minicomputer-based measurement system for use with the detector has been completed. Work is continuing on calibration of the instrument to provide size measurement of PuO_2 particles. Mass spectral interference due to hydrocarbon contamination has been minimized. Performance of the air-sampling direct inlet has been improved.

The gain of the ion detector was improved by angling the target surface 20° away from the incoming ion beam (see Figure 2.13). This increased the yield of secondary electrons about a factor of two by reducing the angle between the incident ions and the target surface. Calibration of the ion detector shows the dc channel to be linear up to about 1.6×10^{-10} A of input ion current (Figure 2.14). Together with the pulse-counting channel this gives a 10 decade range in ion current measurement capability.

A minicomputer-based ion-burst measurement system (I-BMS) for use with the detector has been put into operation. The I-BMS is designed to measure the fast, transient signals which result when a particle is ionized in the DIMS. Ion bursts as short as 10 msec can be measured by accumulating ion-pulse counts and integrating the dc current.

In order to minimize the amount of PuO_2 aerosol which must be generated to test and calibrate the DIMS, initial work is being done with analogs. Analogs can be used to develop techniques for generation of test aerosols, to determine the transmission of different size particles through the inlet, and to determine the relative ionization efficiency of different size particles. Uranium dioxide and CeO_2 have been selected for this role because of their refractory nature, density, and ionization potential and because they also form dioxide ions in the DIMS.

We have measured the duration of ion signals which result at different filament temperatures when a group of UO_2 particles enters the DIMS. As shown in Figure 2.15, at a filament temperature of 1070°C ionization persists for minutes so that individual particle information cannot be obtained. At 1180°C the ion signal shows structure due to particles striking the filament, but the individual events still cannot be separated. As the filament temperature is increased, ionization proceeds more rapidly allowing individual ion bursts to be measured.

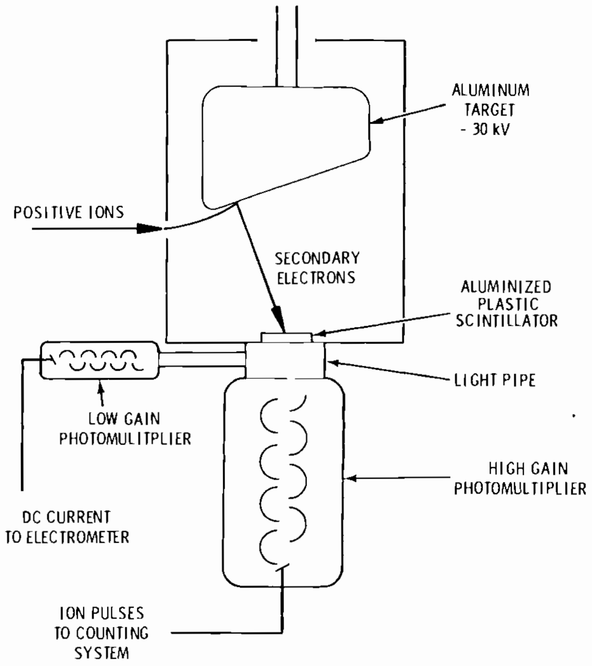

FIGURE 2.13. Ion Detector with Simultaneous Pulse Counting and DC Current Modes of Operation for Wide Dynamic Range

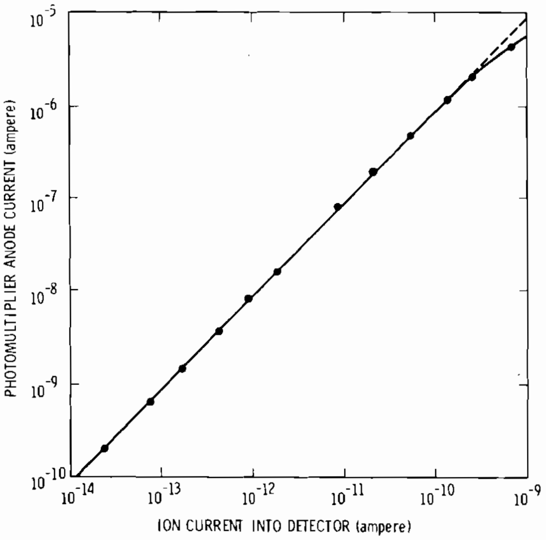

FIGURE 2.14. Calibration Curve of the Ion Detector DC Channel

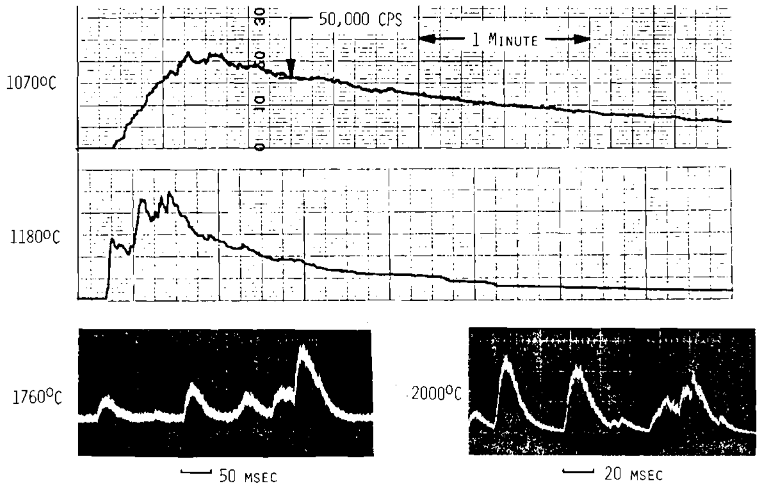

FIGURE 2.15. Ionization of UO^2 Particles on Rhenium in a Direct-Inlet Mass Spectrometer

Cerium dioxide particles exhibit similar behavior. Calibration measurements with monodisperse CeO$_2$ particles will begin shortly.

Mass spectral interference due to hydrocarbon contamination in the vacuum system has been minimized in the region of interest around mass 271 (corresponding to ^{239}Pu^{16}O$_2$). O-rings used on the ion source chamber and as a sliding seal to position the inlet capillary have been replaced with teflon gaskets. With this modification and those reported last year,(28) the hydrocarbon background can be significantly reduced by baking the ion source. Even with serious contamination, the hydrocarbon spectrum diminishes as the filament temperature is increased. Above 1600°C the background in the region around mass 271 is essentially the detector background.

We are continuing work aimed at defining and controlling parameters which affect the performance of the direct inlet. Although the performance of different inlet capillary tubes varies, we have nevertheless obtained some excellent aerosol beams with the present inlet. Aerosol beam deposits were collected by placing transparent tape at the filament position in the ion source so that the aerosol particles impact on the adhesive side of the tape. Figure 2.16 is a photograph of such a deposit and shows a uniform, sharp-edged deposit of only 0.5 mm diameter. The aerosol used was polydisperse Fe$_2$O$_3$ with a geometric mean diameter of about 0.1 μm.

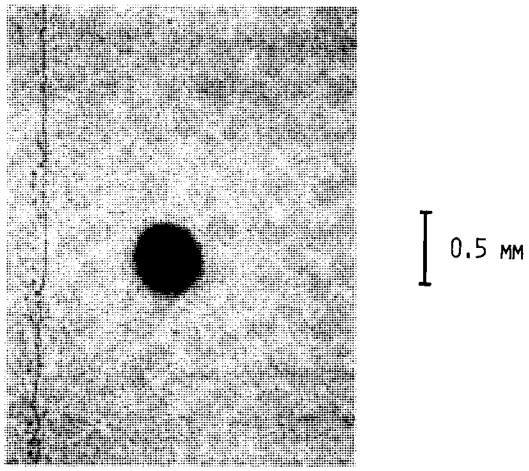

FIGURE 2.16. Aerosol Beam Deposit Collected at the Filament Position of the Direct-Inlet Mass Spectrometer

Figure 2.17 shows what a 0.5 mm-diameter deposit represents in terms of the inlet geometry. The figure is drawn to scale in both the axial and radial directions, but the radial scale is expanded for clarity. We see that the aerosol beam was not merely collimated but focused. Although the geometry would allow a divergence of 0.85° measured relative to the capillary bore, the aerosol beam diverged only 0.05°. To our knowledge, this degree of focusing of an aerosol beam has not previously been reported.

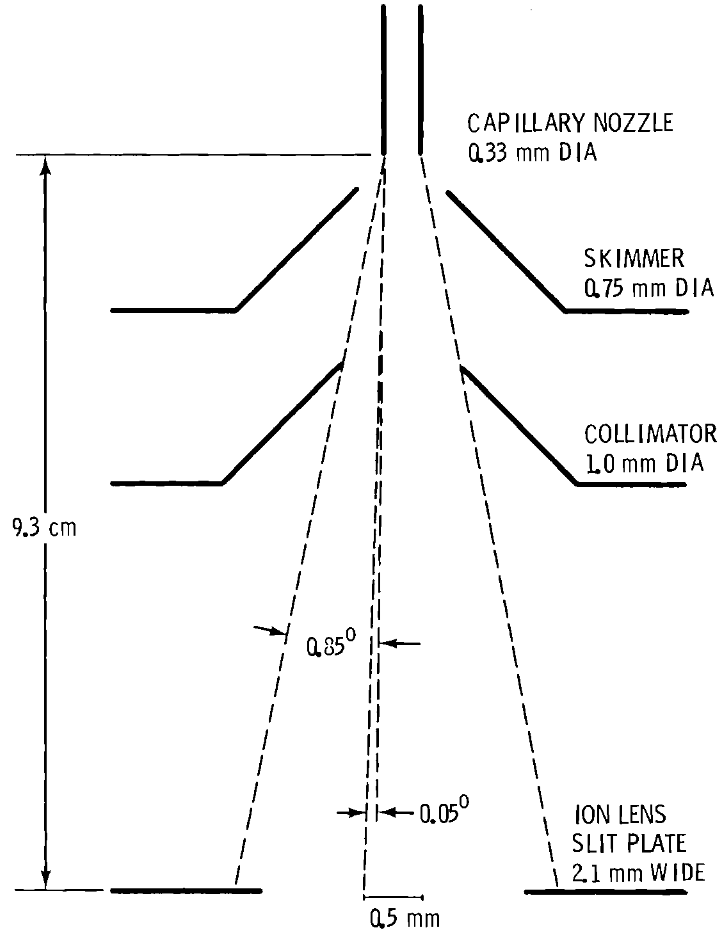

FIGURE 2.17. Divergence of an Aerosol Beam in the Direct Inlet. The Aerosol Used was Polydisperse Fe_2O_3 Having a Geometric Mean Diameter of About 0.1 μm

• Analytical Techniques for Measurement of ^{99}Tc in Environmental Samples

A highly sensitive technique is being developed for measurement of ^{99}Tc in environmental samples. The procedure involves the addition of a known quantity of ^{97}Tc tracer to the sample, chemical separation and purification of the Tc fraction and mass spectrometric measurement of the ^{97}Tc/^{99}Tc isotopic ratio. Calibration of the mass spectrometer has recently been completed, and preliminary measurements of environmental samples have been initiated.

Ultrasensitive Measurement of ^{99}Tc by Mass Spectrometry

J. H. Kaye

From an environmental and hazard viewpoint ^{99}Tc is one of the most troublesome radionuclides produced through nuclear fission. This is due to the long half-life (2.13 x 10^5 years), the volatile nature of the heptoxide, the mobility of the pertechnetate ion in aqueous solution, the high fission yield (over 6%) and the affinity of several organs of the human body for this element. Furthermore, technetium is almost impossible to detect at very low levels by direct counting methods since its half-life is long and it emits only low-energy beta radiation.

The purpose of this study is to develop, by means of mass spectrometry, much more sensitive methods for its detection than are presently available. Currently planned ecological studies within existing DOE programs are awaiting development of the ^{99}Tc analytical procedures. Other programs (e.g., waste management, environmental monitoring) also require availability of a sensitive analysis method for ^{99}Tc.

The method being developed for analysis of ^{99}Tc is based on isotope dilution mass spectrometry. Current sensitivity of this method is about 1 pg ^{99}Tc (0.018 pCi). It is anticipated that the sensitivity may be improved by a factor of 10 to 100.

The basic approach of the method involves first the addition of a known quantity (approximately 300 pg) of ^{97}Tc tracer to the sample. The sample is dissolved by ashing, fusing with sodium peroxide and adding acid to the melt. Sodium hydroxide is added to the solution to precipitate the bulk of any ruthenium which may be present. (Ruthenium is the only stable element with a mass 99 isotope.) Further purification involves anion exchange, cation exchange, solvent extraction and electro-deposition of the technetium as the dioxide onto an iridium filament. Due to the codeposition of molybdenum during the electrodeposition step, it is necessary to dissolve the plated sample and do further solvent extraction purifications. Finally, the sample, containing about 50 μ liters of liquid, is evaporated onto a rhenium filament, reduced with hydrogen gas at elevated temperature to convert the dioxide to technetium metal, and loaded into the mass spectrometer. The isotopic measurement involves determining the ion counting rates at masses 97, 98, 99 and 102. The mass 98 counting rate and the natural abundances of molybdenum 97 and 98 are used to correct the mass 97 counting rate for molybdenum and the mass 102 counting rate may be used similarly to correct the mass 99 counting rate for ruthenium. However, the mass 102 counting rate has normally been insignificant. After these corrections are made, the 97/99 counting rate ratio is used to determine the level of ^{99}Tc in the sample.

A calibration curve of the ^{97}Tc/^{99}Tc ratio has been run for electroplated solutions containing 300 pg of ^{97}Tc and either 0.01, 0.1, 1.0, 10.0 or 100 pg of ^{99}Tc. The calibration curve is linear for quantities of ^{99}Tc of one picogram or greater. For smaller added quantities of ^{99}Tc, the 97/99 mass ratio does not remain constant as a function of time. Causes of this effect are under investigation.

During the past year the procedure for separation of ^{97}Tc from irradiated enriched ^{96}Ru was successfully established. A procedure was also developed for separation of ^{95m}Tc from enriched ^{95}Mo which had been irradiated at the Oak Ridge cyclotron.

A substantial effort during the past year has been directed toward development of special hardware and software for control of the mass spectrometer via a PDP-11 computer system. An interface was built which allows transfer of digital data from the mass spectrometer scaler to the computer. Software allows display of these data during acquisition and generation and display of plots of count rate versus time for each mass after acquisition. Plots of 97/99 count rate ratios versus time, after correction for ^{97}Mo and ^{99}Ru, can also be generated. A special power supply was constructed which allows computer control of the current to the mass spectrometer filament.

Development of the chemical procedures for isolation of Tc from vegetation samples has nearly been completed. Special plants were grown hydroponically indoors to provide vegetation samples low in ^{99}Tc. Analysis of these and other samples is presently underway.

• Radiation Instrumentation—Radiological Chemistry

Program efforts were concentrated in the following areas: development of low-level radiochemical laboratory techniques, in situ monitoring techniques, and activation analysis technology.

Cyclic Activation Analysis

N. A. Wogman and H. G. Rieck

A computer-controlled cyclic neutron activation facility is being assembled for routine multielement analysis of environmental and geological samples. The neutron source for irradiation consists of about 80 mg of ^{252}Cf which is placed in a 93% ^{235}U enriched uranium core. The overall subcritical assembly produces a thermal flux of $\sim 10^{10}$ n/cm^2/sec. This system is coupled to a pneumatic rabbit system and an automatic computer switching device which controls irradiation, decay, counting, and data reduction of a sample.

The radioactive isotopes produced are primarily measured by their characteristic gamma-ray energies with intrinsic Ge detectors, dual Ge(Li) detectors, and NaI(Tl) multidimensional gamma-ray spectrometers. High efficiency (25%), low background, anticoincidence shielded Ge(Li) gamma-ray detectors are used to provide the lowest possible background yet maintaining high peak-to-Compton ratios (1000:1).

Computer control for the system is incorporated in a TN-11/10 analyzer which provides direction for programming of the cyclic activation procedure. This includes the number of cycles, decay periods, counting times, and samples to be inserted for irradiation. This approach is particularly useful for very short-lived radionuclides whose half-lives are in the ranges of seconds to minutes. The data assembled from cyclic activation are transferred to a PDP-11/35 disc system for analysis of the spectra. The data reduction by computer involves a comparison of the standard and unknown spectra for each element to determine the quantity of element (ppm) in a given matrix. Alternatively, the subcritical multiplier system is standardized for a given element in a given matrix, and the standardization approach allows direct computation of the desired elements (ppm) in a sample matrix without involving a specific standard in the irradiation. Such an approach is useful and is primarily used in the cyclic activation analysis where the number of cycles (consisting of the irradiation/decay/count periods) may be as high as 100.

Computer analysis and recording of the cyclic activation data are required due to the vast amounts of the information involved. For example, in 200 seconds of elapsed time, a one-second irradiation, one-second count, produces 100 spectra for a single sample. The on-line analysis of spectra is required to just maintain data control.

The on-line computer/irradiation facility has been evaluated on NBS orchard leaf and USGS BCR-1 standards. The use of computer analysis with the noncoincidence/coincidence Ge(Li) counting system has allowed the measurement of 22 elements in orchard leaf. A 6-g sample of orchard leaf and BCR-1 was irradiated at a total neutron fluence of 1×10^{17} neutrons in the subcritical facility. Following the irradiation, the samples were fused with Na_2O_2 + NaOH mixture and a group chemical separation scheme was performed to isolate the rare earth elements. The solution aliquots were counted for 300-1000 minutes on the various counting systems to measure all the REE. Sensitivities to part-per-billion levels were obtained for some of the REE.

The use of a ^{252}Cf neutron source in a ^{235}U enriched subcritical assembly seems to be a straightforward and safe method of providing a relatively inexpensive and fast activation. The wide-scale use of these multiplier units for developing highly sensitive gamma-ray spectrometers requires the use of computer control and analysis in their expanding application, particularly in cyclic activation.

In Situ Radiation Detection

K. K. Nielson, N. A. Wogman and
R. L. Brodzinski

A portable intrinsic germanium spectrometer has been adapted to in situ analysis of plutonium and americium X-rays and γ-rays for use in decontamination and monitoring of contaminated laboratories. This system consists of a high-efficiency, 19-cm^2 detector mounted in a rotatable (180°) vacuum cryostat for flexible positioning, and connected to a portable multichannel analyzer and cassette tape deck for rapid data accumulation and storage.

Developmental in situ counting of contaminated concrete floors indicated 10-min, 3σ detection limits to be 290 d/m/cm^2 for ^{239}Pu and 9 d/m/cm^2 for ^{241}Am, based respectively on L X-rays (14,17 and 20 keV) and the 26- and 60-keV γ-ray peaks. Although the floor contamination was observed to be on the concrete surface, similar counts of concrete surfaces near a contaminated hood showed the activity to be located at a depth of several millimeters, as determined from X-ray and γ-ray intensity ratios. Although the best detection limits are obtained using low energy photopeaks (restricting sample penetration to $\sim$1 cm of concrete), higher energy γ-rays observed in direct counting of the contaminated hoods could provide both depth and activity information at much greater depths.

Low-Energy Spectrometry in Activation Analysis

K. K. Nielson, J. C. Laul and N. A. Wogman

An intrinsic germanium (IG) detector has been applied to X-ray and γ-ray spectrometry of rare earths in neutron-activated samples. Its improved efficiency and resolution over large conventional Ge(Li) detectors in the 25-120 keV region provides improved detection of Nd, Eu, Tb, Ho, and Yb.

The IG detector also analyzed La, Ce, Sm, Gd, Tm and Lu at equal or slightly higher detection limits than a Ge(Li) at a comparable solid angle.

Comparison of detection limits using X-ray versus γ-ray peaks with the IG detector indicated Eu and Yb are best determined from X-ray peaks, while Ce, Sm, Gd, Tb, Ho, Tm and Lu have more favorable detection limits using low-energy γ-ray peaks. Two count intervals after 4- and 15-days' decay were used for separate analysis of medium and long-lived nuclides. By using a single radiochemical group separation, individual quantities of 13 rare earth elements were determined at ppb levels in biological samples.

2.0 REFERENCES

1. Kim, Y.-K., "Energy Distribution of Secondary Electrons, I. Consistency of Experimental Data." Radiat. Res. 61:21, 1975.
2. Kim, Y.-K., "Energy Distribution of Secondary Electrons, II. Normalization and Extrapolation of Experimental Data." Radiat. Res. 64:205, 1975.
3. Kim, Y.-K., "Energy Distribution of Secondary Electrons." Radiat. Res. 64:96, 1975.
4. Ashley, J., R. Ritchie, and W. Brandt, "Z^3 Effect in the Stopping Power of Matter for Charged Particles." Phys. Rev. B 5:2393, 1972.
5. Watson, R. L. and L. H. Toburen, Phys. Rev. A 7:1853-1863, 1973.
6. Wilson, W. E., "Analytical Expression for Cross Section Data," Pacific Northwest Laboratory Annual Report for 1976. BNWL-2100 PT 4, Battelle, Pacific Northwest Laboratories, Richland, WA 99352, 1977.
7. Daniel, C and F. S. Wood, Fitting Equation to Data. Wiley-Interscience, New York, p. 23, 1971.
8. Mozumber, A., "Track-core Radius of Charged Particles at Relativistic Speed in Condensed Media." J. Chem. Phys. 60:1145, 1974.

9. Miller, J. H. and M. L. West, "Quenching of Benzene Fluorescence in Pulsed Proton Irradiation: Dependence on Proton Energy." J. Chem. Phys. 67:2793, 1977.

10. Frost, A. A. and P. G. Pearson, Kinetics and Mechanism. 2nd edition, John Wiley & Sons, Inc., New York, 1961.

11. Elkind, M. M. and H. Sutton, "X-ray Damage and Recovery in Mammalian Cells in Culture." Nature 184:1293-1295, 1959.

12. Roesch, W. C., "Theory of LET Effects," Pacific Northwest Laboratory Annual Report for 1974. BNWL-1950-PT4, Battelle, Pacific Northwest Laboratories, Richland, WA 99352, pp. 69-71, February 1975.

13. Todd, P, H. S. Winchell, J. M. Feola, and G. E. Jones, "Pulsed High-Intensity Roentgen Rays." Acta. Radiol. 7:22-26, 1968.

14. Roesch, W. C., "Models of the Radiation Sensitivity of Mammalian Cells," Third Symp. Neutron Dosimetry in Biol. and Medicine. G. Burger and H. G. Ebert eds., Commission of the European Communities, Munich, Germany, in press.

15. Malcolm, W. and J. B. Little, "Characterization of Rapid, Temperature-Dependent Split Dose Recovery in Irradiated Mammalian Cells." Rad. Res. 70:705, 1977.

16. Ben Hur, E., M. M. Elkind, and B. V. Bronk, "Thermally Enhanced Radioresponse of Cultured Chinese Hamster Cells: Inhibition of Repair of Sublethal Damage and Enhancement of Lethal Damage." Rad. Res. 58:38-51, 1974.

17. Braby, L. A. and W. C. Roesch, "Temperature Effect on the Radiation Sensitivity and the Repair of Radiation Damage in Chlamydomonas Reinhardi," Pacific Northwest Laboratory Annual Report for 1976. BNWL-2100 PT4, Battelle, Pacific Northwest Laboratories, Richland, WA 99352, pp. 11-12, June 1977.

18. Donlon, T. and A. Norman, "Kinetics of Unscheduled DNA Synthesis Induced by Ionizing Radiation in Human Lymphocytes." Rad. Res. 39:400-412, 1969.

19. Laurie, J., J. S. Orr, and C. J. Foster, "Repair Processes and Cell Survival." Brit. J. Radiol. 45:362-368, 1972.

20. Nachtwey, D. S. and L. A. Braby, "LET and Recovery in Chlamydomonas," Pacific Northwest Laboratory Annual Report for 1974. BNWL-1950 PT4, Battelle, Pacific Northwest Laboratories, Richland, WA 99352, pp. 65-66, February 1975.

21. Braby, L. A. and W. C. Roesch, "Dose Rate Effects and Chlamydomonas," Pacific Northwest Laboratory Annual Report for 1975. BNWL-2000 PT4, Battelle, Pacific Northwest Laboratories, Richland, WA 99352, pp. 67-69, February 1976.

22. Paretzke, H. G., "Comparison of Track Structure Calculations with Experimental Results," Microdosimetry, Proc. Fourth Symposium on Microdosimetry. H. G. Ebert, ed., EURATOM, 5122 d-e-f, 1973.

23. Roesch, W. C. "Microdosimetry of Moving Particulates." Rad. Res. 70:683, 1977.

24. Davis, W. D., "Continuous Mass Spectrometric Analysis of Particulates by Use of Surface Ionization." Environ. Sci. Tech. 11:587-592, 1977.

25. Davis, W. D., "Continuous Mass Spectrometric Determination of Concentration of Particulate Impurities in Air by Use of Surface Ionization." Environ. Sci. Tech. 11:593-596, 1977.

26. Stoffels, J. J., C. R. Lagergren, and A. L. Franklin, "Fast Real-Time Measurement of Extremely Low-Level Airborne Plutonium," Pacific Northwest Laboratory Annual Report for 1974. BNWL-1950 PT4, Battelle, Pacific Northwest Laboratories, Richland, WA 99352, pp. 33-34, February 1975.

27. Stoffels, J. J. and C. R. Lagergren, "Fast-Time Measurement of Extremely Low-Level Airborne Plutonium," Pacific Northwest Laboratory Annual Report for 1975. BNWL-2000 PT4, Battelle, Pacific Northwest Laboratories, Richland, WA, 99352, pp. 33-35, February 1976.

28. Stoffels, J. J. and C. R. Lagergren, "Real-Time Measurement of Pu in Air at Below MPC Levels," Pacific Northwest Laboratory Annual Report for 1976. BNWL-2100 PT4, Battelle, Pacific Northwest Laboratories, Richland, WA 99352, pp. 95-97, June 1977.

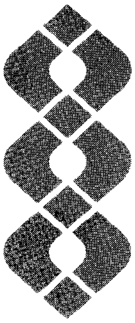

3.0
Geothermal

GEOTHERMAL

- **Heavy Metal and Noxious Gas Emissions from Geothermal Resource Development**

• Heavy Metal and Noxious Gas Emissions from Geothermal Resource Development

Although geothermal energy is generally considered a relatively clean source of power, the high temperature processes which create the hydrothermal provinces result in the mobilization of some undesirable constituents. In this section, we report on a general effort underway to characterize and compare effluents from a number of different geothermal sites. The second report details our results from a preliminary sampling of a geopressured geothermal well.

Heavy Metal Gaseous Emissions from Geothermal Power Plants

D. E. Robertson, J. S. Fruchter,
J. D. Ludwick, E. A. Crecelius,
C. L. Wilkerson, J. C. Evans

The high temperature magmatic processes which create the hydrothermal provinces of high geothermal energy potential also result in the accumulation of undesirable gases and liquids. During the tapping and utilization of geothermal fluids for power production, elevated levels of these naturally produced contaminants can be released to the surrounding environment. We have initiated a study to identify the quantities and chemical forms of volatile and water soluble heavy metals released in geothermal effluents. To date, our studies have been conducted at The Geysers, Cerro Prieto, Niland, East Mesa, Raft River, Heber, and Vermilion Bay, Louisiana geothermal sites.

Of the heavy metals studied, mercury is the most volatile and gms/hour quantities are released as gases from the generating units at The Geysers and Cerro Prieto. Mercury concentrations in effluents from Imperial Valley geothermal wells are slightly lower. Mercury concentrations in Raft River steam and water are one to two orders of magnitude lower than at The Geysers and Cerro Prieto. The mercury levels in gases and hot water from the geopressured well at Vermilion Bay, Louisiana contained extremely low levels of mercury. The volatile mercury at all locations is predominantly elemental Hg° vapor, a surprising observation because of the high concentrations of H_2S present.

Hydrogen sulfide was ubiquitous in the noncondensable gases and ranged in concentration from 6% at several units at The Geysers to several ppm at the Vermilion Bay site. Radon gas is also present in elevated concentrations in the noncondensable geothermal gases, with the highest concentrations observed at The Geysers.

Arsenic primarily follows the liquid phase at the hot water dominated sites and concentrations in the geothermal waters ranged from 28 μg/l in Raft River hot water to 2250 μg/l in the Cerro Prieto brine. At Cerro Prieto, 2480 gm/hr of arsenic are released to an evaporation pond. At Cerro Prieto the arsenic in the fresh brine is primarily in the +3 oxidation state, but appears to oxidize rapidly to the +5 form when exposed to the atmosphere. The arsenic in fresh hot water from Raft River is initially present mainly in the +5 form.

The source-term chemical characterization includes the quantitative measurement of numerous gases, including CO_2, NH_3, N_2, O_2, hydrocarbons and noble gases, and the analyses of numerous major and trace element constituents in the hot waters. We have also begun to examine the environs surrounding established geothermal power plants to identify any accumulations of geothermal pollutants as a result of plant operations. Preliminary data suggest that Hg, B and perhaps As levels have become elevated in soils surrounding several generating units.

Measurement of Potentially Toxic Materials in Geopressured Geothermal Fluids

J. S. Fruchter, D. E. Robertson, and
J. D. Ludwick

In previous work, we found that a number of conventional geothermal wells emitted certain heavy metals or noxious gases at rates comparable to those from coal-fired power plants. These emissions from a geothermal well may be relatively serious because the plant must be located near the wells, leaving little flexibility in the selection of the site. The objective of this work is to determine these same elements and compounds in a geopressured well to see how they compare to conventional geothermal wells and to other energy sources. Geopressured resources differ considerably from conventional geothermal resources in that they are located along the Texas and Louisiana Coasts, an area which has no apparent connection with magmatic or volcanic activity. DOE has at this time a considerable commitment to development of geopressured resources. The measurements reported here were made at El Tigre Lagoon, Vermilion Bay, Louisiana, which was at the time the only operating geopressured well.

Data were obtained for the gases and brine from the El Tigre Lagoon Well. The major constituent of the gas is methane. The gases are quite low in H_2S and Hg compared to gases from most conventional geothermal areas. The brine is also relatively low in F and As. Of the trace constituents measured, B, NH_3, K, Li, Mg and Sr were found in levels typical of those found at other geothermal areas. The high concentration of a number of major constituents, such as Na and Ca, shows that the brine is very concentrated compared to sea water.

4.0

Oil Shale

OIL SHALE

- Oil Shale and Tar Sand Research
  - Oil Shale and Tar Sand Effluent Characterization
  - Oil Shale and Tar Sand Research Materials

• Oil Shale and Tar Sand Research

Oil shale and tar sands are a potential supply of billions of barrels of crude oil for this country's future use. One of the chief concerns in the development of these new industries is to make sure that the conversion processes can be carried out in an environmentally acceptable manner. For this reason, it is important to chemically and physically characterize the effluents from these conversion processes at an early stage of development, preferably at the pilot plant or semi-works stage. The complex nature of the effluents makes it necessary to develop new sampling, analysis and chemical operation techniques. In this section, new or improved techniques for both organic and inorganic analyses are presented, along with applications to fossil fuel research. Also described is a program for providing representative and well-characterized fossil fuel samples for further characterization, environmental, and health effects studies and a program of interlaboratory comparisons to ensure the accuracy of the data.

Improved Computer Program for Neutron Activation Analysis

C. L. Wilkerson, J. C. Laul, and V. L. Crow

Computer programs previously developed in our laboratory for neutron activation analysis (NAA) and Ge(Li) gamma-ray spectrometry have been modified to improve analytical accuracy and to increase the processing efficiency for large numbers of γ-ray spectra. Our modified computer programs for gamma-ray spectrometry do not involve spectrum stripping, smoothing operations, spectrum unscrambling, etc., where shaping of a photopeak is involved. Instead, our approach to γ-ray spectrum analysis is based on the principle of manual selection of a photopeak area and Compton background channels of the identified photopeaks of interest in a spectrum. This approach to computer analysis of Ge(Li) gamma-ray spectra has been thoroughly tested in our laboratory and has proven to be very applicable to quantitative NAA-procedures.

In our present computer analysis system, several Ge(Li) detectors and multichannel analyzers are interfaced to a PDP-15/30 computer. Gamma-ray spectra are transferred directly from a multichannel analyzer to the PDP-15/30 computer by a transfer interface. The list of parameters which may be assigned to each spectra has been modified and now includes: 1) a description of the sample or standard material; 2) spectrum sequence name and number; 3) detector identification; 4) sample counting position or shelf number; 5) gain calibration; 6) date and time of reactor irradiation; 7) date and time of counting; 8) counting interval; 9) actual elapsed time during count; 10) detector dead time; 11) neutron flux and counting geometry correction factors; and 12) sample weight. These parameters and the γ-ray spectra are stored on a DEC tape by the PDP-15/30 computer. Up to 50 2048 channel or 25 4096 channel spectra may be stored on a single DEC tape.

The output format of the analysis program has been expanded to present a more complete and easy-to-read record of computed data. This modification has significantly reduced the time spent in evaluating NAA results. The current program computes elemental concentrations in ppm, the associated error (%), and other data such as gross, net and background counts, counting errors due to the sample and standard, decay correction during counting and from the end of irradiation, corrected counts/min/gm, etc., that are used in computation by the PDP-15/30 computer. The program also lists peak channel and any peak shift, peak width, any background channel shifts, and other identifying parameters mentioned above.

We have tested very successfully our computer program approach on five identical synthetic TEST spectra which were comprised of ^{241}Am, ^{57}Co, ^{60}Co, ^{137}Cs, ^{203}Hg, and ^{46}Sc radionuclides. Each TEST spectra consisted of 35 photopeaks of different intensities in the range of 60-1600 keV. The photopeak channels in the first TEST spectrum were precisely calibrated (1 keV per channel) and served as standards, wherever the photopeak channels in the second and third TEST spectra were shifted by two channels to the right and left, respectively. The peak channels in the fourth and fifth TEST spectra were disproportionally shifted (2-6 channels) by a small to a large gain shift. In each TEST case, the program was able to successfully locate shifted photopeaks and to calculate results which agree in greater than 95% of the cases with manual calculations.

The approach of our computer program has been further tested in the analyses of geological and environmental matrices. We have analyzed in duplicate the USGS standards BCR-1, W-1, and PCC-1, IAEA Soil-5, and NBS coal, fly ash, orchard leaf and bovine liver for some 34 major, minor, and trace elements (Al, As, Ba, Br, Ca, Ce, Cl, Co, Cr, Cs, Eu, Fe, Hf, K, La, Lu, Mg, Mn, Na, Nd, Ni, Rb, Sb, Sc, Se, Sm, Sr, Ta, Tb, Th, Ti, V, Yb, and Zn) by NAA-gamma-ray spectrometry. Our results within the precision (1) in the vast majority of cases agree very well with the recommended reported values.

High Performance Liquid Chromatographic Characterization of Oil Shale Retort Waters

W. D. Felix

During the production of oil from oil shale, water is produced as a byproduct. Both environmental and process considerations lead to interest in the evaluation of changes in the organic content of the process water. Analytical procedures are therefore required which are rapid and quantitative for the determination of organic solute alteration. A high performance liquid chromatographic technique was developed such that fingerprint spectra are produced. This technique has the advantage of being extremely rapid and sensitive. The success of this technique in the present application was in part due to recent improvements in column packing. An RP8, reverse phase, long chain hydrocarbon bonded column of high theoretical plate capacity (10,000-40,000 plates/meter) was used with programmed gradient elution. The solvent of choice was a methanol/water mixture. A typical liquid chromatogram in Figure 4.1 shows the detection capability using an UV sensitive detector at 230 nm. Compounds were identified by comparison with standards and by selective collection of the eluant with subsequent GC/MS analyses. The technique was applied to investigate the changes in retort water stored at 37° and 4°C. Significant differences were noted in the chromatogram for peaks centered around peak numbers 3, 4, 8, 47, 48 and 50. These changes could presumably be ascribed to microbial effects at 37°C. The elution normally requires less than 1 hr with significant resolution of over 60 compounds as detected at wavelengths in the ultra-violet range. Thus, it is possible to obtain characteristic LC spectra against which comparisons may be made of retort water suspected to have been modified by physical or microbial processes. This work was done in conjunction with D. S. Farrier and R. Poulson of the Laramie Energy Research Center, Laramie, Wyoming.

HPLC OF OMEGA-9 RETORT WATER

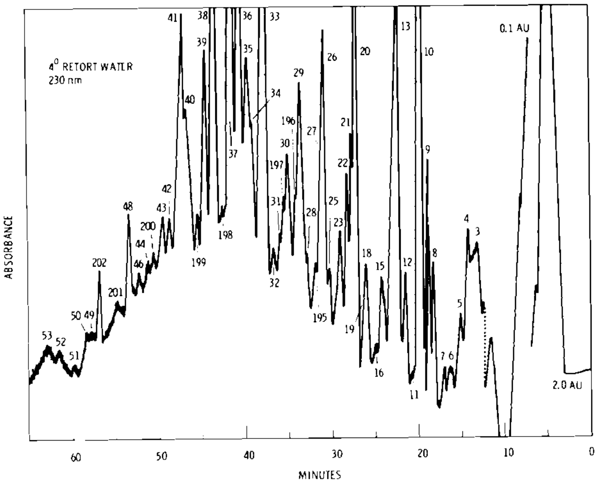

FIGURE 4.1. HPLC (High-Pressure Liquid Chromatogram) of Ω-9 Retort Water at 230 nm

Element Balance Studies at an Oil Shale Research Retort

J. S. Fruchter

Potentially toxic elements are present in raw oil shale at various levels of concentration. The final impact of these elements depends on their fate during the retorting process and on the final physical and chemical form in the effluents from the process. Mass balance studies are a first step in understanding the distribution of an element in the process and waste streams. These studies help to pinpoint those streams which require further study and make sure that significant amounts of the elements are not escaping by unknown pathways. Once the mass balance study is complete, the determinations of the chemical and physical forms of the elements of interest can be carried out.

Reported here is a preliminary mass balance study for the S-11 run of the 125-kg simulated in-situ retort operated by the Lawrence Livermore Laboratory. The element balances for the elements were calculated using the following mass flow balance: raw shale 125.2 kg, spent shale 85.6 kg, dry shale oil 10.54 kg and retort water 3.77 kg. The calculated balances in percent for six elements of interest are shown in Figure 4.2, assuming 100% starting material. The major imbalance occurs for the volatile element Hg. The Hg is probably lost in the offgas stream, which was not measured in this case. Measurements we have made of other offgas streams do indicate that Hg is at times present in retort offgases. Complete measurements of all effluent streams to complete the balance for Hg for other oil shale retort runs are underway. Balances for the refractory elements Fe and Na shown in the figure, as well as a number of other refractory elements, have been found to be satisfactory with most of the elements ending up in the spent shale as expected. The great majority of elements such as As, Se and Sb, which like Hg, might be expected to be volatile, also remained in the spent shale in this case. Significant amounts of As and Se were, however, found also in the product oil and water. Studies are underway to determine the physical forms of these and other elements in the process streams.

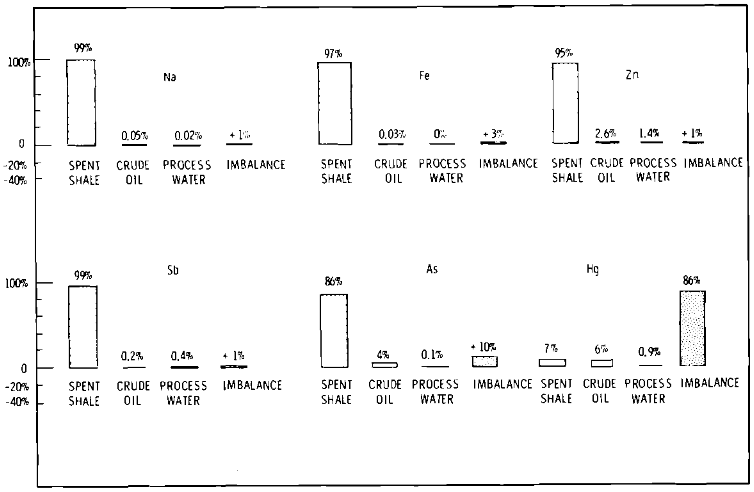

FIGURE 4.2. Material Balances for Selected Elements—Livermore 125Kg Retort-Run S-11

• Oil Shale and Tar Sand Research Materials

Fossil Fuel Research Materials

J. S. Fruchter and M. R. Petersen

The objective of this program is to prepare research materials from feedstock, products, by-products and wastes from fossil fuel pilot operations to be used in characterization, health and environmental programs. The materials are needed so that environmental and health studies can be carried out on homogeneous, representative and well documented samples. In this program, materials from some of the more promising pilot operations as well as several crude petroleums for reference purposes have been 1) obtained; 2) stored in a manner which minimizes degradation; and 3) split into aliquots which are available for distribution to DOE laboratories and others designated by DOE to conduct environmental and health studies. The availability of samples to laboratories for their research programs is also contingent upon the consent of the organization that provided the materials to PNL.

The materials we have obtained and stored to date are listed in Table 4.1. We have also split samples of several of the shale oils and the solvent-refined coal liquids into four fractions (acid, basic, PNA and neutral) using the scheme described in last year's reports. These fractions have been provided to PNL biologists for studies of mutagenicity and toxicity. In addition, samples of air particulates have been obtained from the Paraho site. These samples will be extracted with a battery of solvents for use in mutagenicity tests.

TABLE 4.1 Fossil Fuel Reference Materials[a]

1. Solvent-Refined Coal Process
   - a. Solvent-refined coal
   - b. Mineral residue
   - c. Light oil (naphtha)
   - d. Recycle solvent
   - e. Wash solvent

2. Lawrence Livermore 125 kg Retort
   - a. Mahogany Zone raw shale (24 gal/ton)
   - b. Spent shale (Run S-11)

3. Lawrence Livermore 7 Ton Retort
   - a. Spent shale (Run L-1)
   - b. Crude shale oil (Run L-1)
   - c. Process water (Run L-1)

4. Geokinetics In Situ

   Process water

5. Crude Petroleums
   - a. Wilmington (high N)
   - b. Gato Ridge (high metals, high N, high S)
   - c. Prudhoe Bay (low N, low S)

6. Paraho Semiworks Retort
   - a. Raw shale
   - b. Retorted shale
   - c. Crude shale
   - d. Product water
   - e. Raw shale crushing fines from filter baghouse
   - f. Retorted shale fines from filter baghouse

7. CO_2 Acceptor
   - a. Ash
   - b. Spent Acceptor

---

[a] The availability of samples is contingent upon approval on a case-by-case basis by the organization that made the materials available to PNL

Analysis of Boron in Fossil Fuel and Geothermal Samples

J. S. Fruchter and J. C. Evans

The element boron in its various chemical forms is of considerable interest in environmental studies because of its known toxicity to many plants in relatively low concentrations. It is also one of the most difficult elements to measure accurately in the complex matrices found in fossil fuel and geothermal materials. Many procedures reported in the literature list interferences which make them inapplicable to these samples. After careful consideration, two primary techniques for boron determinations, which are really quite independent of one another, were selected. These techniques were a plasma emission spectroscopy method and the Azomethine (H)colorometric method. Some samples were also checked using a prompt gamma spectrometric method developed elsewhere. Publications on the spectrophotometric determination of low-level B(0-4 ppm) solutions, plant and soil samples using Azomethine (H) suggested application of the method to several of our existing DOE related programs. The method is selective and sensitive on geothermal waters, sea water, shale oil and oil shale process water, and suffers from very few interferences.

The procedure for clear solutions (sea water, geothermal fluids, etc.) is fairly straightforward. Four ml of sample are pipetted into a 25 ml polyethylene bottle. It is important that polyethylene or quartz be used throughout to avoid contamination problems. One ml of a buffer washing solution containing ammonium acetate (pH 4.5) and pentasodium DPTA is added followed by one ml of Azomethine(H) indicator. After thorough mixing, the solution is allowed to stand for one hour. The solution's adsorbance at 415 nm is compared to that of standard boron solutions. A distilled water blank is also run through the procedure.

Liquid materials such as shale oil and shale oil retort water which are not clear must be treated to remove the color without losing the boron. In cases where the color is due to organic compounds, the sample may be wet ashed or low-temperature ashed. During the ashing procedure, the pH must be kept high (8-9) to prevent volatilization of boric acid.

The plasma emission spectroscopy method is detailed in another section of this report. The agreement between the two methods is in general quite good and is illustrated in Table 4.2 for the case of alkaline leachates of soil samples taken near a geothermal plant at The Geysers.

TABLE 4.2 Boron Concentrations in Alkaline Leachates of Soils Taken Near a Geothermal Plant at The Geysers, California

	Azomethine-H Method	Plasma Emission Spectroscopy Method
1	550 μg	580 μg
2	95 μg	103 μg
3	6 μg	4.2 μg
4	14 μg	14.6 μg
5	28 μg	25.1 μg
7	135 μg	150.0 μg
9	22 μg	27.2 μg
10	40 μg	47.5 μg
Blank	0.5 μg	0.018 μg

Oil Shale Analytical Intercomparison Studies

J. S. Fruchter, J. C. Laul, and J. C. Evans

Complex samples such as oil shale materials present a considerable analytical challenge. Therefore, it is important to evaluate the precision and accuracy of various analytical methods used to determine elements and species of interest. Results can be cross checked both by using more than one analytical technique and by comparing results among different laboratories. During the past year we have been attempting to determine each element of interest by at least two methods and have been participating in several interlaboratory comparisons.

Some of the results for one intercomparison sample are shown in Table 4.3. As can be seen, the data were obtained by three different laboratories using four different analytical techniques. In most cases, the agreement is quite good. This good agreement shows that analysts using modern techniques can achieve uniform and reliable results. Other elements for which intercomparisons are available are listed at the bottom of the table.

TABLE 4.3 Intercomparison Study - Spent Shale Livermore S-11

Analyst	Technique	As	Ca	Fe	Sr	Zn
LBL	(NAA)	65 ± 3	14.0 ± 0.6	3.06 ± 0.04	-	-
BNW	(NAA)	68 ± 3	15.1 ± 1.5	3.28 ± 0.05	1076 ± 60	-
LBL	(XRF)	56 ± 3	12.3 ± 0.1	2.94 ± 0.04	944 ± 40	116 ± 4
BNW	(XRF)	58 ± 5	15.7 ± 0.7	3.35 ± 0.75	990 ± 70	125 ± 5
CSM	(XRF)	60 ± 2	15.6 ± 0.5	3.23 ± 0.25	1070 ± 25	105 ± 4
BNWL	(AA)	-	13.9 ± 0.5	3.20 ± 0.31	960 ± 62	-
LBL	(ZAA)	-	-	-	-	109 ± 4

LBL = Lawrence Berkeley Laboratory

BNW = Battelle Northwest

CSM = Colorado School of Mines

Note:
Additional Elements for which Intercomparisons will be Available on Shale and Spent Shale

- Al, Si, Sc, Ti, V, Cr, Mn, Co, Ni, Cu, Se, Mo, Cd, Sb, Cs, Ba, La, Sm, Eu, Hg and Pb

A New Procedure for Analysis of Polynuclear Aromatic Hydrocarbons (PAH)

M. R. Petersen and P. W. Ryan

The usual analytical techniques for PAH compounds involve a separation and preconcentration procedure which may require several days before the PAH's in the sample can be determined quantitatively. One of our efforts during the past year has been to develop a new analytical procedure that is faster than the more lengthy versions and at the same time just as selective and sensitive for PAH's.

Our technique in its present form consists of a GC/MS analysis with selected ion monitoring at the desired m/e ratio; e.g., m/e = 252 for benzofluoroanthenes, benzopyrenes, and perylene. Further selectivity is achieved through use of the appropriate gas chromatography stationary phase and use of argon as a chemical reagent gas. The use of argon as the charge exchange agent is the unique feature that differentiates this technique from other reported procedures using GC/MS. More importantly, the use of argon increases selectivity and sensitivity at least another order of magnitude over other chemical ionization (CI) techniques.

We have used a variety of liquid stationary phases on Chromosorb W with efficient 2-foot packed columns. The liquid phases, SP2100 (SE-30) and SP2250 (OV-17), are stable over long time periods and perform well with temperature programming. Hence, a variety of PAH's can be determined quantitatively. For more sophisticated separations of the isomeric sets such as $C_{20}H_{12}$ (mol wt 228) $C_{22}H_{12}$ (mol wt 252), or $C_{22}H_{12}$ (mol wt 276), etc., we use the high temperature liquid crystal stationary phase N,N'-bis(p-phenyl-benzylidene) α,α'-bi-p-toluidine (BPhBT) developed by researchers at NCI. Its use is limited to isothermal runs at temperatures above the solid nematic transition, 260°C. The liquid crystal phase (3% on Chromosorb W 100-120 mesh AW-DMCS) may be stable for several weeks.

The concentrations of some selected PAH's were determined in the following synthetic fuels: 4 different shale oils from aboveground retorts, 3 light distillates, 2 middle distillates, 3 heavy distillates, 2 solvent refined coals from the SRC (PAMCO) process and Prudhoe Bay crude for comparative purposes. For a comparison of the average benzo(a)pyrene content in these sample types, see Figure 4.3.

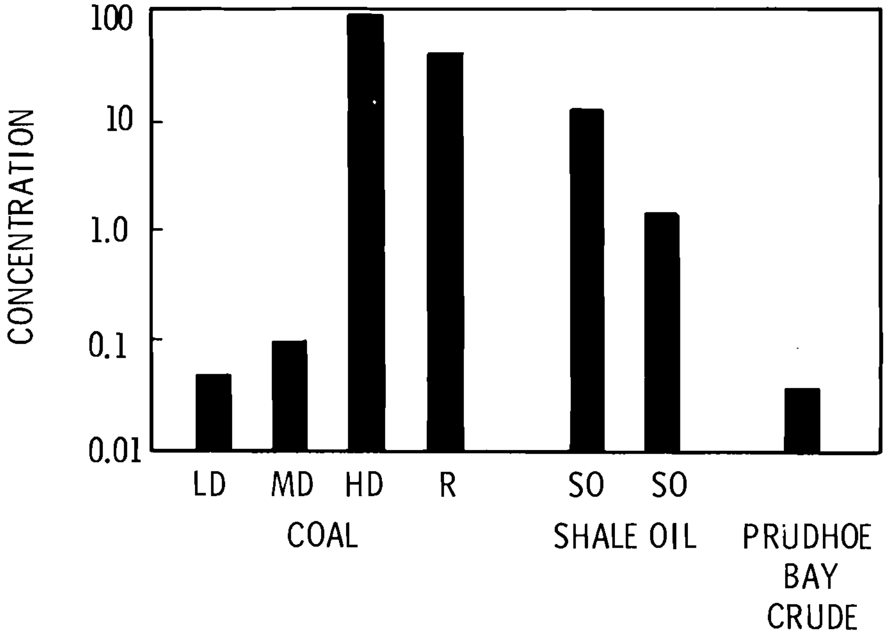

FIGURE 4.3. Comparisons of BaP Concentrations

5.0

Multitechnology

MULTITECHNOLOGY

- Environmental Pollution Analysis—Instrument and Methods Development
- Environmental Pollutant Characterization by Direct-Inlet Mass Spectrometry (DIMS)
- In Situ Pollutant Measurements
- Trace Constituent Analysis by Laser Excitation
- Applications of Holography

• Environmental Pollution Analysis—Instrument and Methods Development

Assessment of energy-related pollutants at their sources and effluents transported through the environment calls for reliable analytical instruments and methods. Analysis methods have been developed for measurement of the chemical forms and quantities of priority pollutant elements, including 1) arsenic, copper, and mercury in fresh, geothermal, and sea waters by precipitation and X-ray fluorescence; and 2) copper, lead, zinc, cadmium, selenium, chromium, and nickel by cathodic stripping voltammetry, and differential pulse polarography. Method development has been completed to allow X-ray fluorescence analysis of sized coal fly ash, urine, and hair. The use of plasma emission spectroscopy is also being evaluated for some 70 pollutant elements.

Plasma Emission Spectroscopy Utilization for Pollutant Analysis

J. C. Evans

A plasma emission spectrograph is being evaluated for elemental analysis of pollutant elements in a variety of environmental matrices. The instrument utilizes a direct discharge argon plasma for its excitation source. Liquid samples are introduced into the plasma by a peristaltic pump nebulizer system. The argon arc of 6000°K minimizes chemical interferences which have commonly plagued atomic absorption analysis. About 70 elements can be measured with this technique. Some elements, such as boron, can be analyzed more easily with greater sensitivity with this system than with atomic absorption or other techniques.

Instrument Development for the Measurement of Organometallics from Energy Production Which May Be Found in Environmental Materials

J. A. Campbell, W. C. Weimer, and N. A. Wogman

Molecular characterization or speciation studies are now underway on organometallic substances which may reside in the environment after release from energy production sources. These toxic compounds normally are found at pico- to nanogram levels in the environment. The detection and identification of such organometallic compounds in the environment present some challenging analytical problems in species collection, species separation from natural matrices, and quantitative identification.

Entrapment on solid adsorbents such as iodine crystals, activated carbon, or silicon rubbers on Chromosorb and condensation in cold traps or baths are the primary methods for the collection of volatile organometallic compounds from air. Gas chromatography and liquid chromatography, coupled with flameless or normal atomic absorption spectrometry, are being employed for separation and detection of the organometallic compounds.

An investigation has also been initiated to determine whether mass spectrometry and gas chromatography/mass spectrometry can identify qualitatively the organometallics which have been separated from environmental materials by a high precision liquid chromatograph column. Mass spectrometry has been used extensively to identify and study individual pure organometallics; however, thus far there have been only limited applications of GC/MS for qualitative and quantitative analyses of organometallic compounds in complex mixtures normally found in environmental materials.

Electrochemical Trace Analysis of Se, Cr, and Ni Species in Environmental Samples

W. C. Weimer and J. C. Kutt

Highly sensitive electrochemical methods are extremely valuable in environmental sample analyses since they respond to individual chemical species. While the usefulness of anodic stripping voltammetry for analysis of low levels of Cu^{+2}, Pb^{+2}, Zn^{+2}, and Cd^{+2} has been well demonstrated, the techniques of cathodic stripping voltammetry and differential pulse polarography have been less extensively investigated. We have been examining these methods for the analysis of Se, Cr, and Ni species in samples from environmental systems.

Cathodic stripping voltammetry with a hanging mercury drop electrode has been used for the analysis of Se^{+4} in several different environmental waters. These include the steam condensate from a geothermal power plant, the seawater leachate of air filters collected near a smelter, and the scrubber waters from an aerosol sampling train used around the Colstrip, Montana, coal-fired steam plant. The detection limit for Se^{+4} in these types of matrices is approximately 0.5 ppb for a 15 ml sample. This high sensitivity, when combined with selective oxidizing and reducing agents, will provide the capability to analyze sub-ppb levels of Se^{-2}, Se^{0}, Se^{+4}, and Se^{+6} in environmental samples.

Differential pulse polarography of Cr^{+6} and Ni^{+2} is also being evaluated for environmental sample analyses. Our limited work thus far has demonstrated very good linearity and reproducibility in the 25-100 ppb concentration range. Present limits of detection for these metal species are approximately 7-9 ppb.

Analysis of Copper in Sea Water by Anodic Stripping Voltammetry (ASV)

E. A. Crecelius and J. M. Gurtisen*

Anodic Stripping Voltammetry (ASV) is an electroanalytical technique that has been used in our laboratory and on shipboard to measure copper in Northwest Coastal waters. Values for total copper and complexed copper are being routinely measured.

The sensitivity and reliability of ASV is dependent upon the response from the working electrode--a Mercury Film Electrode (MFE). The film is deposited on a glassy carbon surface. Copper from the surrounding medium amalgamates with mercury at a specific potential and is subsequently released as the potential is increased in the positive direction. Special preparation of the glassy carbon surface has resulted in the dependability of ASV as an analytical tool.

Deterioration of the electrode can be recognized when severe baseline deviations are detected. A wet lapidary wheel combined with granulated silica as an abrasive is used to resurface the electrode. A distinct carbon deposit becomes apparent on the disk when buffed for one minute at 1800 RPM. A new mercury film is applied by reducing Hg^{+2} at the electrode surface from a 1mg/l solution at -1.0 volts for 45 sec. Measurement of copper concentrations >40 ng/l are being made with this electrode.

Copper concentrations in sea water were determined after treatment to ultraviolet light (U.V.), ozone and acid oxidation in order to release bound copper. ASV is sensitive only to free ionic or labile forms of copper. Acid oxidations of samples at pH 2.2 released the bound copper. No significant increase in measurable copper was obtained by further exposure of the oxidized sample to either ozone or U.V. light. Independent ozone or U.V. light treatments do release some bound copper.

The ASV will not respond to added Cu^{+2} if there is a complexing capacity in sea water. It will respond linearly when all complexing sites are filled. Natural pH levels are maintained while the added copper is allowed to age or complex. Analysis is underway that will determine the effect of plating voltages on complexed copper determinations. Typical copper complexation capacities for Pacific Northwest marine waters range from 5-90 μg Cu/l.

Modification of the Arsenic Speciation Technique Using Hydride Generation

E. A. Crecelius

Several modifications of the arsenic speciation technique that was developed several years ago by Braman and co-workers

---

*Ecosystems Department

have been made. Modifications include adding three additional traps to the system. These are: a water vapor trap, a second CO_2 trap, and a H_2S trap.

A major problem has been water vapor freezing out in the arsine trap, thus causing changes in the gas flow rate through the system. By adding a water vapor trap between the sample reaction chamber and the arsine trap, this problem was eliminated. The water vapor trap is constructed of 8 mm glass tubing as a U-tube with 10 cm long arms, and in operation, it is immersed in an icewater/salt bath.

Samples that contain relatively high concentrations of CO_2 or H_2S, such as wine and geothermal waters, may require special handling to avoid interferences from these gases. Two approaches have been used. Either the sample is acidified and degassed in the reaction chamber for 5 min at 500 ml/min to remove the H_2S and CO_2, or a H_2S trap and an additional CO_2 trap are added to the system. The lead acetate trap (8 mm x 8 cm long glass tube packed with lead acetate) is connected between the water vapor trap and the arsine trap. The additional CO_2 trap (8 mm x 8 cm glass tube packed with NaOH beads) is connected between the water vapor and the H_2S trap.

Experimentally, it was discovered that after the water, CO_2 and H_2S traps were dried and repacked, more consistent results were obtained if the system was "sensitized". This was accomplished by processing a high concentration of standard (50 μg As^{+3} and 100 μg DMAA) through the normal procedure for As^{+3} but not using the detector. After this was complete, the reaction chamber was carefully cleaned, and several reagent blanks were run before the system was standardized. This "sensitizing" procedure apparently saturates arsine absorption sites in the system and decreases the number of analyses required to obtain reproducible calibration curves.

XRF Peak Analysis Method

K. K. Nielson

A novel method for direct analysis of overlapping X-ray peaks has been developed from a unique property of our direct peak analysis method. The overlapping peak analysis takes advantage of the cancellation of equal positive and negative error lobes which result from the interfering peak in the carefully chosen adjacent analysis window. The method has been applied to uranium determination in ores and soils containing high concentrations of the interfering elements Rb and Mo. The U L_α peak was used, and was separated from Rb K_α by 0.78 x FWHM. Detection limits of 7.8 ppm U were obtained in the presence of over 100 ppm Rb.

XRF Analysis of Sized Coal Fly Ash

K. K. Nielson, J. A. Campbell, J. C. Laul, and R. D. Smith

A matrix correction method recently developed at Battelle, Pacific Northwest Laboratories, for XRF analysis of environmental samples was evaluated in the analysis of 29 elements in nine carefully sized fractions of coal fly ash. Comparisons of the results were made with replicate analyses by neutron activation and atomic absorption.

The intercomparison permitted the first meaningful test of the corrections for particle size effects in samples of uniform known particle size. Particle size fractions had mass median diameters of 0.5, 2, 4, 5, 9, 13, 16, 25 and 50 microns, and required corrections of over 50% in concentrations of light elements such as Si and S for particle size effects. The results showed excellent agreement between the various analytical methods despite completely independent calibration methods. The particle size corrections were also demonstrated to be adequate, with no significant particle size-related error being observed.

PIXE Analysis of Fly Ash

K. K. Nielson, N. A. Wogman, J. A. Campbell, and N. F. Mangelson*

An experiment was initiated to measure concentration gradients as a function of depth in coal flyash particles using proton-induced X-ray emission (PIXE). By varying the energy of the exciting protons, varying depths of penetration were achieved in the pelletized flyash samples. Proton energies ranging from 0.4 to 2 MeV were used, and indicated possible weak concentration gradients for several volatile elements in large particles. The minimum depth range covered by this method is on the order of several microns, much greater than traditional "surface" analytical methods such as ESCA.

---

*Brigham Young University

Urine Analysis by XRF

K. K. Nielson and W. D. Felix

A method has been developed for preconcentration of urine samples for multielement analysis by XRF. The procedure consists of an evaporation step, a drying/decomposition step, and a pelletizing step which avoids the potential contamination and chemical recovery problems typical of ion-exchange and precipitation methods.

Quantitative analysis of the resulting pellets gives detection limits in the 10 ppb concentration range for many important transition metals as indicated in Figure 5.1. The two detection limit lines resulted from extremely different degrees of decomposition before pelletizing. The potential rapidity, low cost and wide scope of this mulielement analytical approach make it excellent for screening, diagnostic and basic research on a scale previously impossible.

Hair Analysis by XRF

K. K. Nielson and W. D. Felix

Preliminary tests of a rapid new method for XRF analysis of hair samples have proved highly successful. The method will permit direct quantitative analysis of an unweighed mass of hair, thus eliminating the current most costly analytical step, sample preparation. The mass of hair actually in the X-ray beam and its self-absorption coefficients and other parameters are all estimated from the coherent and incoherent backscatter peaks from the exciting radiation. At least 14 elements are detectable in a single analysis of "normal" hair, including sulfur, which was analyzed with excellent accuracy relative to reported mean values of 4.1%.

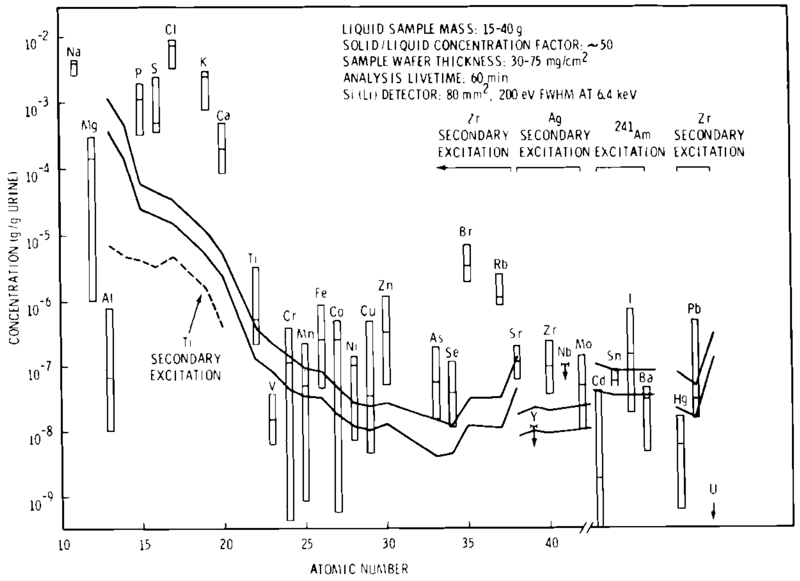

FIGURE 5.1. "Normal" Urine Element Ranges and X-Ray Fluorescence Detection Limits

• Environmental Pollutant Characterization by Direct-Inlet Mass Spectrometry (DIMS)

The utility of direct-inlet mass spectrometry for the detection, characterization and monitoring of important particulate airborne pollutants which arise as by-products of energy production activities is being experimentally determined. The first phase of this new program was the design and assembly of a direct-inlet mass spectrometer system. This was completed in FY-1977. Performance tests of the new instrument are in progress.

Characterizing Environmental Pollutants by DIMS

C. R. Lagergren

Direct-Inlet Mass Spectrometry (DIMS) is a new analytical technique which offers potential advantages in the detection, characterization and monitoring of airborne environmental particulate pollutants. It combines the inherently high sensitivity of surface ionization mass spectrometry with an air sampling system which then makes possible the measurement (on a real-time basis) of pollutant material as it exists in the air. No sample collection or processing procedures are required. In this technique, air that contains particles is introduced as a jet directly into the ion source of a surface ionization mass spectrometer. Particles striking the hot filament form bursts of ions which are then mass analyzed and measured. Burst rates are related to particle concentration in sampled air while the total charge per burst is a measure of particle size.

The sensitivity of the DIMS technique has been demonstrated(1,2) to be sufficiently high to detect individual particles containing Li, Sr, U, Cr, and Pb as small as a few hundredths of a micrometer in diameter. The sensitivity is fundamentally limited by the ionization efficiency attainable for the material involved.

In addition to its high sensitivity, if a characteristic spectrum can be produced from a given material, the technique offers the possiblity of identifying the particle composition as well.

The purpose of this program is to determine experimentally the utility of the DIMS technique for the detection, characterization and monitoring of important particulate airborne pollutants which arise as by-products of energy generating activities. To do this, it is necessary to determine the nature of the ionization produced from specific pollutant materials by surface ionization. The ionization efficiency, cracking patterns (ion spectrum), and time history of signals produced are functions of the nature and temperature of the filament surface as well as the molecular and physical form of the material itself. These quantities and relationships are unknown and need to be developed for successful application of the technique.

The first phase of this program, and the main objective for FY-1977, was the design and assembly of a DIMS system suitable for performing the needed experiments. Figure 5.2 is a schematic representation of the system constructed. The air inlet system is essentially the same as that developed for the DIMS plutonium monitor(3) and provides an adequate beam of particles directed onto a surface ionization filament. A quadrupole mass filter was selected as a mass analyzer for the ions produced because of its ability to be rapidly switched so that selectable portions of the mass spectrum may be observed in a nearly simultaneous fashion. It is positioned with its axis intersecting and perpendicular to that of the particle beam.

A vacuum barrier with a 1/16 in. diameter hole is interposed between the surface ionization filament and the quadrupole in order that the pressure in which the quadrupole operates can be held as low as possible in order to minimize interfering background spectra. The ionizer of the quadrupole was modified so as to provide efficient entrance of ions from the surface ionization filament and at the same time permit ionization by electron impact of the neutral products formed as well. Performance tests of the assembled system are in progress.

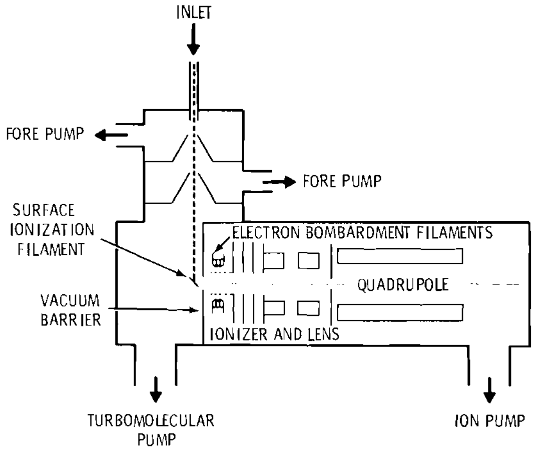

FIGURE 5.2. Schematic Representation of a Direct-Inlet Spectrometer

• **Trace Constituent Analysis by Laser Excitation**

A high resolution pulsed dye laser has been interfaced to a minicomputer for interactive control and data aquisition. This system has been used to study and develop analytical methods for both gas phase polynuclear aromatic hydrocarbons (PNA's) and noble gases. Detection limits of low parts per trillion have been demonstrated for PNA's. Two photon excitation spectra of xenon have shown some isotopic hyperfine structure.

Laser Excitation Application to Trace Constituent Analysis

B. A. Bushaw and T. J. Whitaker

PNA Detection

One of the most difficult analytical problems currently facing environmental studies is the analysis of complex mixtures of "large" molecules at trace levels. The development of real time or near real time methods of analysis is desirable in view of the time involved in analysis by currently accepted methods involving various chromatographic techniques. Laser excitation techniques offer the capability of real time analysis with high sensitivities. However, in real time analysis, there is no opportunity for sample preparation. Thus, careful consideration must be given to the interaction of the subject molecules with a varying carrier matrix if a reliable and reproducible method is to be developed. We have studied the effect of sample conditions on the laser induced fluorescence analysis of gas phase polynuclear aromatic hydrocarbons (PNA's) and found that emission intensities may vary greatly with carrier gas and temperature.

Using pyrene as a representative PNA, we have investigated the effect of atmospheric constituents and sample temperature on relative fluorescence quantum yield. Both a frequency doubled nitrogen laser pumped dye laser and the fourth harmonic of a Nd:YAG laser (266 nm) were used as exciting sources. Plotting the values of vapor pressure as a function of 1/T (a Clausius-Claperyon plot) gave a linear dependence indicating fluorescence to be exponentially dependent upon temperature in the following way:

$$I = A \times 10^{\alpha/\tau}$$

We have determined the value of α for pyrene vapor over the temperature range of 300-400°K to be 884 ± 109. This, along with the value of A, which has been determined for our system, allows the determination of the concentration of the PNA in the sample.

Quenching studies have indicated that O_2 is the only major atmospheric constituent which appreciably attenuates fluorescence intensity in pyrene vapor. Figure 5.3 shows the Stern-Volmer plots of pyrene vapor emission intensity as a function of the log of the partial pressure of both O_2 and N_2 in the sample. From the slope, the quenching rate constant for

$$\text{Pyrene}^* + O_2 \rightarrow \text{Pyrene} + O_2^*$$

is determined to be: $k_1 = 4.0 \pm 0.1 \times 10^{10}$ liter mole^{-1} sec^{-1}.

Since O_2 produces such strong quenching, it would be desirable to pretreat samples by cold trapping the PNA's and then releasing them in a noble gas carrier to provide a maximum sensitivity. In experiments with no O_2 in the sample, we have shown that detection limits in the low parts per trillion range are easily attainable. Even with O_2 present, as would be the case for real time atmospheric analysis, detection limits of about 10 ppb are still possible.

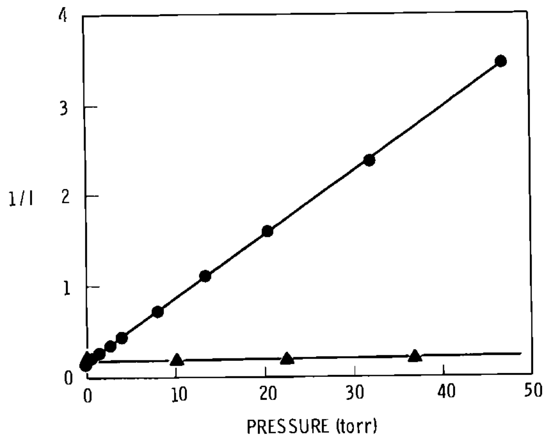

FIGURE 5.3. Stern-Volmer Plots Showing Quenching Effects of Buffer Gases on Pyrene Vapor Fluorescence Intensity: ● O_2, Δ N_2

Two Photon Excitation of Xenon

During the last year, the efforts for development of an isotopically selective method of analysis for noble gases have continued. The previously observed $^1D_2 \rightarrow {}^1S_0$ two-photon excitation of xenon has been examined with higher resolution (Figure 5.4). Some structure, which is attributed to isotopic hyperfine splitting, has now been observed. This structure indicates that the hyperfine splitting constants are on the order of several gigahertz, in agreement with earlier theoretical calculations. Before development into an analytical procedure, further work using higher resolution Doppler cancelling techniques to resolve the isotopic peaks must be carried out. A system which places the sample inside a high resolution confocal interferometer to provide standing wave excitation is currently under development.

Laser Control and Data Acquisition

Computer acquisition, interface to the laser system, and software development were important projects for this year. We now have a minicomputer interactively coupled to the laser system through a versatile system of analog-to-digital, digital-to-analog, and special purpose interfaces. Programs which align the many tuning elements of the laser have allowed the spectrum in Figure 5.4 to be taken at a resolution which was previously impossible by manual tuning of the laser system. These programs also permit continuous high resolution scanning over a range limited only by the output of the dye used in the dye laser. The computer also is used for rapid data acquisition, storage, and analysis.

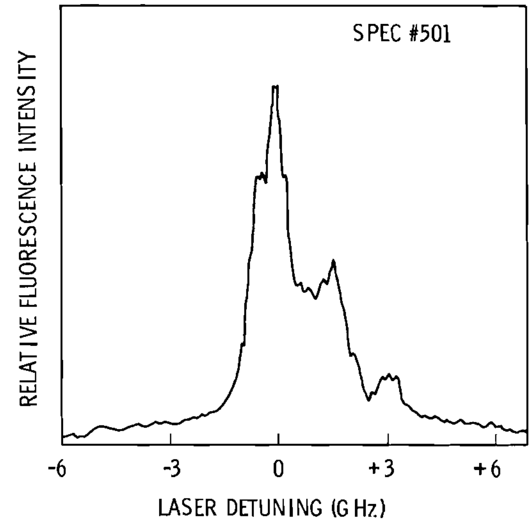

FIGURE 5.4. Two Photon Fluorescence Excitation Spectra of Xenon $^1D_2$ State Showing Partially Resolved Structure

• Applications of Holography

Holography with short laser pulses is being studied to determine its applicability to environmental problems. It has been established that if a simple portable holo-camera were available it would find use in the field and laboratory for characterizing the physical properties and behavior of aerosols, particulates and underwater organisms. To this end we have designed and built such a camera.

Applications of Holography to Environmental Studies

B. P. Hildebrand

Holography, invented in 1948, is a photographic technique capable of recording a scene in three dimensions. This record, the hologram, can be used to reconstruct the scene for later study. The reconstruction is so perfect that it can be used to make precise measurements by means of interferometry, for example. The invention of the laser in the 1960's resulted in a rapid expansion in research of holography and the search for applications. The pulsed laser, in particular, imparted a momentum in the direction of particle holography since transient events could be recorded and studied in the laboratory.

Observations

Commercial pulsed ruby lasers are very expensive and cumbersome, usually weighing hundreds of pounds and requiring a source of power. This is probably the major reason that holography has not reached its full potential in any but the most specialized applications. During this year we succeeded in building a small battery-powered ruby laser starting with a Metz 402 photographer's flash unit. We also adapted a 35 mm Pentax camera body to hold Kodak SO-173 film on which Gabor holograms are recorded. The photograph on Figure 5.5 shows the flash unit with its battery pack, and the Pentax camera.

The laser cavity was made from 20 mm I.D., 50 mm long, quartz tubing silvered on the outside and capped with flat mirrors. A commercial 2 mm x 50 mm ruby rod, reflection coated on both ends, was mounted along side the flashlamps near the center of the tube. Figure 5.6 shows the components and Figure 5.7 the completed cavity. The flash lamp is triggered by the camera using all the existing circuitry in the camera and flash unit. The completed camera (in breadboard form) is shown in Figure 5.8. The aerosol or target to be recorded is introduced between the camera and laser. The laser beam is, of course, expanded to fill the aperture of the camera. Note also the narrow band filter in place of a lens in the camera. This filter blocks out all the ambient light so that the camera can be used in full sunlight.

Measurements indicate that full output of the laser is 12-15 milli-Joules, enough to overexpose the film. We have, therefore, modified the flash unit to shorten the length of the pulse to provide optimum exposure. This was done by utilizing an existing circuit in the unit. Figure 5.9 is an example of the image of two water droplets (about 100 μm) in a cloud of spray, taken with this camera.

Conclusions

We have succeeded in building a light portable ruby laser at very low cost. This laser is adequate for obtaining holograms of slow moving aerosol clouds and particles (1 mm/sec). For faster motion, we will need to build a Q-switch to shorten the pulse from its current 1-2 msec. This will be done with the same goal of simplicity and portability.

FIGURE 5.5. Flash Unit with Battery Pack and Pentax Camera for Use in Ruby Laser System

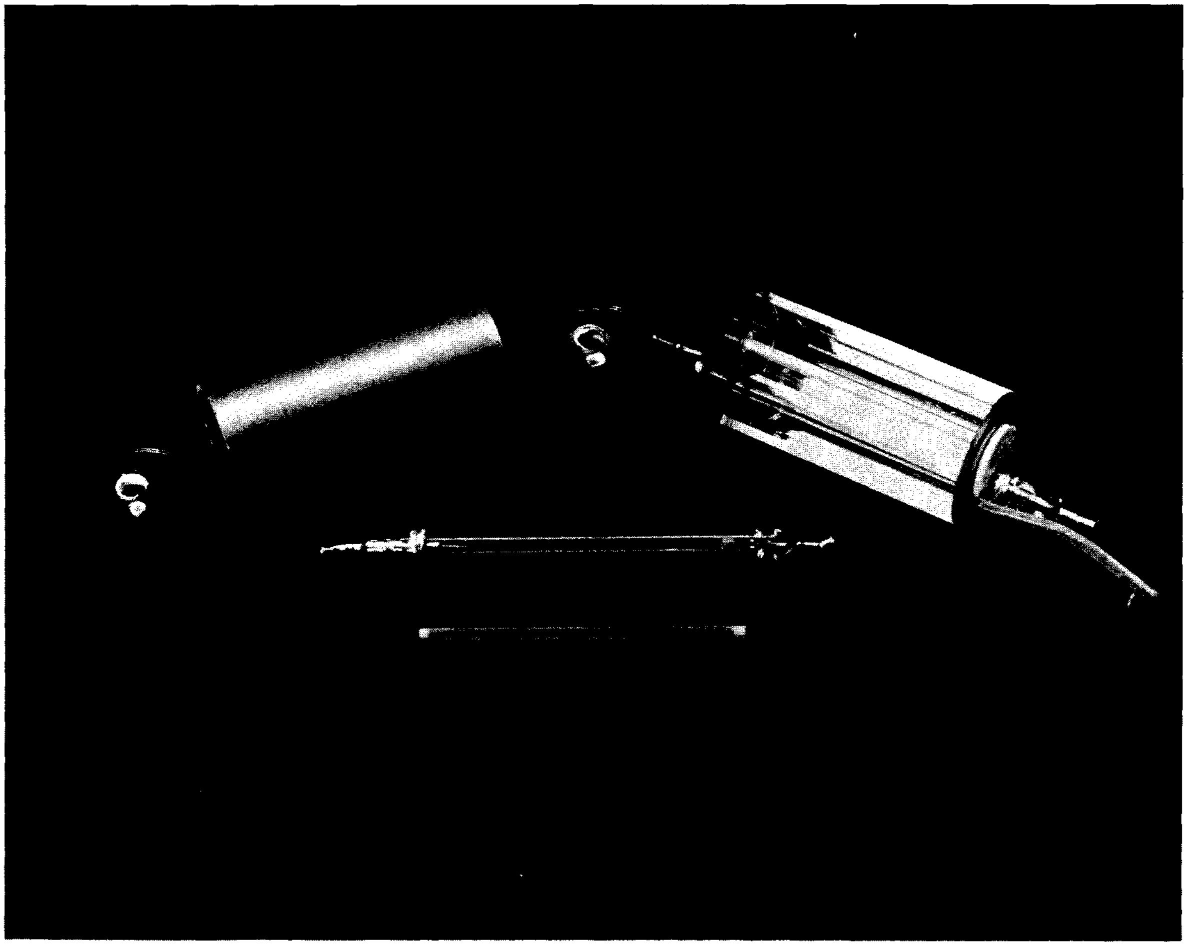

FIGURE 5.6. The Components for the Ruby Laser Cavity

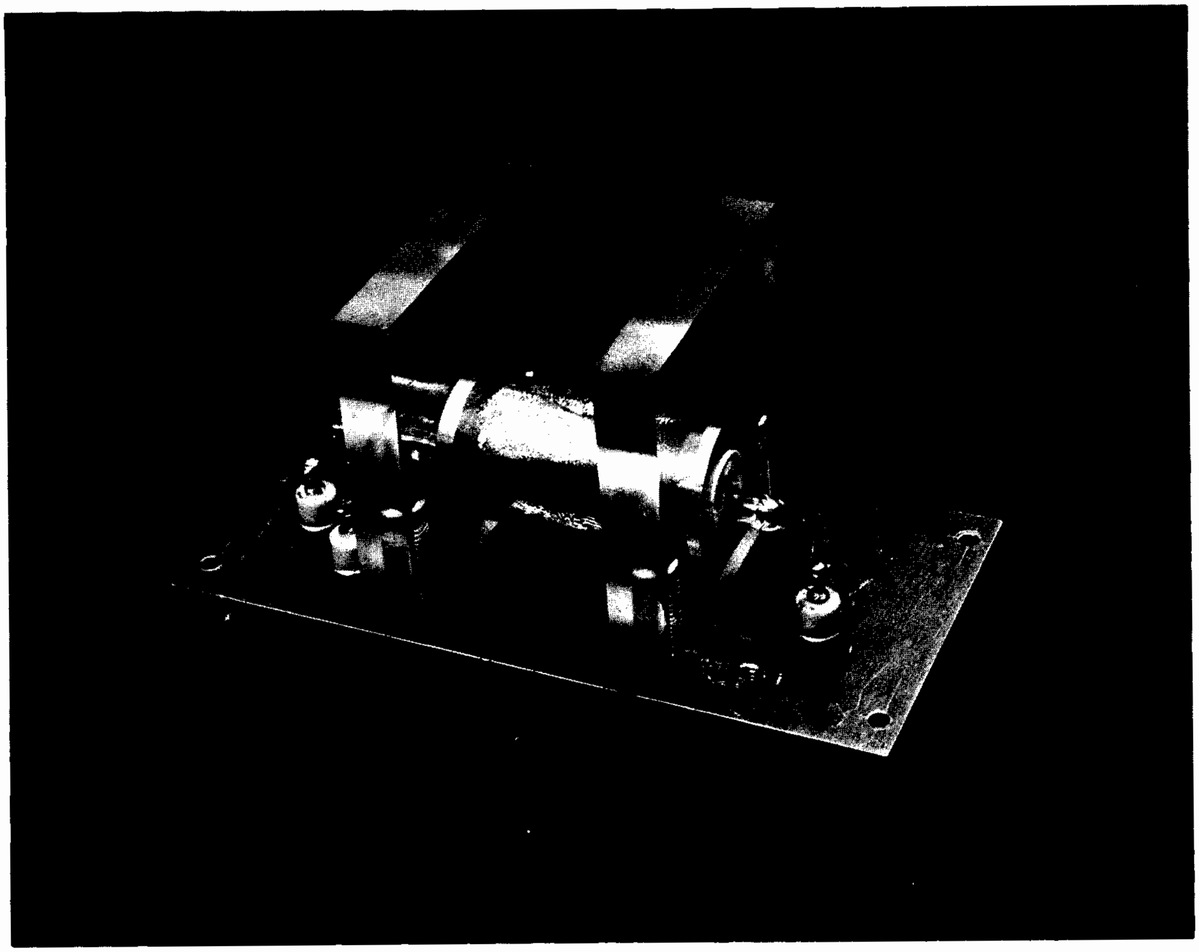

FIGURE 5.7. The Completed Ruby Laser Cavity

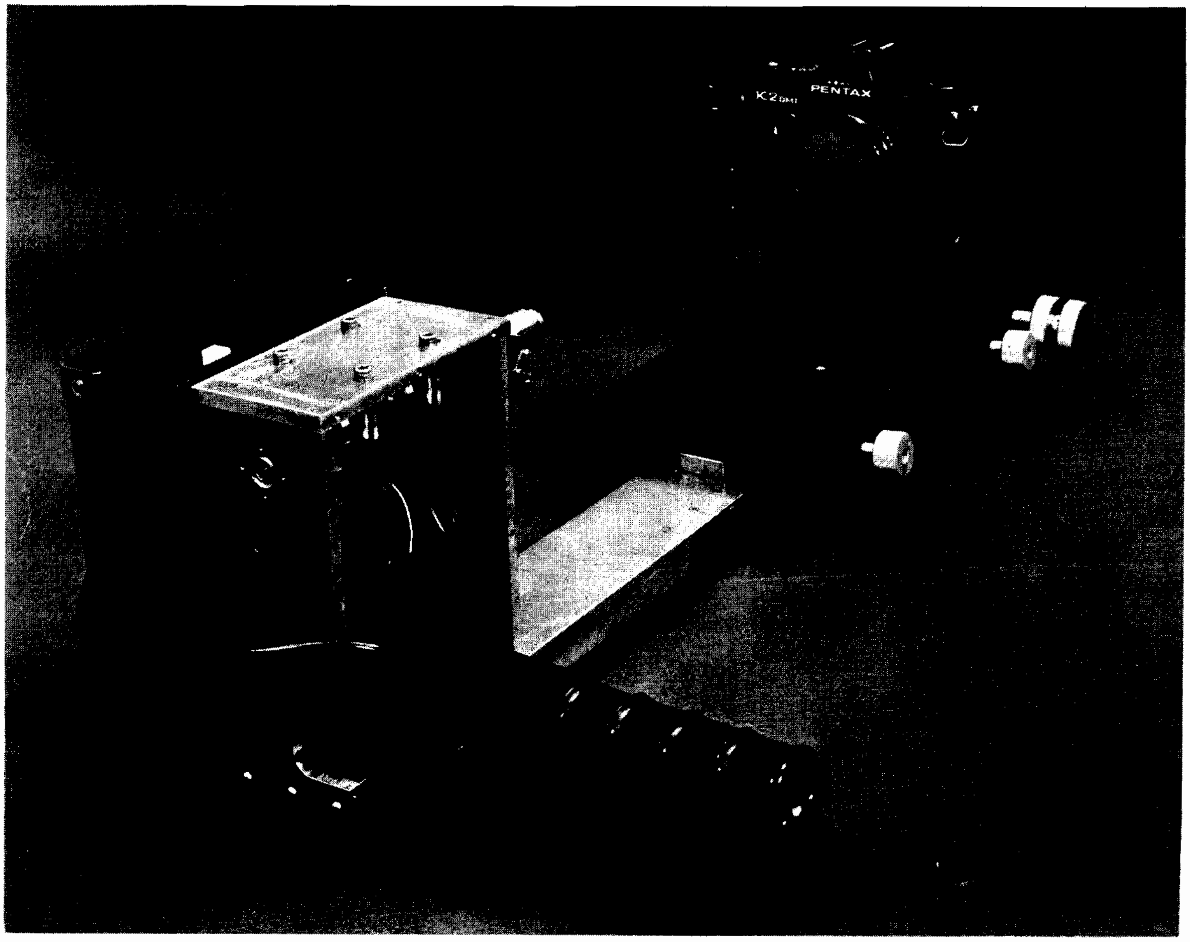

FIGURE 5.8. The Completed Camera System for Ruby Laser Holography Use

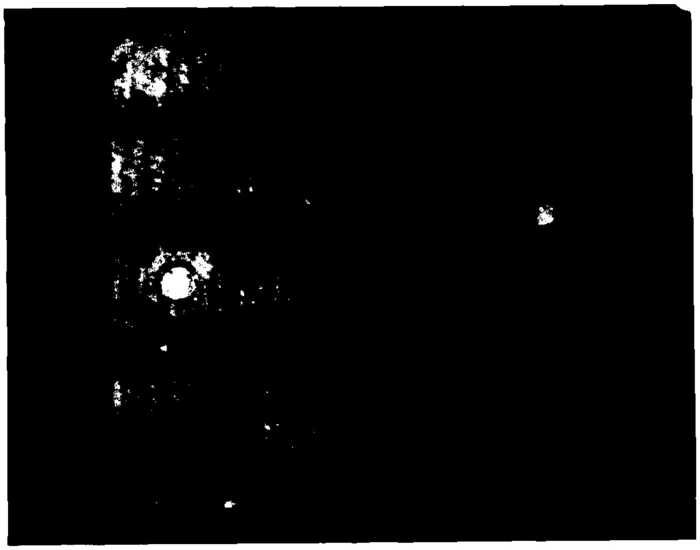

FIGURE 5.9. A Ruby Laser Image of Two Water Droplets (about 100 μm) in a Cloud of Spray

5.0 REFERENCES

1. W. D. Davis, "Continuous Mass Spectrometric Analysis of Particulates by Use of Surface Ionization." Environ. Sci. Tech. 11:587-592, 1977.

2. W. D. Davis, "Continuous Mass Spectrometric Determination of Concentration of Particulate Impurities in Air by Use of Surface Ionization." Environ. Sci. Tech. 11:593-596, 1977.

3. J. J. Stoffels and C. R. Lagergren, "Fast Real-Time Measurement of Extremely Low-Level Airborne Plutonium," in Pacific Northwest Laboratory Annual Report for 1977. PNL-2500 PT4, Battelle, Pacific Northwest Laboratories, Richland, WA 99352, 1978.

PUBLICATIONS AND PRESENTATIONS

PUBLICATIONS

Abel, K. H. and E. A. Crecelius, "Copper Speciation in Sea Water Determined by Anodic Stripping Voltammetry." Abstract to be published by AAS from presentation at AAS meeting, Denver, CO, Feb. 23-25, 1977.

Anders, O. U., J. I Kim, H. I. Al-Shahristani, R. L. Brodzinski, G. F. Clemente, R. Cornelis, J. J. M. DeGoeij, F. Girardi, G. Guzzi, K. Heydorn, L. Kosta, F. Lux, S. Meloni, J. Mitchell, J. W. Morgan, J. V. Niewobniczanski, R. M. Park, J. Pauwels, T. G. Pierce, H. Rook, B. Sansoni and R. E. Wainerdi, "Representative Sampling and Proper Use of Reference Materials." Anal. Chem. 49:33A, 1977.

Beamer, J. L., M. M. Malin, G. W. R. Endres, F. T. Cross and M. F. Sullivan, "Ureteral Dosimetry of Swine Exposed to Intracervical Irradiation." Radiation Research 67:558, 1976.

Bishop, J. K. B., J. M. Edmond, D. R. Ketten, M. P. Bacon and W. B. Silker, "The Chemistry, Biology, and Vertical Flux of Particulate Matter from the Upper 400 m of the Equatorial Atlantic Ocean." Deep-Sea Research, 24:511-548, 1977.

Braby, L. A., W. C. Roesch, and J. M. Nelson, "Temperature Effect on the Production and Repair of Radiation Damage in Chlamydomonas reinhardi." Radiation Research 70:684, 1977.

Brodzinski, R. L., J. C. Langford, M. T. Thomas and O. K. Harling, "Rapid Chemical Separations for Thermal Neutron Activation Analysis of Niobium and Vanadium and Application to Controlled Thermonuclear Reactor Materials Studies." J. Radionanal. Chem. 38, No. 1:179-184, 1977.

Chaturvedi, R. P., D. J. Lynch, L. H. Toburen and W. E. Wilson, "Molecular Effects in K-Shell Ionization of Fluorine." Phys. Lett. 61a:101-103, 1977.

Crecelius, E. A., "Arsenite and Arsenate Levels in Wine." Bull. of Environ. Contam. & Toxicol. 18:227-230, 1977.

Crecelius, E. A., "Changes in the Chemical Speciation of Arsenic Following Ingestion by Man." Environ. Health Persp. 3:147-150, 1977.

Crecelius, E. A., D. E. Robertson, J. S. Fruchter and J. D. Ludwick, "Chemical Forms of Mercury and Arsenic Emitted by a Geothermal Power Plant." Trace Substances in Environmental Health-X. pp. 287-293, 1977.

Crecelius, E. A., "Modification to the Arsenic Speciation Techniques Using Hydride Generation." Analy. Chem. (Accepted for publication).

Criswell, T. L., L. H. Toburen and M. E. Rudd, "Energy and Angular Distributions of Electrons Ejected from Argon by 5 keV to 1.5 MeV Protons." Phys. Rev. A. 16:508-517, 1977.

Cross, F. T., G. W. R. Endres and M. F. Sullivan, "Dose to the G. I. Tract from Ingested Insoluble Beta Emitters." Radiation Research. (In press).

Dionne, P. J., T. P. Harrington, D. L. Stevens, F. T. Cross and G. E. Dagle, "Modeling the Early Translocation of Inhaled $^{239}Pu(NO_3)_4$ in Dogs." Health Physics Society Twenty-Second Annual Meeting, July 1977. (Abstract)

Fruchter, J. S., J. C. Laul, P. W. Ryan, M. R. Petersen and M. E. Turner, "High Precision Trace Element and Organic Constituent Analysis of Oil Shale and Tar Sands." Advances in Chemistry Series, American Chemical Soc. (In press).

Fruchter, J. S., M. R. Petersen and P. W. Ryan, Quarterly Progress Report--Characterization of Substances in Products, Effluents and Wastes from Synthetic Fuel Development Processes. BNWL-2224, Battelle, Pacific Northwest Laboratories, Richland, WA 99352, January 1977.

Gordon, R. L., F. P. Brauer, D. M. Robertson and H. G. Rieck, Jr., Monitoring Methods for Particulate and Gaseous Effluent from Waste Solidification Processes. BNWL-2229, Battelle, Pacific Northwest Laboratories, Richland, WA 99352, March 15, 1977.

Kalkwarf, D. R. and D. L. Frasco, "Lysis of Phospholipid Membranes with Radiation-Induced Free Radicals." Radiation Research 70:647, 1977, (Abstract).

Kalkwarf, D. R., Safety Evaluation of Cation Exchange Resins. BNWL-2391, Battelle, Pacific Northwest Laboratories, Richland, WA 99352, August 1977.

Kaye, J. H., J. S. Rapids and N. E. Ballou, "Determination of Subpicogram Levels of Technitium-99 by Isotope Dilution Mass Spectrometry." BNWL-SA-6254S, Battelle, Pacific Northwest Laboratories, Richland, WA 99352, April 12, 1977.

Laul, J. C. and L. A. Rancitelli, "Multielement Analysis of Sequential Instrumental and Radiochemical Neutron Activation." J. of Radioanalytical Chem. 38:461-475, 1977.

Ludwick, J. D., T. D. Fox and S. R. Garcia, "Elemental Concentrations of Northern Hemispheric Air at Quillayute, Washington." Atoms. Environment 11:1083-1087, 1977.

Mangelson, N. F., M. W. Hill, K. K. Neilson and J. F. Ryder, "Proton-Induced X-ray Emission Analysis of Biological Samples: Some Approaches and Applications." Nucl. Inst. & Methods 142:133-142, 1977.

Manson, S. T. and L. H. Toburen, "Energy and Angular Distribution of Electrons Ejected from Kr by 1 MeV Proton Impact Ionization: Theory and Experiment," X ICPEAC Abstracts of Papers. ed. by M. Barat and J. Reinhardt (Commissariat A L'Energie Atomique, Paris), p. 1006-1007, 1977.

Manson, S. T., L. H. Toburen and Y.-K. Kim, "Energy Distribution of Secondary Electrons Ejected from Krypton by Proton Impact Ionization," X ICPEAC Abstracts of Papers. ed. by M. Barat and J. Reinhardt (Commissariat A L'Energie Atomique, Paris), p. 988-989, 1977.

Miller, J. H. and M. L. West, "Quenching of Benzene Fluorescence in Pulsed Proton Irradiation: Dependence on Proton Energy." J. Chem. Phys. 67:2793-2797, 1977.

Miller, J. H., "Z^3 Effect in the Ionization Cross Section of Argon by 1.2 and 2.0 MeV Alpha Particles." Phys. Rev. A. (Accepted for publication).

Miller, J. H. and M. L. West, "Quenching of Flourescence in Binary Liquid Scintillators." Presented APS meeting, San Diego, March 21, 1977, published Bull. Am. Phys. Soc. 22:391, 1977.

Nelson, J. M., L. A. Braby and W. C. Roesch, "Determination of Mean Recovery Time Following Split-Dose or Portracted Irradiation." Radiation Research 70:708, 1977.

Nelson, F. W., K. K. Nielson, N. F. Mangelson, M. W. Hill and R. T. Matheny, "Preliminary Studies of the Trace Element Composition of Obsidian Artifacts from Northern Campeche, Mexico." American Antiquity 42:209-225, 1977.

Nelson, J. M., "Preparation of Monocellular Dispersions of Mammalian Neoplastic Cells from Solid Tumors," Tissue Culture Association Manual. Vol. 2, No. 2, 1976.

Nielson, H. L., N. A. Wogman and R. L. Brodzinski, "In-Situ Subterranean Gamma-Ray Spectroscopy." Nucl. Instr. & Methods 143:395, 1977.

Nielson, K. K., "Application of Direct Peak Analysis to Energy-Dispersive X-ray Flourescence Spectra." X-ray Spectrometry 7. (In press).

Nielson, K. K., "Matrix Corrections for Energy Dispersive X-ray Flourescence Analysis of Environmental Samples of Coherent/Incoherent Scattered X-rays." Anal. Chem. 49:641-648, 1977.

Nielson, K. K. and S. R. Garcia, "Use of X-ray Scattering in Absorption Corrections for X-ray Fluorescence Analysis of Aerosol-Loaded Filters." Adv. in X-ray Anal. 20:497-506, 1977.

Popowich, R. J., W. E. Wilson and L. H. Toburen, "Comparison of Electron Emission Cross Section for He Ions, Alpha Particles and Protons on Water Vapor." Radiation Research 70:618, 1977.

Reeder, P. L., J. F. Wright and L. J. Alquist, "Average Neutron Energies from Separated Delayed-Neutron Precursors." Phys. Rev. C., 15(6):2098-2107, June 1977.

Reeder, P. L., J. F. Wright and L. J. Alquist, "Delayed-Neutron Emission Probabilities of Separated Isotopes of Br, Rb, I, and Cs." Phys. Rev. C. 15(6):2108-2118, June 1977.

Reeder, P. L., L. J. Alquist and F. H. Ruddy, "Neutron and Gamma Spectroscopy of Rb, In, and Cs Delayed-Neutron Precursors." BNWL-SA-6237A, Battelle, Pacific Northwest Laboratories, Richland, WA 99352, March 29, 1977.

Robertson, D. E., E. A. Crecelius, J. S. Fruchter and J. D. Ludwick, "Mercury Emissions from Geothermal Power Plants." Science 196(4294): 1094-1097, 1977.

Roesch, W. C., "Microdosimetry Theory." Phys., Med. Biol. 22:560, 1977.

Roesch, W. C., "Microdosimetry of Internal Sources." Radiation Research 70:494-510, 1977.

Roesch, W. C., "Microdosimetry of Moving Particulates." Radiation Research 70:683, 1977.

Roesch, W. C., "Models of the Radiation Sensitivity of Mammalian Cells." Third Symposium on Neutron Dosimetry in Biology and Medicine, Munich, BNWL-SA-6288, Battelle, Pacific Northwest Laboratories, Richland, WA 99352, 1977.

Rudd, M. E., L. H. Toburen and N. Stolterfoht, "Differential Cross Sections for Ejection of Electrons from Helium by Protons." Atomic Data and Nuclear Data Tables 18:413-432, 1976.

Ryan, P. W. and M. R. Petersen, "Direct Analysis for Polynuclear Aromatic Hydrocarbons at the ppb Level by GC/MS." BNWL-SA-6469, Battelle, Pacific Northwest Laboratories, Richland, WA 99352, August 1977.

Saalfeld, F. E., J. J. DeCorpo, R. D. Smith and J. R. Wyatt, "Mass Spectrometric Studies of Low Temperature Flames. II. Concentration Profiles and Reactions of Additives in Flames." Advances in Mass Spectrometry 7, 1977.

Schneiderman, M. H., L. A. Braby and W. C. Roesch, "Division Delay After Low X-ray Doses and Treatment with Cycloheximide." Radiation Research 70:130-140, 1977.

Silker, W. B., "Comment on 'Probable Error in the Use of Cosmogenic Radionuclides of Beryllium for Ocean Transport Studies' by Thomas A. Gosink." Marine Science Communications 3(3):271-276, 1977.

Smith, T. J., E. A. Crecelius and J. D. Reading, "Airborne Arsenic Exposure and Excretion of Methylated Arsenic Compounds." Environ. Health Persp. 3:89-93, 1977.

Smith, R. D. and P. W. Ryan, "Chemical Ionization-Mass Spectrometry as a Tool for the Elimination of Surface Related Phenomena in the Spectra of Unstable Compounds." (Accepted by Analytical Chemistry), 1977.

Smith, R. D. and J. H. Futrell, "Internal Energy Effects in Proton Transfer Reactions." Advances in Mass Spectrometry 7, 1977.

Stoffels, J. J., C. R. Lagergren and P. J. Hof, "A Wide Dynamic Range Ion Detection and Measurement System." PNL-SA-6094, Battelle, Pacific Northwest Laboratories, Richland, WA 99352, 1977.

Strebin, R. S., Jr., and D. M. Robertson, "Alpha-Energy and Mass Analyses of Plutonium from a Single Sample Mount." J. of Radioanalytical Chemistry. (Accepted for publication).

Strebin, R. S., Jr. and D. M. Robertson, "Isotopic Composition Measurement on Sub-Picogram Amounts of Plutonium." Analytica Chimica Acta, 91:267-272, 1977.

Strebin, R. S., Jr., J. W. Johnson and D. M. Robertson, "Wide-Range Density Separation of Mineral Particles in a Single Fluid System." American Mineralogist, 62:374-376, 1977.

Sullivan, M. F. and F. T. Cross, "The Role of Target Cells in the Toxicity of Ingested Reactor Core Products." Radiation Research Society Annual Meeting, May 1977. (Abstract).

Sullivan, M. F., F. T. Cross, G. W. R. Endres, et al., "The Long-Term Effects of an Intracavitary Treatment with Californium-252 on Normal Tissue." Proceedings of a Symposium on Radiological Research Needed for the Improvement of Radiotherapy, Vienna, Austria, November 1976. (In press).
Paper No. IAEA-SM-212/57.

Sullivan, M. F., F. T. Cross, G. W. R. Endres, et al., "The Response of Normal Tissues to an Intracavitary Exposure from Californium-252." Proceedings of International Symposium of Cf-252 Utilitzation, Brussels, Belgium, April 1976. (In press).

Sullivan, J. F., J. L. Beamer, T. D. Mahony, F. T. Cross, J. E. Lung and G. W. R. Endres, "The Long-Term Effects of Intracavitary Treatment with Californium-252." Radiation Research. (In press).

Toburen, L. H. and W. E. Wilson, "Ionization of Noble Gases by Equal Velocity He$^+$, He^{++} and H$^+$ Ions," X ICPEAC Abstracts of Papers. ed. by M. Barat and J. Reinhardt (Commissariat A L'Energie Atomique, Paris), p. 1006-1007, 1977.

Toburen, L. H. and W. E. Wilson, "Energy and Angular Distributions of Electrons Ejected from Water Vapor by 0.3-1.5 MeV Protons." J. Chem. Phys. 66:5202-5213, 1977.

Toburen, L. H., W. E. Wilson and L. E. Porter, "Energy and Angular Distributions of Electrons Ejected in the Ionization of SF$_6$ and TeF$_6$ by Fast Portons." J. Chem. Phys. 6(9):4212-4221, November 1977.

Toburen, L. H., S. T. Manson and Y.-K. Kim, "Energy Distributions of Secondary Electrons III: Projectile Energy Dependence for Ionization of He, Ne and Ar by Protons." Phys. Rev. A., December 1977.

Weimer, W. C. and D. E. Armstrong, "Determination of Inositol Phosphate Esters in Lake Sediments." Analytica Chimica Acta 94:35-47, 1977.

West, M. and J. H. Miller, "Track Structure Effects in the Radioluminescence of Benzene in Cyclohexane." Radiation Research 70:617-618, 1977.

West, M. L. and J. H. Miller, "Quenching of Benzene Fluorescence in Pulsed Proton Irradiation: Temperature Dependence." Submitted for publication, J. Phys. Chem., 1977.

Wilson, W. E., "Radiological Physics and Dosimetry Research with a Small Positive Ion Accelerator." Proceedings of Fourth Conference on Scientific and Industrial Applications of Small Accelerators, CONF-761059, pp. 481-492, 1976.

Wilson, W. E., A Method for Calculating Single-Event Distributions for Point Source Alpha Emitters. BNWL-2254, Battelle, Pacific Northwest Laboratories, Richland, WA 99352, Sept. 1977.

Wilson, W. E., L. H. Toburen and R. J. Popowich, "Comparison of the Track Structure of H^+ and He^{++} Ions in Water Vapor." Med. Phys. 4:344, 1977.

Wogman, N. A., H. G. Rieck, Jr., J. C. Laul and K. W. MacMurdo, "High Sensitivity Isotope Analysis with a ^{252}Cf-^{235}U Fueled Subcritical Multiplier and Low Background Photon Detector Systems." Nucl. Inst. & Methods, 1977.

Wogman, N. A., "The Present State of Nuclear Techniques Applicable to Pollution Studies in Groundwater." IAEA Advisory Group, Proceedings on the IAEA Symposium on Nuclear Techniques in Water Pollution Studies, Cracow, Poland, December 6-9, 1976.

Wogman, N. A., "In Situ X-ray Fluorescence in ^{252}Cf Neutron Activation Analysis for Marine and Terrestrial Mineral Exploration." Proceedings of the IAEA Symposium on Nuclear Techniques in Exploration, Extraction, and Processing of Mineral Resources, Vienna, Austria, March 7-11, 1977.

Wogman, N. A., R. L. Brodzinski and L. Van Middlesworth, "Radium Accumulation in Animal Thyroid Glands: A Possible Method for Uranium and Thorium Prospecting." Jour. of Radionanal. Chem., 1977.

Wehner, A. P., C. L. Wilkerson, W. C. Cannon, R. L. Buschbom and T. M. Tanner, "Pulmonary Deposition, Translocation and Clearance of Inhaled Neutron-Activated Talc in Hamsters." Fd Cosmet. Toxicol. 15;213-224, 1977.

Wyatt, J. R., J. J. Decorpo, R. D. Smith and F. E. Saalfeld, "Mass Spectral Studies of Polymeric Sulfur Nitride." Advances in Mass Spectrometry 7, 1977.

PRESENTATIONS

Abel, K. H. and E. A. Crecelius, "Copper Speciation in Sea Water Determined by Anodic Stripping Voltammetry." Abstract to be published by AAS from presentation at AAS meeting, Denver, CO, Feb. 23-25, 1977.

Abel, K. H. and D. E. Robertson, "Elemental Composition of Alaska Outer Continental Shelf Suspended Particulates and Surficial Sediments." Presented at the American Society of Limnology and Oceanography Pacific Section Meeting, San Francisco State University, San Francisco, CA, June 12-16, 1977.

Abel, K. H., D. E. Robertson, E. A. Crecelius and W. B. Silker, "Speciation Studies of Radionuclides in Low-Level Wastes and Process Waters for a Pressurized Water Reactor." Proceedings of Fourth Joint Conference on Sensing of Environmental Pollutants, American Chemical Society, New Orleans, LA, Nov. 6-11, 1977.

Braby, L. A., W. C. Roesch and J. M. Nelson, "Temperature Effect on the Production and Repair of Radiation Damage in Chlamydomonas reinhardi." Radiation Research Society, San Juan, 1977, published Radiation Research 70:684, 1977.

Brauer, F. P. and W. A. Mizlaff, "Evaluation of Well-Type Ge(Li) Detectors for Low-Level Radiochemical Analysis." Presented at the 1977 Nuclear Science Symposium, San Francisco, CA, October 19-21, 1977, BNWL-SA-6301.

Brauer, F. P., J. E. Fager, J. H. Kaye and R. J. Sorenson, "A Mobile Nondestructive Assay Verification and Measurement System." BNWL-SA-6113, Battelle, Pacific Northwest Laboratories, Richland, WA 99352. Presented at the Institute of Nuclear Materials Management 18th Annual Meeting, Washington, DC, June 29-30, 1977.

Brauer, F. P., J. M. Kelley, R. W. Goles and J. E. Fager, "Measurement of Environmental ^{241}Am and the Pu/Am Ratio by Photon Spectrometry." Presented at the 1976 Nuclear Science Symposium and Scintillation and Semiconductor Counter Symposium, IEEE/NPSS, New Orleans, LA, October 20-22, 1976. IEEE Trans. on Nucl. Sci. NS-24, February 19, pp. 591-595.

Brauer, F. P., H. G. Rieck, Jr., J. H. Kaye and R. W. Goles, "Sampling and Measurement of Long-Lived Radionuclides in Environmental Samples." Proceedings of Fourth Joint Conference on Sensing of Environmental Pollutants, New Orleans, LA, November 6-11, 1977.

Bushaw, B. A. and T. J. Whitaker, "Laser Induced Fluorescence Analysis of Polynuclear Aromatics in the Atmosphere." Proceedings of Fourth Joint Conference on Sensing of Environmental Pollutants, New Orleans, LA, November 6-11, 1977.

Crecelius, E. A., "The Production of Bromine, Bromite and Chlorine in Seawater by Ozonization." Proceedings of Symposium on Advanced Ozone Technology, Toronto, Canada, Nov. 18, 1977.

Dionne, P. J., T. P. Harrington, D. L. Stevens, F. T. Cross and G. E. Dagle, "Modeling the Early Translocation of Inhaled $^{239}Pu(NO_3)_4$ in Dogs." Health Physics Society Twenty-Second Annual Meeting, July 1977. (Abstract)

Felix, W. D., D. S. Farrier and R. E. Poulson, "High Performance Liquid Chromatographic Characterization of Oil Shale Retort Waters." Presented at the Second Pacific Chemical Engineering Congress (Pachec '77), Denver, CO, August 28-31, 1977.

Fruchter, J. S., J. C. Laul, M. R. Petersen, P. W. Ryan and M. E. Turner, "High Precision Trace Element and Organic Constituent Analysis of Oil Shale and Solvent-Refined Coal Materials." Proceedings of Symposium on Analytical Chemistry of Tar Sands and Oil Shale, American Chemical Society, New Orleans, LA, March 20-25, 1977.

Laul, J. C., W. C. Weimer and L. A. Rancitelli, "Biogeochemical Distribution of Rare Earths and Other Trace Elements in Plants and Soils." Proceedings of Second Symposium on the Origin and Distribution of the Elements, Paris, France, May 10-13, 1977.

Laul, J. C., "Neutron Activation Analysis in Geological Materials." Presented at the Atomic Energy Review, IAEA, Vienna, Austria, 1977.

Laul, J. C., K.K. Nielson and N. A. Wogman, "Trace Rare Earth Analysis by Neutron Activation and γ-Ray/X-ray Spectrometry." Proceedings of Third Int. Conference in Nuclear Methods in Environmental and Energy Research, Columbia, MO, October 10-12, 1977.

Miller, J. H. and M. L. West, "Quenching of Fluorescence in Binary Liquid Scintillators." Presented APS meeting, San Diego, CA, March 21, 1977. Published Bull. Am. Phys. Soc. 22:391, 1977.

Nelson, J. M., L. A. Braby and W. C. Roesch, "Determination of Mean Recovery Time Following Split-Dose or Protracted Irradiation." Radiation Research Society, San Juan, 1977, published Radiation Research 70:708.

Nielson, K. K. and D. R. Kalkwarf, "Multi-element Analysis of Urine Using Energy Dispersive X-ray Fluorescence." Proceedings of Symposium on Electron Microscopy and X-ray Applications to Environmental and Occupational Health Analyses, Denver, CO, May 25-27, 1977.

Nielson, K. K., N. A. Wogman and R. L. Brodzinski, "X-ray Fluorescence Capabilities for Uranium Ore Analysis." Proceedings of the Twenty-sixth Denver X-ray Conference, Denver, CO, August 3-5, 1977.

Petersen, M. R. and P. W. Ryan, "Analysis of Complex Samples for Trace Amounts of Polynuclear Aromatic Compounds." Proceedings of the Northwest Regional ACS Meeting, Portland, OR, June 15-17, 1977.

Roesch, W. C., "Microdosimetry of Moving Particulates." Presented at Radiation Research Society Meeting, San Juan, May 7, 1977. Published Radiation Research 70:638.

Roesch, W. C., "Models of the Radiation Sensitivity of Mammalian Cells." Third Symposium on Neutron Dosimetry in Biology and Medicine, Munich, 1977.

Smith, R. D., J. A. Campbell and W. D. Felix, "A Flow Tube Combustion Reactor-Mass Spectrometer for the Study of Post Combustion Processes. Proceedings of the Twenty-fifth Annual Conference of the American Society for Mass Spectrometry, Washington, DC, May 29-June 3, 1977.

Stoffels, J. J., C. R. Lagergren and P. J. Hof, "A Wide Dynamic Range Ion Detection and Measurement System." Twenty-fifth Annual Conference on Mass Spectrometry and Allied Topics, Washington, DC May 30-June 3, 1977.

Sullivan, J. F. and F. T. Cross, "The Role of Target Cells in the Toxicity of Ingested Reactor Core Products." Radiation Research Society Annual Meeting, May 1977 (Abstract).

Sullivan, M. F., F. T. Cross, G. W. R. Endres, et. al., "The Long-Term Effects of an Intracavitary Treatment with Californium-252 on Normal Tissue." Proceedings of a Symposium on Radiological Research Needed for the Improvement of Radiotherapy, Vienna, Austria, November 1976. (In press).
Paper No. IAEA-SM-212/57.

Sullivan, M. F., F. T. Cross, G. W. R. Endres, et al., "The Response of Normal Tissues to an Intracavitary Exposure from Californium-252." Proceedings of International Symposium of Cf-252 Utilization, Brussels, Belgium, April 1976. (In press)

Weimer, W. C. and J. C. Langford, "Comparative Biogeochemical Behaviors of Iron-55 and Stable Iron in the Marine Environment." Presented at AAAS-ASLO Pacific Division Conference, San Francisco, CA, June 20-22, 1977.

Weimer, W. C., J. C. Laul, J. C. Kutt and E. A. Bondietti, "Plant Uptake of Am, Cm, and the Chemical Analog Nd." Presented at Third Int. Conference on Nuclear Methods in Energy and Environmental Research, Columbia, MO, October 10-13, 1977.

West, M. L. and J. H. Miller, "Track Structure Effects in the Radioluminescence of Benzene in Cyclohexane." Presented at Radiation Research Meeting, San Juan, May 7, 1977, published Radiation Research 70:617-618, 1977.

Whitaker, T. J. and B. A. Bushaw, "Analysis of Radioactive Noble Gases by Two-Photon Induced Fluorescence." Proceedings of Fourth Joint Conference on Sensing of Environmental Pollutants, New Orleans, LA, Nov. 6-11, 1977

Wilson, W. E., "Radiological Physics and Dosimetry Research with a Small Positive Ion Accelerator." Proceedings of Fourth Conference on Scientific and Industrial Applications of Small Accelerators, CONF-761059, p. 481-492, 1976.

Wilson, W. E., L. H. Toburen and R. J. Popowich, "Comparison of the Track Structure of H^+, He^+ and He^{++} Ions in Water Vapor." Presented AAPM Meeting, Cincinnati, July 31, 1977, published Med. Phys. 4:344, 1977.

ORGANIZATION CHARTS

DEPARTMENT STAFF

AUTHOR INDEX

DISTRIBUTION

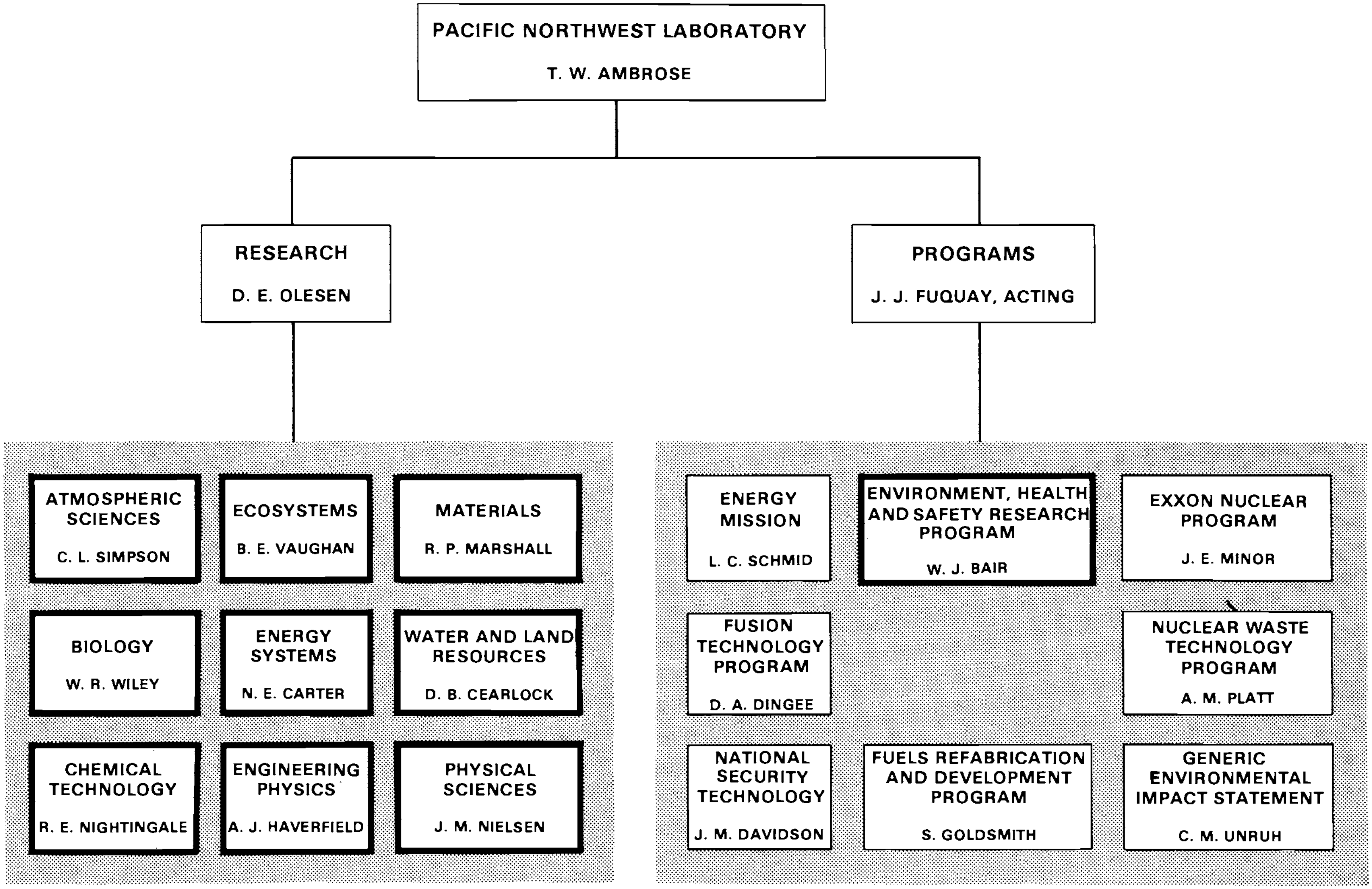

NOTE: HEAVY BLACK LINES DENOTE ORGANIZATIONAL COMPONENTS IN WHICH ENVIRONMENT, HEALTH, AND SAFETY RESEARCH IS BEING CONDUCTED.

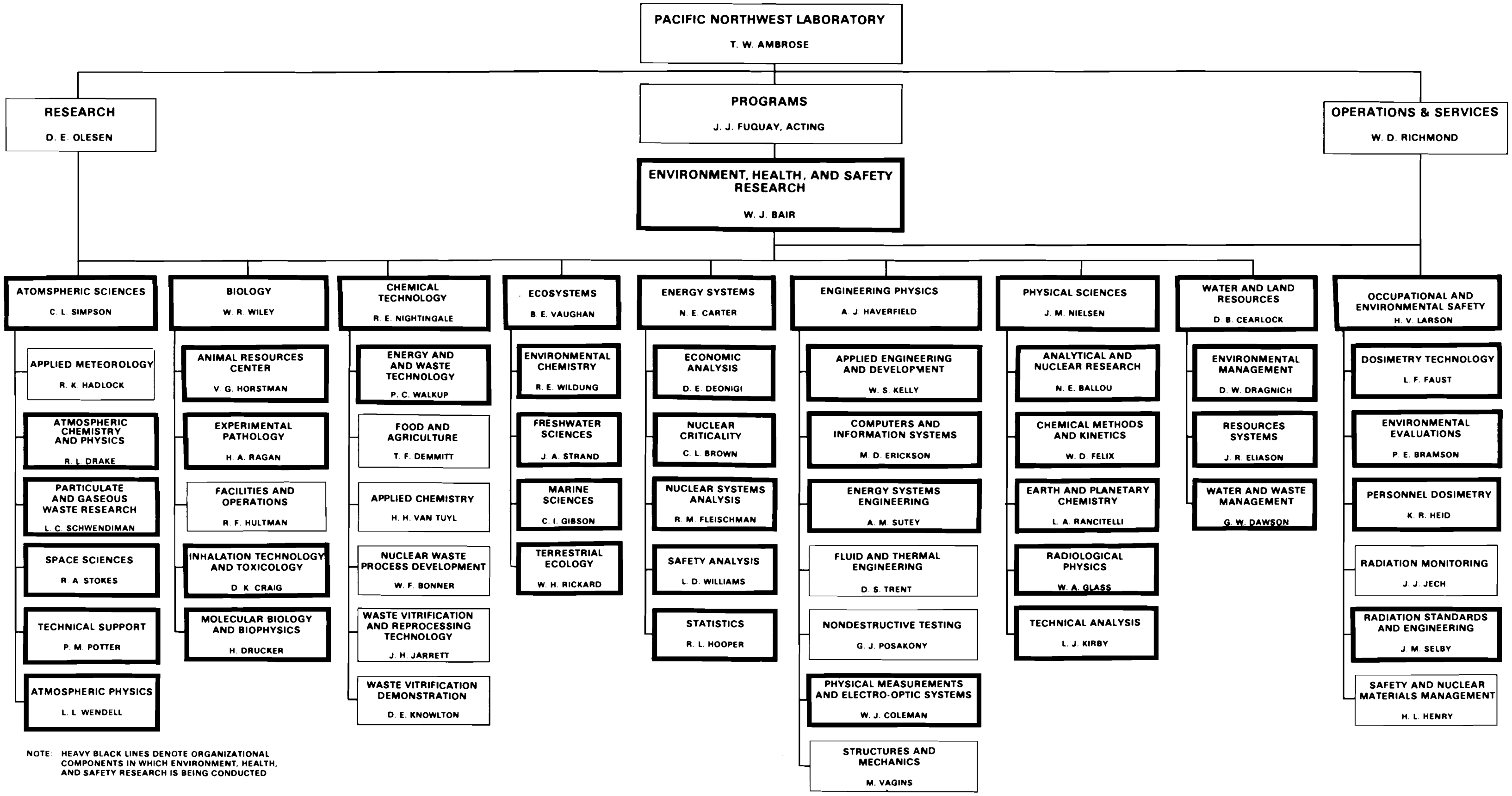

NOTE: HEAVY BLACK LINES DENOTE ORGANIZATIONAL COMPONENTS IN WHICH ENVIRONMENT, HEALTH, AND SAFETY RESEARCH IS BEING CONDUCTED

DEPARTMENT STAFF

PHYSICAL SCIENCES DEPARTMENT
(7HA0)

November 1, 1977

JM (Julian) Nielsen, Manager
FL (Louise) Barton, Secretary
***SE (Susan) King, Clerk

RW (Dick) Perkins, Assoc. Manager
RM (Rose) Garcia, Secretary

#GM (Gary) Garnant, Editor/Writer

#WE (Bill) Gross, Financial Specialist
°°°JC (Jim) Langford, Quality Assurance Specialist

EI (Earl) Wandling, Specialist, Building Management

Radiological Physics
(7HA3)

WA (Bill) Glass, Manager
JA (Judy) Ewing, Secretary

Radiological Research Group

WC (Bill) Roesch, Technical Leader, Radiation Biophysics
LH (Larry) Toburen, Technical Leader, Radiation Physics

LA (Les) Braby
JH (John) Miller
JM (John) Nelson
CA (Charlie) Ratcliffe
ML (Martin) West
WE (Walt) Wilson

JE (Jim) Choate
***MS (Mike) Creek
MK (Marvin) Lein
R (Rudy) Rodriquez

Accelerator Facility
(7HA4)

Analytical and Nuclear Research
(7HA5)

NE (Nate) Ballou, Manager
GJ (Jean) Clark, Secretary
DE (Dewey) Hunter, Secretary

FP (Fred) Brauer
+MW (Martin) Cole
JE (Jon) Fager
RW (Ron) Goles
RL (Dick) Gordon
+DC (Doug) Hamilton
JH (Jim) Kaye
JM (Jim) Kelley
CR (Bob) Lagergren
WA (Bill) Mitzlaff
PL (Paul) Reeder
DM (Dean) Robertson
JJ (Jim) Stoffels
RS (Bob) Strebin
H (Harvey) Tenny
RA (Ray) Warner

NL (Lois) Abbey
LA (Lee) Bond
***PD (Pat) Draze
DR (Don) Ells
RM (Rose Ann) Graves
MS (Mike) Rapids
LW (Lena) Schock
SC (Shirley) Simpson

Technical Analysis
(7HA6)

LJ ("Rip") Kirby, Manager

AC (Art) Case
VW (Bill) Thomas, Jr.

VC (Velma) Beard
JD (Jerry) Forsythe
DT (Dottie) Harless
PA (Pat) Wodarz

Earth and Planetary Chemistry
(7HA7)

LA (Lou) Rancitelli, Manager
ES (Betty) Getchell, Secretary

KH (Keith) Abel
DP (Don) Brown
††EA (Eric) Crecelius
JC (John) Evans
JS (John) Fruchter
SR (Sammy) Garcia
JC (JC) Laul
JD (Don) Ludwick
†††RL (Rick) McKeever
†††KB (Khris) Olsen
HG (George) Rieck, Jr.
DE (Dave) Robertson
WB (Wyatt) Silker
ME (Mary) Turner
CL (Connie) Wilkerson
JA (Jim) Young

LL (Lavern) Baker
EF (Ermel) Briggs
BG (Chris) Christensen
DA (Dave) Cochran
CL (Chuck) Nelson
††CW (Clay) Philbrick
JH (Jim) Reeves
WC (Wayne) Richey
RW (Ron) Sanders

Chemical Methods and Kinetics
(7HA8)

WD (Dale) Felix, Manager
KA (Kelly) Corrigan, Secretary

RL (Ron) Brodzinski
BA (Bruce) Bushaw
JA (Jim) Campbell
PO (Pete) Jackson
DR (Don) Kalkwarf
JC (John) Kutt
°°°JC (Jim) Langford
JR (John) Morrey
HL (Howard) Nielson
KK (Kirk) Nielson
MR (Mike) Petersen
DM (Don) Schoengold
RD (Dick) Smith
CW (Chuck) Thomas
++JC (Chuck) Templeton
WC (Wally) Weimer
TJ (Tom) Whitaker
NA (Ned) Wogman

GG (Gwen) Brodaczynski
RM (Rush) Campbell
DR (Don) Edwards
JG (Grant) Pratt
C (Chuck) Veverka, Jr.

LEGEND:
*Part-time employee, included in total.
***Hourly employee, included in total.
°°°Dual assignment, included only once.
+S&E Program, not included in total.
++NORCUS appointment, not included in total.
#Assigned from another organization, not included in total.
††Offsite, Marine Research Lab., Sequim, Washington.
†††Offsite, Colstrip, Montana.

Total Number of Exempt	=	65
Total Number of Non-Exempt	=	38
TOTAL		103

AUTHOR INDEX

DISTRIBUTION

No. of
Copies

A. A. Churm, Director
Patent Division
DOE - Chicago Operations
Office
9800 South Cass Ave.
Argonne, IL 60439

3 J. L. Liverman
Acting Assistant Secretary
Department of Energy
Office of the Assistant
Secretary for Environment
Washington, DC 20545

W. R. Albers
Department of Energy
Office of the Assistant
Secretary for Environment
Office of Occupational and
Environmental Safety
Washington, DC 20545

R. W. Barber
Department of Energy
Office of the Assistant
Secretary for Environment
Office of Reactor Safety
Research Coordination
Washington, DC 20545

N. F. Barr
Department of Energy
Office of the Assistant
Secretary for Environment
Division of Regional
Assessments
Washington, DC 20545

J. W. Benson
Department of Energy
Office of the Assistant
Secretary for Environment
Washington, DC 20545

L. C. Brazley
Department of Energy
Office of the Assistant
Secretary for Environment
Office of NEPA Oversight
Washington, DC 20545

W. A. Brobst
Department of Energy
Office of the Assistant
Secretary for Environment
Office of Environmental
Control Technology
Washington, DC 20545

No. of
Copies

W. W. Burr, Jr.
Department of Energy
Office of the Assistant
Secretary for Environment
Office of Biomedical and
Environmental Research
Washington, DC 20545

C. E. Carter
Department of Energy
Office of the Assistant
Secretary for Environment
Office of Biomedical and
Envrionmental Research
Washington, DC 20545

R. J. Catlin
Department of Energy
Office of Assistant
Secretary for Environment
Office of NEPA Oversight
Washington, DC 20545

J. A. Coleman
Department of Energy
Office of the Assistant
Secretary for Environment
Office of Technology Impacts
Washington, DC 20545

R. A. Conaway
Department of Energy
Office of the Assistant
Secretary for Environment
Office of Program Coordination
Washington, DC 20545

L. J. Deal
Department of Energy
Office of the Assistant
Secretary for Environment
Office of Occupational and
Environmental Safety
Washington, DC 20545

G. P. Dix
Department of Energy
Office of the Assistant
Secretary for Environment
Office of Occupational and
Environmental Safety
Washington, DC 20545

No. of
Copies

C. W. Edington
Department of Energy
Office of the Assistant
Secretary for Environment
Office of Biomedical and
Environmental Research
Washington, DC 20545

H. G. Fish
Department of Energy
Office of the Assistant
Secretary for Environment
Office of Program Coordination
Washington, DC 20545

R. E. Grossman
Department of Energy
Office of the Assistant
Secretary for Environment
Office of NEPA Oversight
Washington, DC 20545

J. H. Harley
Environmental Monitoring
Laboratory
376 Hudson St.
New York, NY 10014

H. Hollister
Department of Energy
Office of the Assistant
Secretary for Environment
Office of Occupational and
Environmental Safety
Washington, DC 20545

P. W. House
Department of Energy
Office of the Assistant
Secretary for Environment
Office of Technology Impacts
Washington, DC 20545

R. L. Leith
Department of Energy
Office of the Assistant
Secretary for Environment
Office of Program Coordination
Washington, DC 20545

F. A. Leone
Department of Energy
Office of the Assistant
Secretary for Environment
Office of NEPA Oversight
Washington, DC 20545

No. of
Copies

W. J. Little, Jr.
Department of Energy
Office of the Assistant
Secretary for Environment
Office of Planning
Coordination
Washington, DC 20545

K. E. Lockridge
Department of Energy
Office of the Assistant
Secretary for Environment
Office of Planning Coordination
Washington, DC 20545

J. N. Maddox
Department of Energy
Office of the Assistant
Secretary for Environment
Office of Program Coordination
Washington, DC 20545

W. J. McCool
Department of Energy
Office of the Assistant
Secretary for Environment
Office of Occupational and
Environmental Safety
Washington, DC 20545

B. F. McCully
Department of Energy
Office of the Assistant
Secretary for Environment
Office of Program Coordination
Washington, DC 20545

M. L. Minthorn, Jr.
Department of Energy
Office of the Assistant
Secretary for Environment
Office of Biomedical and
Environmental Research
Washington, DC 20545

D. Monti
Department of Energy
Office of the Assistant
Secretary for Environment
Division of Technology
Overview
Washington, DC 20545

W. E. Mott
Department of Energy
Office of the Assistant
Secretary for Environment
Office of Environmental
Control Technology
Washington, DC 20545

No. of
Copies

W. H. Pennington
Department of Energy
Office of the Assistant
Secretary for Environment
Office of NEPA Oversight
Washington, DC 20545

R. W. Ramsey, Jr.
Department of Energy
Office of the Assistant
Secretary for Environment
Office of Environmental
Control Technology
Washington, DC 20545

D. M. Ross
Department of Energy
Office of the Assistant
Secretary for Environment
Office of Occupational and
Environmental Safety
Washington, DC 20545

D. E. Shaw
Department of Energy
Office of the Assistant
Secretary for Environment
OMC
Washington, DC 20545

R. D. Shull
Department of Energy
Office of the Assistant
Secretary for Environment
Division of Environmental
Impacts
Washington, DC 20545

N. F. Simpson
Department of Energy
Office of the Assistant
Secretary for Environment
Office of Program Coordination
Washington, DC 20545

D. H. Slade
Department of Energy
Office of the Assistant
Secretary for Environment
Office of Biomedical and
Environmental Research
Washington, DC 20545

J. Snyder
Department of Energy
Office of the Assistant
Secretary for Environment
Office of Planning
Coordination
Washington, DC 20545

No. of
Copies

J. B. Stronberg
Department of Energy
Office of the Assistant
Secretary for Environment
Washington, DC 20545

J. Swinebroad
Department of Energy
Office of the Assistant
Secretary for Environment
Office of Biomedical and
Environmental Research
Washington, DC 20545

A. R. Vincent
Department of Energy
Office of the Assistant
Secretary for Environment
Office of Planning
Coordination
Washington, DC 20545

B. W. Wachholz
Department of Energy
Office of the Assistant
Secretary for Environment
Division of Policy Analysis
Washington, DC 20545

W. W. Weyzen
Department of Energy
Office of the Assistant
Secretary for Environment
Office of Biomedical and
Environmental Research
Washington, DC 20545

J. C. Whitnah
Department of Energy
Office of the Assistant
Secretary for Environment
Washington, DC 20545

T. Williams
Department of Energy
Office of the Assistant
Secretary for Environment
Division of Policy Analysis
Washington, DC 20545

R. W. Wood
Department of Energy
Office of the Assistant
Secretary for Environment
Office of Biomedical and
Environmental Research
Washington, DC 20545

No. of
<u>Copies</u>

C. W. Fischer
Department of Energy
Office of Assistant Secretary
for Energy Information
Administration
Washington, DC 20545

Major General J. K. Bratton
Department of Energy
Office of the Assistant
Secretary for Defense
Programs
Washington, DC 20545

G. C. Facer
Department of Energy
Office of the Assistant
Secretary for Defense
Programs
Washington, DC 20545

Admiral H. G. Rickover
Department of Energy
Office of the Assistant
Secretary for Defense
Programs
Washington, DC 20545

A. D. Starbird
Department of Energy
Office of the Assistant
Secretary for Defense
Programs
Washington, DC 20545

C. B. Curtis
Department of Energy
Office of the Assistant
Secretary for Federal
Energy Regulatory
Commission
Washington, DC 20545

W. E. Molloy
Department of Energy
Office of the Assistant
Secretary for Federal
Energy Regulatory
Commission
Washington, DC 20545

H. P. Wald
Department of Energy
Office of the Assistant
Secretary for Federal
Energy Regulatory
Commission
Washington, DC 20545

No. of
<u>Copies</u>

D. Beattle
Department of Energy
Office of the Assistant
Secretary for Conservation
and Solar Applications
Washington, DC 20545

T. Noel
Department of Energy
Office of the Assistant
Secretary for Resource
Applications
Washington, DC 20545

J. Belding
Department of Energy
Office of the Assistant
Secretary for Energy
Technology
Washington, DC 20545

J. Bresee
Department of Energy
Office of the Assistant
Secretary for Energy
Technology
Washington, DC 20545

G. W. Cunningham
Department of Energy
Office of the Assistant
Secretary for Energy
Technology
Washington, DC 20545

T. J. Dobry
Department of Energy
Office of the Assistant
Secretary for Energy
Technology
Washington, DC 20545

H. Guthrie
Department of Energy
Office of the Assistant
Secretary for Energy
Technology
Washington, DC 20545

E. E. Kintner
Department of Energy
Office of the Assistant
Secretary for Energy
Technology
Washington, DC 20545

No. of
<u>Copies</u>

F. A. Koomanoff
Department of Energy
Office of the Assistant
Secretary for Energy
Technology
Washington, DC 20545

C. Kuhlman
Department of Energy
Office of the Assistant
Secretary for Energy
Technology
Washington, DC 20545

R. Loose
Department of Energy
Office of the Assistant
Secretary for Energy
Technology
Washington, DC 20545

W. E. Lotz
Department of Energy
Office of the Assistant
Secretary for Energy
Technology
Washington, DC 20545

M. B. Neuworth
Department of Energy
Office of the Assistant
Secretary for Energy
Technology
Washington, DC 20545

F. F. Parry
Department of Energy
Office of the Assistant
Secretary for Energy
Technology
Washington, DC 20545

G. Perdirtz
Department of Energy
Office of the Assistant
Secretary for Energy
Technology
Washington, DC 20545

H. F. Soule
Department of Energy
Office of the Assistant
Secretary for Energy
Technology
Washington, DC 20545

No. of
Copies

R. D. Thorne
Department of Energy
Office of the Assistant
Secretary for Energy
Technology
Washington, DC 20545

P. C. White
Department of Energy
Office of the Assistant
Secretary for Energy
Technology
Washington, DC 20545

E. Willis
Department of Energy
Office of the Assistant
Secretary for Energy
Technology
Washington, DC 20545

W. Bateman
Department of Energy
Office of the Assistant
Secretary for Energy
Research
Washington, DC 20545

3 J. M. Deutch
Department of Energy
Office of the Assistant
Secretary for Energy
Research
Washington, DC 20545

D. R. Israel
Department of Energy
Office of the Assistant
Secretary for Energy
Research
Washington, DC 20545

J. S. Kane
Department of Energy
Office of the Assistant
Secretary for Energy
Research
Washington, DC 20545

H. D. Bruner, M.D.
Department of Energy
Office of Biomedical and
Environmental Research
Washington, DC 20545

R. L. Butenhoff
Department of Energy
Office of Biomedical and
Environmental Research
Washington, DC 20545

No. of
Copies

J. S. Kirby-Smith
Department of Energy
Office of Biomedical and
Environmental Research
Washington, DC 20545

R. P. Blaunstein
Department of Energy
Office of Biomedical and
Environmental Research
Washington, DC 20545

G. Goldstein
Department of Energy
Office of Biomedical and
Environmental Research
Washington, DC 20545

F. Hudson
Department of Energy
Office of Biomedical and
Environmental Research
Washington, DC 20545

D. W. Cole, Jr.
Department of Energy
Office of Biomedical and
Environmental Research
Washington, DC 20545

W. G. Belter
Department of Energy
Office of Technology
Overview
Washington, DC 20545

R. D. Cooper
Department of Energy
Office of Technology
Overview
Washington, DC 20545

R. M. Jimeson
Department of Energy
Office of Technology
Overview
Washington, DC 20545

J. R. Maher
Department of Energy
Office of Technology
Overview
Washington, DC 20545

G. Hagey
Department of Energy
Office of Technology
Overview
Washington, DC 20545

No. of
Copies

H. R. Wasson
Department of Energy
Office of Technology
Overview
Washington, DC 20545

H. P. Smith
Department of Energy
Office of Safety, Standards
and Compliance
Washington, DC 20545

E. J. Vallario
Department of Energy
Office of Safety, Standards
and Compliance
Washington, DC 20545

A. A. Schoen
Department of Energy
Office of Safety, Standards
and Compliance
Washington, DC 20545

F. R. Zintz
Department of Energy
Office of Safety, Standards
and Compliance
Washington, DC 20545

C. I. York
Department of Energy
Office of Safety, Standards
and Compliance
Washington, DC 20545

D. E. Patterson
Department of Energy
Office of Safety, Standards
and Compliance
Washington, DC 20545

E. K. Loop
Department of Energy
Office of Safety, Standards
and Compliance
Washington, DC 20545

M. A. Bell
Department of Energy
Office of Safety, Standards
and Compliance
Washington, DC 20545

J. D. Griffith
Department of Energy
Development and Demonstration
Branch
Washington, DC 20555

No. of
Copies

J. J. Davis
Office of Nuclear Regulatory
Research
U.S. Nuclear Regulatory
Commission
Washington, DC 20555

E. E. Held
Office of Standards
Development
U.S. Nuclear Regulatory
Commission
Washington, DC 20555

J. O'Toole
Ames Laboratory
Iowa State University
Ames, IA 50010

P. F. Gustafson
Argonne National Laboratory
9700 South Cass Ave.
Argonne, IL 60439

J. Sedlet
Argonne National Laboratory
9700 South Cass Ave.
Argonne, IL 60439

C. Jackson
DOE - San Francisco
Operations Office
133 Broadway
Wells Fargo Building
Oakland, CA 94616

C. W. Sill
Department of Energy
Idaho Operations Office
P.O. Box 2108
Idaho Falls, ID 83401

J. H. Spickard
Department of Energy
Idaho Operations
Commission
550 Second Street
Idaho Falls, ID 83401

D. M. Gardiner
Department of Energy
Chicago Operations Office
9800 South Cass Ave.
Argonne, IL 60439

No. of
Copies

M. E. Gates
Department of Energy
Nevada Operations Office
P.O. Box 14100
Las Vegas, NV 89114

R. Ray
Department of Energy
Nevada Operations Office
P.O. Box 14100
Las Vegas, NV 89114

P. B. Dunnaway
Department of Energy
Nevada Operations Office
P.O. Box 14100
Las Vegas, NV 89114

J. R. Roeder
Department of Energy
Albuquerque Operations Office
P.O. Box 5400
Albuquerque, NM 87115

E. W. Bean
Rocky Flats Area Office
Department of Energy
Albuquerque Operations Office
P.O. Box 928
Golden, CO 80401

J. F. Stevens
Dayton Area Office
Department of Energy
Albuquerque Operations Office
P.O. Box 66
Miamisburg, OH 45342

W. Reese
Department of Energy
Savannah River Operations
Office
P.O. Box A
Aiken, SC 29801

J. A. Lenhard
Department of Energy
Oak Ridge Operations
Office
P.O. Box E
Oak Ridge, TN 37830

J. S. Ball
Bartlesville Energy Research
Center
Department of Energy
P.O. Box 1398
Bartlesville, OK 74003

No. of
Copies

G. H. Gronhovd
Grand Forks Energy Research
Center
Department of Energy
Box 8213, University Station
Grand Forks, ND 58202

A. W. Decora
Laramie Energy Research Center
Department of Energy
P.O. Box 3395
University Station
Laramie, WY 83071

D. Farrier
Laramie Energy Research
Center
Department of Energy
P.O. Box 3395
University Station
Laramie, WY 82701

H. Jensen
Laramie Energy Research
Center
Department of Energy
P.O. Box 3395
University Station
Laramie, WY 82701

R. D. Kerr
Laramie Energy Research
Center
Department of Energy
P.O. Box 3395
University Station
Laramie, WY 82701

A. A. Pitrolo
Morgantown Energy Research
Center
Department of Energy
P.O. Box 880
Morgantown, WV 26505

I. Wender
Pittsburgh Energy Research
Center
Department of Energy
4800 Forbes Avenue
Pittsburgh, PA 15213

B. M. Erickson
Department of Energy
Schenectady Naval
Reactors Office
P.O. Box 1069
Schenectady, NY 12301

No. of
Copies

NRC Advisory Committee on
Reactor Safeguards
Washington, DC 20555

W. Cool
Nuclear Regulatory Commission
Washington, DC 20545

R. Alexander
Nuclear Regulatory Commission
Washington, DC 20545

2 J. J. Davis
Assistant Director of Research
Nuclear Regulatory Commission
Washington, DC 20545

D. D. Dominick
Office of Categorical
Programs
Environmental Protection
Agency
Washington, DC 20460

S. M. Greenfield
Environmental Protection
Agency
Washington, DC 20460

D. Smith
Environmental Protection
Agency
Washington, DC 20460

W. Mills
Environmental Protection
Agency
Washington, DC 20460

M. K. Hubbert
Department of the Interior
U.S. Geological Survey
Water Resources Division
Washington, DC 20242

D. N. Breiter
National Bureau of Standards
A121, Building 222
Washington, DC 20234

J. R. DeNoe
National Bureau of Standards
A121, Building 222
Washington, DC 20234

J. W. McCaslin
INEL, Aerojet Nuclear
550 Second Street
Idaho Falls, ID 83401

No. of
Copies

R. C. Yoder
Rockwell International
P.O. Box 888
Golden, CO 80401

A. R. Boulogne
E.I. DuPont de Nemours
and Company, Aiken
Savannah River Laboratory
Technical Information
Service
Room 773A
Aiken, SC 29801

K. MacMurdo
E.I. DuPont de Nemours
and Company, Aiken
Savannah River Laboratory
Technical Information
Service
Room 773A
Aiken, SC 29801

C. M. Patterson
E.I. DuPont de Nemours
and Company
Savannah River Plant
Aiken, SC 29801

B. C. Rusche
E.I. DuPont de Nemours
and Company, Aiken
Savannah River Laboratory
Technical Information
Service
Room 773A
Aiken, SC 29801

W. B. Scott
E.I. DuPont de Nemours
and Company, Aiken
Savannah River Laboratory
Technical Information
Service
Room 773A
Aiken, SC 29801

Technical Information
Service
Room 773A
Savannah River Laboratory
E.I. DuPont de Nemours
and Company
Aiken, SC 29801

R. J. Beyers
Savannah River Ecology
Laboratory
University of Georgia
Savannah River Plant
P.O. Box A
Aiken, SC 29801

No. of
Copies

C. L. Karl
National Lead Company
of Ohio
P.O. Box 39158
Cincinnati, OH 45239

R. L. Kathren
Portland General Electric
621 S.W. Alder
Portland, OR 97205

V. P. Bond
Brookhaven National
Laboratory
Upton, Long Island, NY
11973

L. P. Hatch
Brookhaven National
Laboratory
Research Library
Reference Section
Information Division
Upton, Long Island, NY
11973

C. B. Meinhold
Brookhaven National
Laboratory
Upton, Long Island, NY 11973

Librarian
Research Library, Reference
Bookhaven National
Laboratory
Upton, Long Island, NY 11973

B. Manowitz
Radiation Division
Brookhaven National
Laboratory
Upton, Long Island, NY
11973

G. M. Woodwell
Brookhaven National
Laboratory
Research Library
Reference Section
Information Division
Upton, Long Island, NY
11973

C. R. Richmond
Oak Ridge National
Laboratory
P.O. Box X
Oak Ridge, TN 37830

No. of
Copies

S. I. Auerbach
Oak Ridge National
Laboratory
Oak Ridge Operations
Office
P.O. Box X
Oak Ridge, TN 37830

J. A. Auxier
Oak Ridge National
Laboratory
P.O. Box X
Oak Ridge, TN 37830

G. D. O'Kelley
Oak Ridge National
Laboratory
Oak Ridge Operations
Office
P.O. Box X
Oak Ridge, TN 37830

E. G. Struxness
Oak Ridge National
Laboratory
Oak Ridge Operations
Office
P.O. Box X
Oak Ridge, TN 37830

J. E. Turner
Oak Ridge National
Laboratory
Oak Ridge Operations
Office
P.O. Box X
Oak Ridge, TN 37830

Gustafson
Argonne National
Laboratory
9700 South Cass Ave.
Argonne, IL 60439

W. K. Sinclair
Argonne National
Laboratory
9700 South Cass Ave.
Argonne, IL 60439

E. L. Alpen
Lawrence Berkeley Laboratory
University of California
Building 90, Room 2056
No. 1 Cyclotron Road
Berkeley, CA 94720

No. of
Copies

R. E. Heft
Lawrence Radiation
Laboratory
University of California
Lawrence Livermore
Laboratory
Technical Information
Department, L-3
P.O. Box 808
Livermore, CA 94550

G. H. Higgins
Lawrence Radiation
Laboratory
University of California
Lawrence Livermore
Laboratory
Technical Information
Department, L-3
P.O. Box 808
Livermore, CA 94550

J. B. Knox
Lawrence Radiation
Laboratory
University of California
Lawrence Livermore
Laboratory
Technical Information
Department, L-3
P.O. Box 808
Livermore, CA 94550

M. L. Mendelsohn
University of California
Lawrence Livermore
Laboratory
P.O. Box 808
Livermore, CA 94550

P. Phelps
Lawrence Radiation
Laboratory
University of California
Lawrence Livermore
Laboratory
Technical Information
Department, L-3
P.O. Box 808
Livermore, CA 94550

B. W. Shore
Lawrence Radiation
Laboratory
University of California
Lawrence Livermore
Laboratory
Technical Information
Department, L-3
P.O. Box 808
Livermore, CA 94550

No. of
Copies

Librarian
Lawrence Radiation
Laboratory
University of California
Technical Information
Department, L-3
P.O. Box 808
Livermore, CA 94550

G. L. Voelz
University of California
Los Alamos Scientific
Laboratory
P.O. Box 1663
Los Alamos, NM 87545

Librarian
Los Alamos Scientific
Laboratory
P.O. Box 1663
Los Alamos, NM 87545

J. W. Healy
Los Alamos Scientific
Laboratory
University of California
P.O. Box 1663
Los Alamos, NM 87545

M. F. Milligan
Los Alamos Scientific
Laboratory
University of California
P.O. Box 1663
Los Alamos, NM 87545

R. O. McClellan
Inhalation Toxicology
Research Institute
Lovelace Foundation for
Medical Education and
Research
P.O. Box 5890
Albuquerque, NM 87115

K. A. Smith
Sandia Laboratories
P.O. Box 5800
Albuquerque, NM 87115

J. O'Toole
Battelle Human Affairs
Research Center
4000 N.E. 41st St.
P.O. Box 3595
Seattle, WA 98105

No. of
Copies

J. E. Rasmussen
Battelle Human Affairs
Research Center
4000 N.E. 41st Street
P.O. Box 5395
Seattle, WA 98105

Librarian
Batelle Memorial Institute
Columbus Laboratories
505 King Avenue
Columbus, OH 53201

R. S. Paul
Batelle Memorial Institute
Columbus Laboratories
505 King Avenue
Columbus, OH 53201

B. D. Breitenstein
Hanford Environmental
Health Foundation
Richland, WA 99352

P. A. Fuqua
Hanford Environmental
Health Foundation
Richland, WA 99352

Librarian, Building 465
Atomic Energy Research
Establishment
Harwell, Didcot
OXON OXII ORD, ENGLAND

H. Daw
Director, Division of
Health, Safety and Waste
Management
International Atomic Energy
Agency
Vienna 1, Kaerntnerring 11,
AUSTRIA

Director, Office of Nuclear
Safety and Environmental
Protection
International Atomic Energy
Agency
1010 Vienna, Kaerntnerring 11,
P.O. Box 590
AUSTRIA

J. Z. Minczewski
International Atomic Energy
Agency
Vienna 1, Kaerntenerring 11,
AUSTRIA

No. of
Copies

Director
Joint Center for Graduate
Study
100 Sprout Road
Richland, WA 99352

David Rall, Director
NIEHS
P.O. Box 12233
Research Triangle
Park, NC 27709

D. Beirman
Chief, Document Service
Branch
Central Intelligence
Agency
Attn: CRS/DPSD/DSB/IAS/
409779/DB
Washington, DC 20505

Council on Environmental
Quality
72 Jackson Place, N.W.
Washington, DC 20006

A. Barbreau
Centre d'Etudes
Nucléaires de Saclay
P.O. Box 2, Saclay
Fig-sur-yvette
(S & O)
FRANCE

F. Duhamel
Centre d'Etudes
Nucléaires de Saclay
P.O. Box 2, Saclay
Fig-sur-yvette
(S & O)
FRANCE

Librarian
Centre d'Etudes
Nucléaires de Saclay
P.O. Box 2, Saclay
Fig-sur-Yvette
(S&O)
FRANCE

P. Slizewicz
Centre d'Etudes
Nucléaires de Saclay
P.O. Box 2, Saclay
Fig-sur-yvette
(S & O)
FRANCE

No. of
Copies

A. M. Menoux
Commissariat à l'Energie
Atomique
Centre d'Etudes
Nucléaires Fontenay-aux-
Roses,
PB n°, 6-9226 Fontenay-
aux-Roses,
FRANCE

M. Rzekiecki
Commissariat à l'Energie
Atomique
Centre d'Etudes
Nucléaires de Cadarache
BP n 13-St. Paul
Les Durance
FRANCE

Director
Commissariat à l'Energie
Atomique
Centre d'Etudes
Nucléaires de Fontenay-aux-
Roses (Seine)
FRANCE

Librarian
Commonwealth Scientific and
Industrial Research
Organization
314 Albert Street
P.O. Box 89
East Melbourne, Victoria
AUSTRIALIA

Director
Commonwealth Scientific and
Industrial Research
Organization
Aspendal, Victoria,
AUSTRALIA

B. B. Hicks
Commonwealth Scientific and
Industrial Research
Organization
Aspendal, Victoria
AUSTRALIA

E. Wallauschek
ENEA (OECD) Health and
Safety Office
38, Blvd. Suchet
Paris IVI,
FRANCE

M. Saiki
National Institute of
Radiological Sciences
Environmental Hygiene
Division
4-9-1, Anagawa
Chiba-shi
JAPAN

No. of
Copies

M. Suzuki
National Institute of
Radiological Sciences
Environmental Hygiene
Division
4-9-1, Anagawa
Chiba-shi
JAPAN

Director
National Institute of
Radiological Sciences
4-9-1, Anagawa
Chiba-shi
JAPAN

Librarian
Australian AEC
Riverina Laboratory
P.O. Box 226
Deniliquin
New South Wales
AUSTRALIA 2710

A. M. Marko
Director
Atomic Energy of
Canada Ltd.
Biology and Health
Physics Division
Chalk River Nuclear
Laboratories
Chalk River, Ontario
KOJ IJO
CANADA

C. A. Mawson
Atomic Energy of
Canada Ltd.
Chalk River, Ontario
CANADA

I. Ophel
Atomic Energy of
Canada Ltd.
Chalk River, Ontario
CANADA

F. D. Sowby
International Commission on
Radiological Protection
Clifton Avenue
Sutton, Surrey
ENGLAND

W. R. Ney
Executive Director
National Council on
Radiation Protection
and Measurements
7910 Woodmont Ave.
Suite 1061
Washington, DC 20014

No. of
Copies

L. Bustad, Dean
College of Veterinary
Medicine
Washington State University
Pullman, WA 99163

R. H. Filby
Director
Nuclear Radiation Center
Washington State University
Pullman, WA 99163

G. W. Dolphin
National Radiological
Protection Board
Harwell, Didcot
Oxfordshire OXII ORQ
ENGLAND

A. K. Ganguly
Atomic Energy Establishment
Trombay, Bombay 73
INDIA

Librarian
Atomic Energy Research
Establishment
Harwell, Berks
ENGLAND

A. W. R. Wilson
Australian AEC
Post Office Coogee
New South Wales
AUSTRALIA

D. J. Beninson
Comision Nacional de
Energia Atomica
Buenos Aires
ARGENTINA

E. Vander Elst
Comision Nacional de
Energia Atomica
Buenos Aires
ARGENTINA

V. R. Thayer
E.I. DuPont de Nemours
and Company
Polymer Intermediate
Department
Department of Energy
Wilmington, DE 19898

Librarian
Eurochemic Library
B 2400
MOL
BELGIUM

No. of
Copies

W. B. Heroy
Geotechnical Corporation
Box 28277
Dallas, TX 75228

H. Krause
Gesselschaft Kernforschung
mbH
Karlsruhe 5
WEST GERMANY

J. Harley
Environmental Measurements
Laboratory
Department of Energy
376 Hudson St.
New York, NY 10014

5 Librarian
Ministry of Agriculture
Fisheries and Food
Laboratory
Lowestoft, Suffolk
ENGLAND

J. J. Rasmussen
Montana Energy Research
Center
P.O. Box 3809
Butte, MT 59701

M. Haworth
Montana Power
(Colstrip)
P.O. Box 419
Colstrip, MT 59323

Library
Ontario Hydro
620 University Ave.
Toronto, Ontario
CANADA

A. G. Sharkey
Pittsburgh Energy Research
Center
4800 Forbes Ave.
Pittsburgh, PA 15213

E. D. Goldberg
Schripps Institute of
Oceanography
University of California
La Jolla, CA 92093

D. Lal
Schripps Institute of
Oceanography
University of California
La Jolla, CA 92093

No. of
Copies

R. L. Dobson
World Health Organization
Case Postale No. 5
CH-1211
Geneva 20
SWITZERLAND

Librarian
World Meteorological
Organization
Geneva
SWITZERLAND

22 United States

J. R. Arnold
Chemistry Department
University of California
San Diego
La Jolla, CA 92037

W. Broecker
Lamont Geological
Observatory
Columbia University
Palisades, NY 10964

Education and Information
Section
Health Physics Division
Oak Ridge National
Laboratory
Oak Ridge, TN 37830

M. C. Gaske
Assistant to Executive
Secretary
Advisory Committee on
Reactor Safeguards
U.S. Nuclear Regulatory
Commission
Washington, DC 20555

C. Gordon
Department of Botany
University of Montana
Missoula, MT 59801

N. Harley
New York University
Medical Center
550 First Ave.
New York, NY 10016

D. P. Kharkar
LFE Corporation
Environmental Analysis
Laboratories
2030 Wright Ave.
Richmond, CA 94804

No. of
Copies

H. W. Kirby
Monsanto Research
Corporation
Mound Laboratory
Miamisburg, OH 45342

P. K. Kuroda
Department of Chemistry
University of Arkansas
Fayetteville, AR 72701

P. LaFleur
Nuclear Recator Laboratory
National Bureau of Standards
Gaithersburg, MD 20760

A. Levin
Battelle Memorial Institute
2030 M. Street NW
Washington, DC 20545

D. G. McCauley
Code 304, Michelson Lab.
Department of the Navy
Naval Weapons Center
China Lake, CA 93555

C. Menninga
Physics Department
Calvin College
1331 Franklin St. S.E.
Grand Rapids, MI 49506

D. Montgomery
Environmental Protection
Agency
26 W. St. Clair St.
Cincinnati, OH 4526

A. Seymour
Laboratory of Radiation
Ecology
University of Washington
College of Fisheries
Seattle, WA 98105

W. Singlevich
Air Force Technical
Applications Center/TD-4
Patrick AFB, FL 32925

C. V. Theis
U.S. Geological Survey
P.O. Box 436
Albuquerque, NM 87106

No. of
Copies

D. Uhl
Nuclear Engineering and
Operations Department
Electric Power Research
Institute
3412 Hillview Ave.
P.O. Box 10412
Palo Alto, CA 94303

8 Foreign

J. C. Dalton
U.K. Atomic Energy
Authority
Windscale Works, P.G.
Sellafield, Seascale,
Cumberland
ENGLAND

D. P. Meyerhof
Environmental Radioactivity
Section
Nuclear Safety Division
Radiation Protection
Bureau
Brookfield Road
Ottawa, Ontario K1A 1C1
CANADA

K. Edvarson
Forsvarets Forskningsanstalt
Res. Institute of National
Defence
Avdelning 4,
Stockholm 80
SWEDEN

F. Girardi
C.C.R. EURATOM-ISPRA
(VERESE)
ITALY

S. Jackson
U.K. Atomic Energy
Authority
Harwell, Didcot
Berkshire
ENGLAND

A. Malvicini
Chief, Protection Service
C.C.R. EURATOM-ISPRA
(VERESE)
ITALY

D. P. Meyerhoff
Environmental Radioactivity
Section
Nuclear Safety Division
Radiation Protection
Bureau
Brookfield Road
Ottawa, Ontario
K1A1C1
CANADA

No. of
Copies

J. K. Miettinen
University of Helsinki
Department of
Radiochemistry
Unionkatu 35, Helsinki
FINLAND

R. V. Osborne
Atomic Energy of
Canada, Ltd.
Chalk River, Ontario
CANADA

D. H. Peirson
AERE (Atomic Energy
Research Establishment)
Health Physics and
Medical Division
B. 364
Harwell, Didcot, Berkshire
ENGLAND

ONSITE

8 DOE Richland Operations Office

P. F. Dunigan
J. L. Landon
W. Lei
H. E. Ransom
P. R. Rhodes
F. R. Standerfer
M. W. Tiernan
J. D. White

3 Hanford Environmental Health Foundation

W. D. Norwood
Medical Library (2)

No. of
Copies

154 Battelle-Northwest

T. W. Ambrose
W. J. Bair (20)
N. E. Ballou
J. B. Burnham
N. E. Carter
D. B. Cearlock
J. R. Corley
G. M. Dalen
J. M. Davidson
H. Drucker
C. E. Elderkin
S. J. Farmer
W. D. Felix (15)
J. W. Finnigan
R. F. Foster
J. C. Fox (5)
J. J. Fuquay
C. I. Gibson
W. A. Glass (10)
A. J. Haverfield (5)
D. L. Hessel
R. L. Hooper
V. G. Horstman
L. J. Kriby
H. V. Larson
R. C. Liikala
S. Marks
R. P. Marshall
I. C. Nelson (5)
J. M. Nielsen (10)
R. E. Nightingale
D. E. Olesen
J. F. Park
R. W. Perkins (5)

No. of
Copies

Battelle-Northwest (Contd)

L. A. Rancitelli (15)
W. D. Richmond
C. L. Simpson
W. H. Swift
W. L. Templeton
R. C. Thompson
C. M. Unruh
B. E. Vaughan
W. R. Wiley
Biology Library (2)
Technical Information (5)
Technical Publications (2)1 BE

3 Battelle Seattle

G. W. Duncan
J. Hébert
S. Nealey